Metallomics Research

SPECIAL ISSUE

Selenium Research:

Integrated Chemistry and Biology

Vol.**4**/No.**3**

November 2024

Index

Index

A Selenium Analog of Glutathione. Synthesis and Applications

Michio Iwaoka[1, 2]*

[1] Department of Chemistry, School of Science, Tokai University, Kitakaname, Hiratsuka-shi, Kanagawa 259-1292, Japan
[2] Institute of Advanced Biosciences, Tokai University, Kitakaname, Hiratsuka-shi, Kanagawa 259-1292, Japan

Abstract

Selenoglutathione (GSeH) is a water-soluble tripeptide, in which the sulfur atom of biologically important reductant glutathione (GSH) is replaced by a selenium atom, and exhibits a higher reducing activity than GSH. In this review, we overview the research on this selenium analogue of glutathione and look ahead to future research directions. Both solid-phase and liquid-phase methods can be used to chemically synthesize selenoglutathione diselenide (GSeSeG), the oxidized form of GSeH. Lesser amounts of GSeH are also found in the metabolic products of yeast and certain plants (garlic, sunflower sprouts, etc.) grown in a high-selenium medium. In the meantime, a biological method for the synthesis of GSeH using mutated yeast has recently been reported. Various applications of selenoglutathione in the field of biochemistry have already been explored. It has been reported that GSeSeG is an efficient catalyst for the oxidative folding of proteins. GSeSeG is also an excellent radical scavenger and potential detoxifier of intracellular xenobiotics. Recently, it has also been reported that GSeSeG has stress-reducing and antibacterial properties. Because GSeSeG has low toxicity, its unique reactivity is expected to be widely applied in the fields of applied biology and medicine.

Statements about COI: There is no conflict of interest to declare.

1. Introduction

Selenium is an essential micronutrient, usually present as selenocysteine (Sec) in the body and contained in the reaction center of various enzymes [1,2]. Sec is a natural amino acid, in which the sulfur atom of cysteine (Cys) is replaced by a selenium atom, and is known as the 21st proteinogenic amino acid [3]. Research on the synthesis and function of peptides containing Sec is being actively conducted [4]. The chemical synthesis of artificial proteins, in which Cys has been mutated to Sec, and their unique biological functions are also attracting large interest of researchers [5–8]. In recent decades, the biological functions of selenouracil derivatives, which were found in nucleic acids, have also been actively studied [9,10]. The progress of these research reveals the potential of these selenium analogs of biomolecules as possible candidates of drug discovery [8].

Glutathione (GSH) is a water-soluble tripeptide with a molecular structure of γ-Glu-Cys-Gly, which is abundant in cells and plays important roles in

*Correspondence
Michio Iwaoka
Department of Chemistry, School of Science, Tokai University
Kitakaname, Hiratsuka-shi, Kanagawa 259-1292, Japan
Tel ; +81-463-58-1211
E-mail ; miwaoka@tokai.ac.jp

maintaining redox homeostasis in the body and relieving stress through various redox reactions, such as decomposing free radicals and reactive oxygen species (ROS) like peroxides, decomposing methylglyoxal (MG), which causes fatal glycative stress, and reacting with and eliminating harmful intracellular xenobiotics [11,12]. Since selenium atoms have a higher polarizability and higher redox reactivity than sulfur atoms [13], selenoglutathione (GSeH, **1**), a selenium analogue of GSH, which has Sec instead of Cys in GSH, is expected to have physiological functions far superior to those of GSH. The selenol group (-SeH) of **1** is easily oxidized by oxygen dissolved in the solvent to form a diselenide (-SeSe-) due to its high reactivity. The resulting selenoglutathione diselenide (GSeSeG, **2**) is a stable compound, and the diselenide (SeSe) bond of **2** does not decompose even when left at room temperature for more than a month. This reflects the other side of the high reactivity (reducibility) of the reduced form GSeH (**1**) and means that selenoglutathione usually exists as the oxidized form GSeSeG (**2**). To bring out the unique reactivity of GSeH (**1**), it is necessary to activate the diselenide **2** to the selenol **1** by reduction.

Hilvert and coworkers previously reported that diselenide **2** is reduced by the enzyme glutathione reductase (GR) in the presence of NADPH to produce selenol **1** (Eq. 1) [14]. Diselenide **2** is structurally almost equivalent to GSSG, so GR recognizes **2** as a substrate. It has been reported that the substrate affinity of **2** for GR is approximately one-tenth that of GSSG [14]. On the other hand, it has recently been shown that selenol **1** can also be produced by the reaction of diselenide **2** with excess GSH (Eq. 2) [15]. These results indicate that **2** can be activated to produce **1** in cells by both enzymatic (Eq. 1) and nonenzymatic (Eq. 2) reactions.

$$\text{GSeSeG (}\textbf{2}\text{) + NADPH + H}^+ \xrightarrow{\text{GR}} \text{2GSeH (}\textbf{1}\text{) + NADP}^+ \quad \text{(Eq. 1)}$$

$$\text{GSeSeG (}\textbf{2}\text{) + 2GSH} \rightleftharpoons \text{2GSeH (}\textbf{1}\text{) + GSSG} \quad \text{(Eq. 2)}$$

In this review, we provide an overview of the research results on selenoglutathione reported in the literature and prospects for future research. In particular, we focus on the development of synthetic methods for selenoglutathione and the applications of the unique reactivity to biochemical reactions (**Fig. 1**). Section 2 describes the chemical synthesis of selenoglutathione, and Section 3 describes its formation and metabolism in vivo. Section 4 details recent research results on the applications of selenoglutathione (4.1 Protein folding, 4.2 Radical scavenging, 4.3 Detoxification of intracellular xenobiotics, 4.4 Stress reduction, and 4.5 Antibacterial activity). Section 5 briefly discusses future applications of selenoglutathione in the fields of applied biology and medicinal research based on the recent achievements.
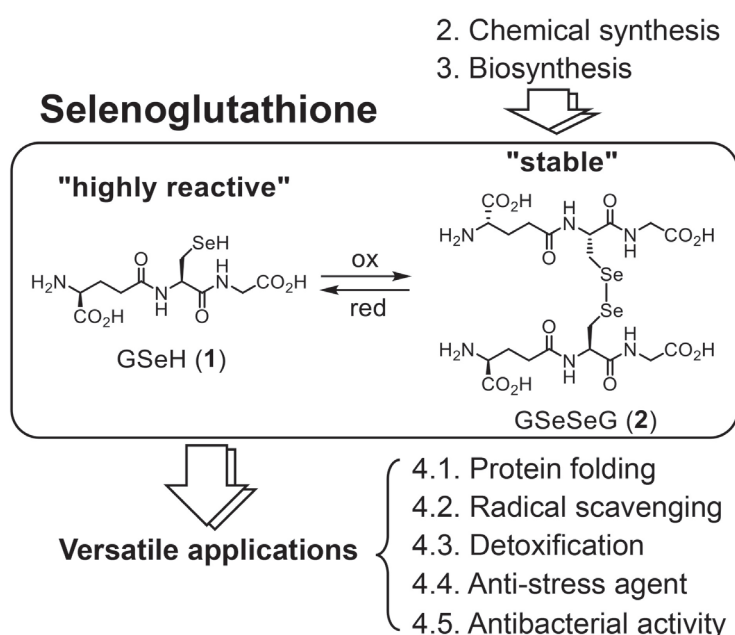

Fig. 1. | Synthesis and applications of selenoglutathione.
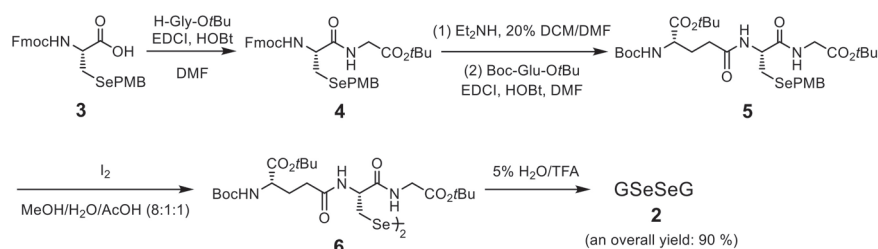
2. Chemical synthesis of GSeSeG

The chemical synthesis of selenoglutathione was reported as early as the 1960s [16,17]. In the early studies, a liquid-phase method was used as the synthesis method. In 1993, Tamura [18] also used a liquid-phase method to synthesize 0.13 g of GSeSeG (**2**) as an ammonium salt from *N*-Fmoc-*Se*-(*p*-methoxybenzyl)-L-selenocysteine (Fmoc-Sec(PMB)-OH, **3**) as a starting material, and succeeded in characterizing selenoglutathione by various spectra for the first time. However, the overall yield of diselenide **2** was low at 9 %, so the liquid-phase synthesis method was not used in subsequent studies for a while. In the 2000s, Beld [14] reported the chemical synthesis of **2** by a solid-phase method, which is easier to carry out experimentally (**Scheme 1**). They reacted activated selenocysteine (Fmoc-Sec(PMB)-OPfp) and γ-glutamic acid (Boc-Glu(OPfp)-O*t*Bu) sequentially with Fmoc-Gly-loaded WANG resin using an automated peptide synthesizer. The tripeptide was then removed from the resin and deprotected using a trifluoroacetic acid (TFA):trimethylsilane bromide (TMSBr):thioanisole:*m*-cresol (750:132:120:50) cocktail to obtain diselenide **2** in an overall yield of 33 %.
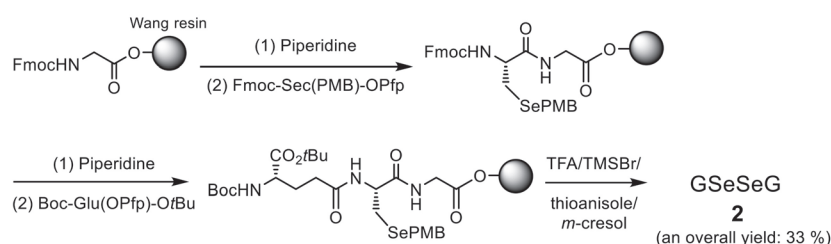
Scheme 1. | Solid-phase synthesis of GSeSeG (2) by Beld et al. [14].

Yoshida [19] used a manual solid-phase method to synthesize **2** in 9 % overall yield by sequentially reacting HOBt/DCC-activated selenocysteine (Fmoc-Sec(PMB)-OBt) and glutamic acid (Boc-Glu(OBt)-O*t*Bu) with Fmoc-Gly-loaded Alko-PEG resin, cleaving the peptide form the resin with a TFA:H_2O:phenol:thioanisole:ethanedithiol (825:50:50:50:25) cocktail, and then deprotecting the PMB group on the selenium atom of the Sec residue with TFA and 2,2'-dithiobis(5-nitropyridine) (DTNP). However, the solid-phase methods require the addition of excess amino acid reagents during amino acid coupling. In addition, the efficiency of peptide cleavage from the resin was poor, and diselenide **2** was only obtained in low yields.

Considering that selenoglutathione is a short peptide and that the synthetic raw material, a selenocysteine derivative, is expensive (see below), it seems that the liquid-phase method is more suitable for large-scale synthesis than the solid-phase method. Therefore, Shimodaira [20] reconsidered Tamura's liquid-phase synthesis method of GSeSeG (**2**). As a result, they succeeded in obtaining the target product **2** from the starting material **3** in an overall yield of 90 % by the synthetic route shown in **Scheme 2**. First, **3** was activated with HOBt/EDCI and reacted with glycine (H-Gly-O*t*Bu) to afford dipeptide **4** in 98 % yield. Next, the Fmoc group of **4** was deprotected with diethylamine, and then glutamic acid (Boc-Glu-O*t*Bu), activated with HOBt/EDCI, was reacted with it to yield tripeptide **5** quantitatively. After removing the PMB group on the selenium atom with iodine, the resulting **6** was purified, and finally the other protecting groups were deprotected with 5 % H_2O-TFA to afford the target compound **2**. Further investigations revealed that **2** could be quantitatively obtained without going through **6** by treating tripeptide **5** with 20 % thioanisole-TFA. These synthetic methods are the most efficient of the previously reported synthetic methods for GSeSeG (**2**), allowing a gram sclae synthesis of **2**. However, in the latter shortcut route, the

Scheme 2. | Highly efficient liquid-phase synthesis of GSeSeG (2) by Shimodaira et al. [20].

deprotecting agent thioanisole may remain as an impurity even after purification and lyophilization. Therefore, the route of Scheme 2 is a steady method to obtain the target compound, although the yield is somewhat reduced.

The synthesis of selenoglutathione requires a selenocysteine derivative with appropriate protecting groups on the amino and selenol groups. The Sec derivative **3** is often used to synthesize Sec-containing peptides (selenopeptides) using the routine Fmoc method. Compound **3** is commercially available, but is expensive. It can also be synthesized from inexpensive L-serine or L-cysteine through several reaction steps and purification [21,22]. However, care must be taken as racemization may occur when selenium is introduced into the amino acid sidechain by substitution reaction [22]. It is also possible to synthesize **3** from commercially available L-selenocystine (the oxidized dimer of Sec) [23], but L-selenocystine is also expensive. In any case, an appropriate route for obtaining **3** should be selected in light of the research aims.

The synthesis of GSeH derivatives has also been reported (**Fig. 2**). Yonezawa [24] reported the synthesis of GSe-Me (**7**) and GSe-Bn (**8**), in which the selenium atom is protected with a Me or Bn group. Lapcinska [25] reported the synthesis of selenoglutathione derivatives **9**, in which the amino group is protected with a Boc group, the carboxyl group with a *t*Bu or Bn ester, and various coumarins are bound to the selenium atom. These derivatives are also interesting from the perspective of applying selenoglutathione in the field of biochemistry.
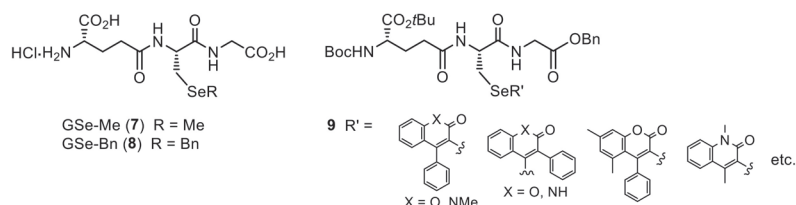
Fig. 2. | **Synthesized derivatives of GSeH (1).**

3. GSeH derivatives found in metabolites

Previously, GSeH (**1**) was thought not to exist in nature [26,27], but as research progressed, it became increasingly clear that **1** does exist in nature in very small amounts.

Van Dorst [28] grew *Lolium perenne* plants in soil containing $^{75}SeO_3^{2-}$ and analyzed the selenium content in the soil and plants by radiometric analysis. As a result, it was confirmed that **1** was formed in the soil. Lobinski and coworkers [29,30] suggested the presence of GSe-Me (**7**) and its oxidized seleninyl derivative GSeO$_2$-Me in the metabolites of selenium-rich yeast by LC-ICP-MS analysis. Although the selenium atom is methylated, these results suggest that **1** is generated during metabolism. Rao [31] fed yeast with selenomethionine (Sem) and treated the metabolites with iodoacetic acid (IAA) or *p*-(hydroxymercuric)benzoic acid sodium salt (PHMB), and analyzed the products by HPLC and MS analysis. As a result, GSe-CH$_2$CO$_2$H and GSe-Hg(C$_6$H$_4$)CO$_2$H were formed within 2 hours, indicating the production of GSeH (**1**). Lobinski and coworkers [32] identified 64 selenium compounds in the metabolic products of selenium-enriched yeast using reversed-phase/hydrophilic ion interaction (HILIC) liquid chromatography–electrospray hybrid quadrupole trap/Orbitrap mass spectrometry, and showed that **1** was
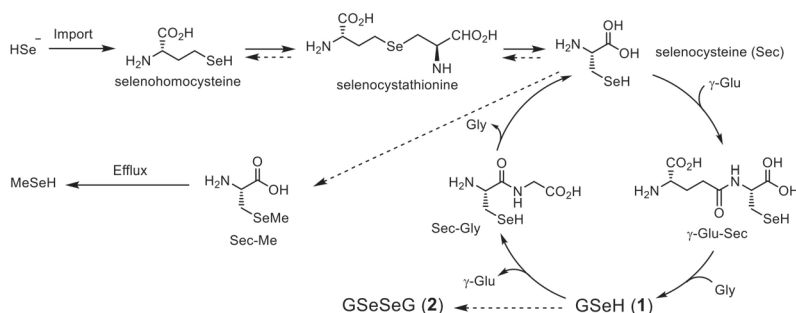
Fig. 3. | **Proposed metabolic formation and degradation of GSeH (1) in selenium yeast.**
This figure was drawn using the data reported by Lobinski and coworkers [32].

among them. Furthermore, they estimated that the metabolic process of selenoglutathione by selenium-enriched yeast is similar to that of natural glutathione, as illustrated in **Fig. 3**.

Ruszczyńska [33] found GSe-Me (**7**) and methylthio-selenoglutathione (GSe-SMe) in garlic, sunflower sprouts and radish sprouts grown in a high-selenium medium using HPLC-ICP-MS and HPLC-ESI Orbitrap-MS/MS analysis. Similarly, the presence of GSe-SMe in the metabolites of the feed yeast *Candida utilis* ATCC 9950 has been reported [34]. As mentioned above, it has been revealed that selenoglutathione or its derivatives exist in the metabolites of yeast and certain plants. However, the amount of GSeH (**1**) is small and was observed when the organisms were grown in a medium containing a high concentration of selenium compounds. Therefore, it is more appropriate to consider it as a passive metabolic product rather than an active synthesis of GSeH (**1**) by the organism for particular purposes.

Recently, Gao [35] obtained a strain that synthesizes substantial amounts of GSH by mutating the yeast *Saccharomyces boulardii* with atmospheric and room temperature plasma (ARTP) mutagenesis, and succeeded in synthesizing a freeze-dried powder of GSeH (**1**), containing GSH (18 %) as an impurity, by culturing the strain in a medium containing sodium selenite (Na_2SO_3). The obtained powder was slightly yellow, and the structure of **1** was characterized by LC-MS analysis. This in vivo method of the synthesis is interesting as a new approach to selenoglutathione in addition to the chemical synthesis of **2** described in Section 2.

4. Applications of selenoglutathione to biochemical reactions

With the availability of GSeH (**1**) and GSeSeG (**2**), research on the reactivity of selenoglutathione and its applications in various biochemical reactions have been promoted in recent years. These pioneering studies have gradually unveiled the unique reactivity of selenoglutathione. Representative applications are described in detail below.

4.1. Protein folding

The first substantial application of selenoglutathione to biochemical reactions was in the oxidative folding of proteins. The research on this subject has been actively conducted by Hilvert and coworkers since the late 2000s [14,36–38]. Proteins that have disulfide bonds (SS bonds) in their molecules lose their three-dimensional structure and become denatured when the SS bonds are reduced. However, when an appropriate small molecule oxidant, such as GSSG and oxidized dithiothreitol (DTT^{ox}), is added to this denatured state (R), the protein gradually retrieves its native folded structure (N) through the formation and rearrangement of SS bonds [39]. The process from R to N is oxidative folding of proteins. The oxidant used in this process is the disulfide reagent RSSR, which has a redox potential close to that of the SS bonds of proteins. These reagents cooperatively promote the SS bond formation and SS bond rearrangement reactions at a moderate velocity, ultimately inducing the native protein (N) [40–43]. On the other hand, selenoxide reagents ($>Se=O$), which have strong oxidizing power, are also known to be useful for oxidative folding of proteins [44]. When selenoxide is used, the SS bond formation reaction takes precedence, followed by a slow SS bond exchange reaction, and the protein gradually folds during this latter process. A use of this reagent makes it possible to clearly determine the protein folding pathways [45].

Conversely, the diselenide reagent (RSeSeR) is much less effective as an oxidizing agent than RSSR, so it is expected that RSeSeR will not promote the formation of SS bonds in proteins and will not be useful for oxidative folding. However, when GSeSeG (**2**) was actually applied, it was found that the folding of bovine pancreatic ribonuclease A (RNase A) and trypsin inhibitor (BPTI) proceeded faster than when GSSG was used (**Fig. 4a**) [14,38]. The reasons for this unexpected result would be several folds, such as because the gain in energy obtained by the formation of the three-dimensional structure of the protein exceeds the energy deficit when the R state is oxidized by GSeSeG (**2**). In addition, since GSeH (**1**) generated by the reaction between R and **2** has strong nucleophilicity, it is also assumable that **1** effectively accelerate the rearrangement of SS bonds in the folding intermediates. It was also found that GSeSeG (**2**) catalytically folds proteins because GSeH (**1**) is easily oxidized by dissolved oxygen [36]. These factors likely accelerate oxidative folding cooperatively.

GSeSeG (**2**) was found to be useful for the oxidative folding of various SS-containing proteins, such as hirudin,

lysozyme, human epidermal growth factor, and interferon α-2a [37]. However, in the case of bovine serum albumin (BSA), which has 17 SS bonds, and antibody Fab fragments, which are considered difficult to fold, it was necessary to use high concentrations (~mM) of GSeSeG (**2**) [37]. In addition to **2**, various small molecule diselenide reagents have been developed as useful folding reagents [46–48]. Some of them have been shown to have even better catalytic activity than **2** [46].

Unique applications that take advantage of the reaction (Eq. 1), in which GSeSeG (**2**) is reduced by GR to generate active GSeH (**1**), have also been reported. Shimodaira [20] showed in vitro that when misfolded RNase A with random SS bonds was treated with **2** in the presence of NADPH and GR, the SS bonds of the misfolded protein were reduced by the generated **1**, and the rearrangement of the SS bonds proceeded to efficiently generate the N state (**Fig. 4b**). Thus, GSeSeG (**2**) would be useful for refolding of misfolded proteins.
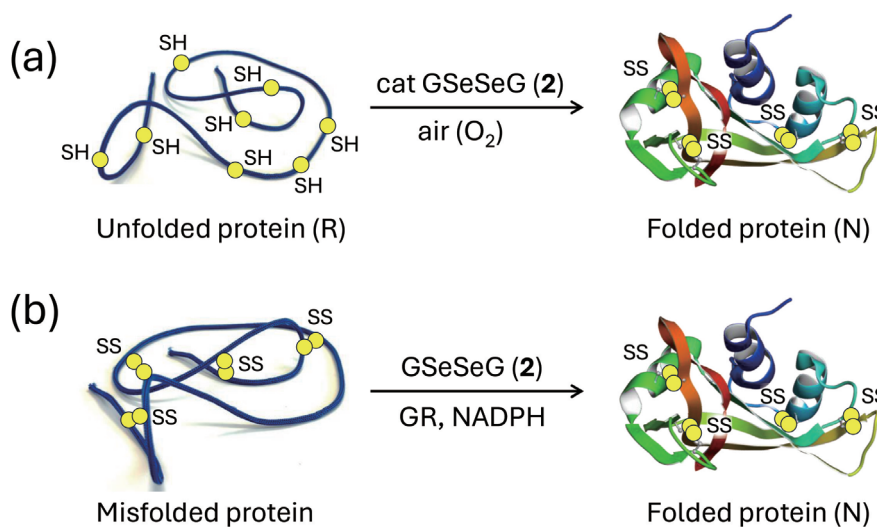
Fig. 4. | **Applications of GSeSeG (2) in protein folding.**
(a) Catalytic folding of proteins. (b) Refolding of misfolded proteins.

Hilvert and coworkers [49] applied GSeSeG (**2**) to the in vivo oxidative folding of β-galactosidase using a DsbA-deficient *E. Coli* strain. As a result, the production of the native state of β-galactosidase was confirmed using 1.0 μM of **2**. Thus, **2** would mediate protein folding in vivo as well as in vitro, but the effect was significantly worse than that of GSSG. Special ingenuity may be required to apply GSeSeG (**2**) to in vivo protein folding.

4.2. Radical scavenging

GSeH (**1**) is also useful as a radical scavenger. Radical species can cause lipid peroxidation and other oxidative stress. Koppenol and coworkers [50] used pulse radiolysis to monitor the reaction of *N*-acetyl-tyrosyine radical (free Tyr·) with Sec, GSeH (**1**), or GSH and estimated the reaction rate constants (*k*'s). The reaction of free Tyr· with Sec is shown in Eq. 3. The rate constant for the reaction of **1** with free Tyr· is $k_{GSeH} = 5 \times 10^8$ M^{-1} s^{-1}, which is slightly smaller than that of Sec ($k_{Sec} = 8 \times 10^8$ M^{-1} s^{-1}), but it is 10^5 larger than that of GSH ($k_{GSH} = 2.4 \times 10^3$ M^{-1} s^{-1}) [50]. The Sec radical generated by the reaction interacts with another Sec molecule to form a dimer radical anion with a two-center-three-electron bond (Eq. 4), which should then decompose. Interestingly, the reaction rate constant of **1** with the tyrosine radical in insulin (insulin-Tyr·) was found to be 10^2 smaller than that with free Tyr· [50]. This is likely due to steric hindrance caused by the folded structure of insulin. The ability of GSeH (**1**) as a radical scavenger is comparable to that of ascorbic acid [51].

$$Tyr\cdot + Sec^- \xrightarrow{k_{Sec}} Tyr^- + Sec\cdot \qquad (Eq. 3)$$

$$Sec\cdot + Sec^- \longrightarrow (Sec\therefore Sec)^- \qquad (Eq. 4)$$
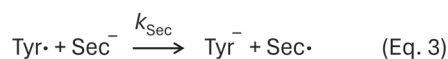
4.3. Detoxification of xenobiotics

Glutathione transferases (GSTs) are enzymes that catalyze the reaction of intracellular xenobiotics (X) with GSH to form glutathione conjugates (GS-X) [52]. It has been demonstrated that GSeH (**1**) exerts GST-like detoxifying effects against organic mercury and allergenic aromatic chloride compounds.

Khan [53] followed the reaction of methylmercury (CH_3HgOH) with **1** by real-time ^1H and ^{199}Hg NMR spectroscopy and confirmed the formation of $(CH_3Hg)_2Se$ and a black precipitate of HgSe(s). Similar reactions were also observed with selenomethionine (Sem) and selenocysteine (Sec). From the analysis of the reaction products, Khan speculated that the reaction proceeded as follows (**Fig. 5**): Selenoglutathione (GSe^-) reacts with CH_3Hg^+ to form GSe-$HgCH_3$, which further reacts with GSe^- to produce $(CH_3Hg)_2Se$, GSeSeG (**2**), and G^-. $(CH_3Hg)_2Se$ disproportionates to form $(CH_3)_2Hg$ and HgSe(s). This study indicates that GSeH (**1**) may contribute to the detoxification of organic mercury.

$$CH_3Hg^+ + GSe^- \text{ (1)} \rightleftharpoons GSe\text{-}HgCH_3$$

$$2\ GSe\text{-}HgCH_3 + GSe^- \text{ (1)} \rightleftharpoons (CH_3Hg)_2Se + GSeSeG \text{ (2)} + G^-$$

$$(CH_3Hg)_2Se \longrightarrow (CH_3)_2Hg + HgSe(s)$$

$$(CH_3)_2Hg + H^+ \longrightarrow CH_3Hg^+ + CH_4$$
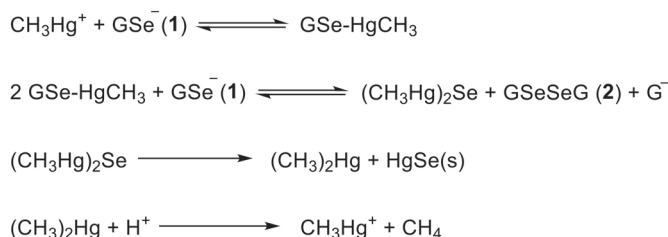
Fig. 5. | **Detoxification of methyl mercury by GSeH (1)** [53].

Recently, Kanamori [15] investigated the GST-like activity of GSeSeG (**2**) using 1-chloro-2,4-dinitrobenzene (CDNB) as a model substance for allergenic aromatic compounds. CDNB (1 mM) and GSH (2 mM) were reacted in the presence of **2**, and the amount of the resulting conjugate (GS-DNB) was determined by the change in absorbance at 340 nm (**Fig. 6**). The results showed that although the activity of **2** was lower than that of the GST enzyme (0.15 unit/mL), **2** exhibited significant GST-like activity in a concentration-dependent manner in the range of 0.05 to 0.5 mM.
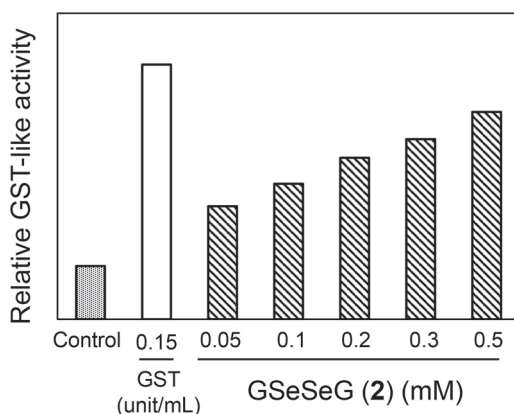
Fig. 6. | **Relative GST-like activity of GSeSeG (2) against CDNB.**
This figure was drawn using the data reported by Kanamori et al. [15].

When the reaction products were analyzed by HPLC, only one peak was observed in the presence of GST, which was identified to be GS-DNB by mass spectrometry. The same product peak was also observed in the control, indicating that the reaction between GSH and CDNB proceeded slightly even in the absence of the GST enzyme (**Scheme 3**). On the other hand, in the presence of **2**, two peaks were observed by HPLC, and mass spectrometry confirmed that these were GS-DNB and GSe-DNB, a conjugate of selenoglutathione and CDNB. Since **2** did not react
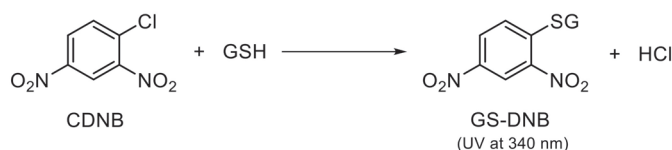
Scheme 3. | **Reaction of GSH with CDNB.**

directly with CDNB, it was assumed that **2** reacted with GSH, which was present in the reaction solution, to produce **1**, which was subsequently reacted with CDNB to generate GSe-DNB (**Scheme 4**). Thus, it was demonstrated that **1** can be generated by a nonenzymatic process between **2** and GSH (Eq. 2). This suggests that under the conditions of high GSH concentration like within cells, GSeH (**1**) is produced from GSeSeG (**2**). This is an important finding in light of biochemical applications of selenoglutathione.
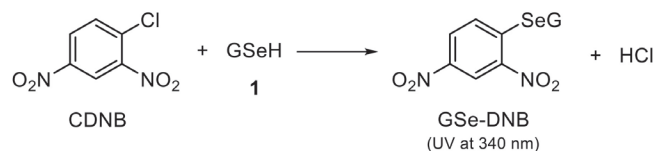
Scheme 4. | **Reaction of GSeH (1) with CDNB.**

4.4. Mitigation of oxidative and glycative stresses

Hydrogen peroxides (H_2O_2) and hypochlorous acid (HOCl) cause oxidative stress in cells. Similarly, methylglyoxal (MG) induces fatal glycative stress in cells. Recent experiments in cell-free and cell-based systems have demonstrated that selenoglutathione effectively alleviates these stresses. This section summarizes the interactions of GSeH (**1**) and GSeSeG(**2**) with H_2O_2, HOCl, and MG.

Glutathione peroxidase (GPx) is an antioxidant enzyme that has Sec at its active center [11,54]. This selenoenzyme uses GSH to degrade H_2O_2 or hydroperoxides (ROOH) generated in the body into harmless water or alcohol, respectively. Singh [55] previously reported in detail on the GPx-like antioxidant activity of Sec. In the active center of GPx, it is known that Sec does not exist alone but form a catalytic triad (or plausible tetrad) with proximate polar amino acids, such as Gln and Trp [56,57]. The interactions between these polar amino acid sidechains and the selenium atom of Sec are studied extensively, but the details of their role remain controversial [58–62].

Yoshida [19] reported that GSeSeG (**2**) exhibits high GPx-like antioxidant activity against H_2O_2 in the presence of GR and NADPH in a cell-free system. GSeH (**1**), which is generated from **2** by the reaction of Eq. 1, reacts rapidly with H_2O_2 to produce selenenic acid GSeOH and H_2O. GSeOH can be further oxidized to seleninic acid $GSeO_2H$, but in the presence of an enough concentration of GSH, GSeOH reacts rapidly with GSH to produce selenenyl sulfide GSeSG, which is a fairly stable intermediate. As far as the reaction was traced by NMR, it could not be reduced to GSeH even when excess GSH was added [20]. However, GSeSG is structurally equivalent to GSSG, just like **2**. Therefore, it would be reduced to **1** in the presence of GR and NADPH (Eq. 5). The reason why **2** exhibits high GPx-like activity is probably because the stable GSeSG intermediate is reduced by the action of GR. The updated GPx-like catalytic cycle of **2** is illustrated in **Fig. 7**. Shimodaira [20] used the synthesized **2** to follow a series of reactions using ^{77}Se NMR and succeeded in characterizing some of the reaction intermediates.
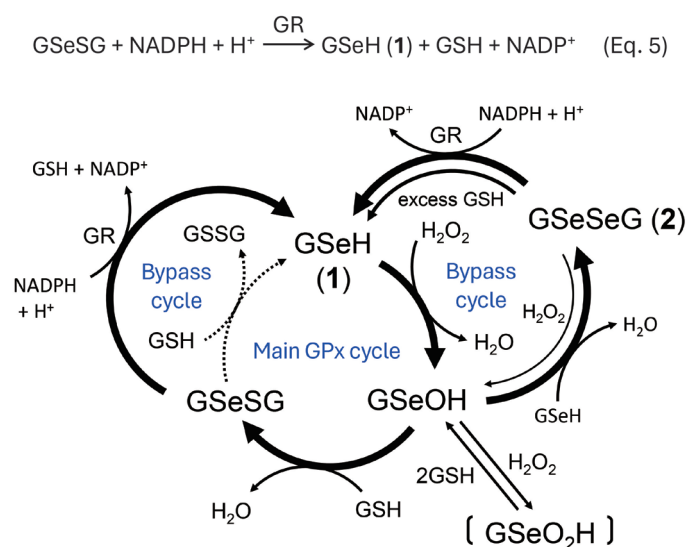
$$\text{GSeSG} + \text{NADPH} + \text{H}^+ \xrightarrow{\text{GR}} \text{GSeH (1)} + \text{GSH} + \text{NADP}^+ \quad \text{(Eq. 5)}$$

Fig. 7. | **GPx-like catalytic cycle of GSeSeG (2) updated.**

Recently, Kanamori [15] attempted to quantify the remaining H_2O_2 in the reaction of **1** (1 mM), which was generated by the method of Eq. 1, with H_2O_2 (0.1 mM) by FOX assay. The FOX assay is a common method to quantify the concentration of H_2O_2 in a sample solution by utilizing the reaction, in which Fe^{2+} is oxidized to Fe^{3+} [63]. The reaction was performed under conditions, in which GPx (0.014 units/mL) and/or GSH (2 mM) were added to the assay solution to mimic the intracellular environment. The remaining rate of H_2O_2 under various reaction conditions is shown in **Fig. 8**.
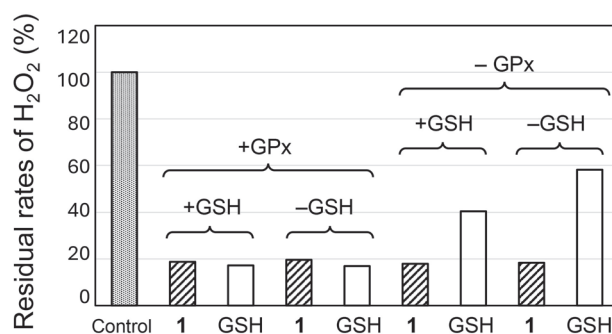
Fig. 8. Residual rates of H_2O_2 30 min after the reaction with GSeH (1) or GSH in the presence or absence of GPx (0.014 units/mL) and/or additional GSH (2 mM).
$[H_2O_2]_0 = 0.1$ mM, $[GSeH]_0 = [GSH]_0 = 1$ mM. This figure was drawn using the data reported by Kanamori et al. [15].

GSeH (**1**) always showed a low H_2O_2 residual rate (<20%) regardless of the addition of GPx or GSH (2 mM). This indicates that **1** reacts directly with H_2O_2 through a nonenzymatic process. In contrast, the reduction of H_2O_2 concentration by GSH depended on the presence of both GPx and GSH (2 mM) in the assay solution. In the presence of GPx, the reduction of H_2O_2 by GSH is also catalyzed by the enzyme. In fact, the residual H_2O_2 increased in the absence of GPx. Looking at the residual H_2O_2 in the absence of both GPx and GSH (2 mM), it was obvious that GSH can also react directly with H_2O_2, but its reducing ability is significantly lower than that of GSeH (**1**). This reflects the fact that the selenol group (-SeH) has a stronger reducing ability than the thiol group (-SH).

Carrol [64] reported the reaction rate constants (k's) of GSeH (**1**) and GSeSeG (**2**) with various reactive oxygen species by precise reaction kinetic analysis. The reaction rate constants of **1** and **2** with HOCl were $k = 3.2 \times 10^8$ and $1.9–2.59 \times 10^7$ $M^{-1} s^{-1}$, respectively, showing that selenoglutathione is an excellent antioxidant against HOCl. This is presumably due to the fact that selenium has a higher polarizability than sulfur.

Glyoxalase I (GLO1) is an enzyme that uses GSH to degrade methylglyoxal (MG), which causes glycative stress (**Scheme 5**) [65,66]. GSH reacts with MG to generate a hemithioacetal intermediate, which is then isomerized to *S*-lactoylglutathione by the action of GLO1. Kanamori [15] reacted GSeH (**1**) or GSH, which was generated from GSeSeG or GSSG, respectively, using GR and NADPH, with an equivalent amount of MG and measured the proportion of unreacted MG in the reaction solution by reacting MG with 1,2-diamino-4,5-methylenedioxybenzene dihydrochloride (MDB). The amount of the MG-MDB adduct formed was determined by measuring the fluorescence of the solution at 393 nm (**Scheme 6**) [67]. The results are shown in **Fig. 9**. It was observed that MG was rapidly consumed in the presence of **1** (approximately 50% in 30 min), whereas the reaction between GSH and MG was slow. Although this experiment did not allow the identification of the reaction product between **1** and MG, it was confirmed that **2** exhibited GLO1-like anti-glycative stress activity in the presence of GR and NADPH.
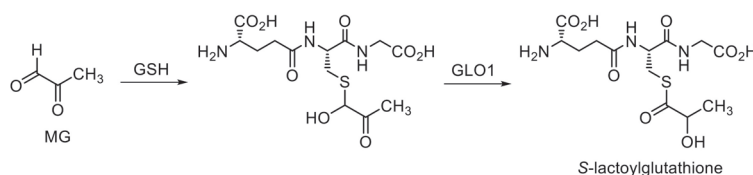
Scheme 5. Reaction between methylglyoxal (MG) and GSH in the presence of GLO1.
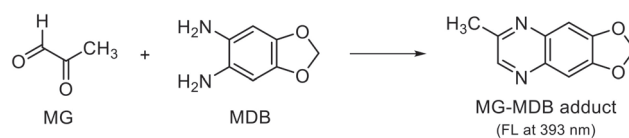
Scheme 6. | **Reaction between methylglyoxal (MG) and MDB.**
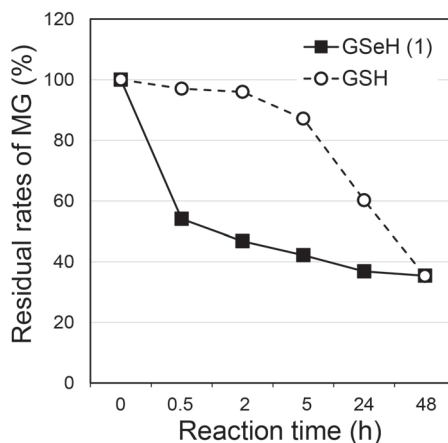
Fig. 9. | **Anti-glycative stress activity of GSeH (1) determined by the reaction with MG in comparison with GSH.**
This figure was drawn using the data reported by Kanamori et al. [15].

The results of the cell-free assays shown in **Figs. 8 and 9** revealed that **2** can exert anti-stress activity through GPx-like and GLO1-like mechanisms in the coexistence of GR and NADPH, thus indicating that **2** is an effective enzyme mimic of GPx and GLO1 and may be applied as a precatalyst to suppress oxidative and glycative stress in cells.

It was also revealed that **2** exhibits significant antioxidative and anti-glycative stress activities in cell culture systems. Kanamori [15] pretreated HeLa cells with **2** and then MG (4 mM), exposed the cells to oxidative stress by adding H_2O_2 (1.2 mM), and investigated the cell viability. The results are shown in **Fig. 10**.

When cells were not treated with MG nor H_2O_2, the cell viability remained constant (about 100%) even when treated with 50 μM of **2**. This indicates that **2** is non-toxic at concentrations up to at least 50 μM. This property of **2** was in significant contrast to a high toxicity of selenite (Na_2SeO_3) to HeLa cells ($LD_{50} = 1.2$ μM) [68]. On the other hand, when H_2O_2 (1.2 mM) was added to the cells, a decrease in the viability was observed for cells not pretreated with **2**. This evidenced that **2** exhibits antioxidative stress activity in HeLa cells. Furthermore, when cells were pretreated with MG, the cell viability was significantly reduced due to glycative stress caused by MG. However, the cell viability was improved when the cells were pretreated with **2**. Thus, **2** exhibited antioxidative and anti-glycative stress activities in the cell culture system as well as in the cell-free system, suggesting the possibility of applying **2** as an anti-stress agent.

3 μM GSeSeG (**2**)	+	−	+	−
4 mM MG	−	−	+	+
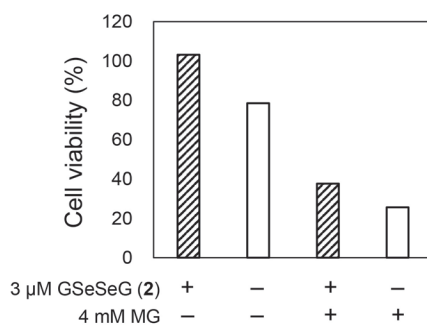
Fig. 10. | **Viabilities of HeLa cells in the presence of 1.2 mM H_2O_2. The cells were pretreated with GSeSeG (2) (3.0 μM) and then MG (4 mM).**
This figure was drawn using the data reported by Kanamori et al. [15].

4.5. Antibacterial activity

As mentioned in Section 3, Gao [35] recently reported the preparation of antibacterial hydrogels using selenoglutathione. By doping GSeH (**1**), which was synthesized using mutant yeast, into cellulose nanocrystals together with glutathione (GSH) and biosynthesized selenium nanoparticles, an elastic hydrogel with antibacterial properties against *E. coli* and *S. aureus* was obtained. This gel also exhibited significant antioxidant and radical-scavenging capacities. The authors expected to apply the hydrogels to strain sensors. Antibacterial activities of selenoglutathione have been only little explored to date.

5. Future perspective

Selenoglutathione, a selenium analog of glutathione, was once difficult to obtain. Therefore, it was only limitedly applied to the biological research in the past. However, in recent years, chemical synthesis protocols for GSeSeG (**2**) using not only solid-phase [14] but also liquid-phase methods [20] have been established, and various derivatives of selenoglutathione are now available. Furthermore, GSeH (**1**) can be obtained by culturing mutated yeast [35]. In the future, applied research of selenoglutathione (**1** and **2**) thus obtained will be actively conducted. In this review, we introduced its recent applications as a protein folding agent, a radical scavenger, a detoxifier for intracellular xenobiotics, an anti-stress agent, and an antibacterial agent as the examples that have already been reported. In the application to oxidative folding of proteins, **2** is an efficient catalyst (Section 4.1). **2** is also excellent as a radical scavenger (Section 4.2) and a detoxifier for intracellular xenobiotics (Section 4.3). It has also been reported recently that **2** has stress-reducing effects (Section 4.4) and antibacterial effects (Section 4.5). Although most of these applications are basic research in cell-free systems, some have already been performed using cell systems. These pioneering studies have revealed that selenoglutathione has a much higher biological activity than the corresponding glutathione. The enhanced activity is mainly due to the fact that the selenol group of GSeH (**1**) is more reactive (reducible) than the thiol group.

The unique reactivity of selenoglutathione is expected to be widely applied in the fields of applied biology and medicine in the future. When applying selenium compounds to living organisms, it is necessary to evaluate their toxicity. Since GSeSeG (**2**) is highly water-soluble like GSSG, the toxicity of this small tripeptide dimer in vivo is expected to be low [68]. In fact, **2** showed no toxicity to HeLa cells at concentrations up to at least 50 µM [15]. The low toxicity of **2** will be a great advantage in the development of new biological functions of selenoglutathione and its application to medicines.

References

[1] Dogaru CB, Muscurel C, Duţă C, Stoian I. "Alphabet" Selenoproteins: Their Characteristics and Physiological Roles. *Int. J. Mol. Sci.* 2023;24:15992.

[2] Zhang F, Li X, Wei Y. Selenium and Selenoproteins in Health. *Biomol.* 2023;13:799.

[3] Turanov AA, Xu XM, Carlson BA, Yoo MH, Gladyshev VN, Hatfield DL. Biosynthesis of Selenocysteine, the 21st Amino Acid in the Genetic Code, and a Novel Pathway for Cysteine Biosynthesis. *Adv. Nutr.* 2011;2:122–128.

[4] Iwaoka M, Shimodaira S. Synthesis and catalytic functions of selenopeptides. *Organochalcogen Compounds: Synthesis, Catalysis, and New Protocols with Greener Perspectives*, edited by Lenardao EJ, Santi C, Perin G, Alves D, Elsevier, 2022, Chapter 6, pp. 195-218.

[5] Mousa R, Notis Dardashti R, Metanis N. Selenium and Selenocysteine in Protein Chemistry. *Angew. Chemie Int. Ed.* 2017;56:15818–15827.

[6] Moroder L, Musiol HJ. Amino acid chalcogen analogues as tools in peptide and protein research. *J. Pept. Sci.* 2020;26:1–15.

[7] Mousa R, Hidmi T, Pomyalov S, Lansky S, Khouri L, Shalev DE, Shoham G, Metanis N. Diselenide crosslinks for enhanced and simplified oxidative protein folding. *Commun. Chem.* 2021;4:30.

[8] Iwaoka M. Chalcogen-containing Protein and Nucleic Acid Derivatives – Synthesis and Applications. *Chalcogen Chemistry: Fundamentals and Applications*, edited by Lippolis V, Santi C, Lenardao EJ, Braga AL, The Royal Society of Chemistry, 2023, Chapter 24, pp. 625-647.

[9] Leszczynska G, Cypryk M, Gostynski B, Sadowska K, Herman P, Bujacz G, Lodyga-Chruscinska E, Sochacka E, Nawrot B. C5-Substituted 2-Selenouridines Ensure Efficient Base Pairing with Guanosine; Consequences for Reading the NNG-3' Synonymous mRNA Codons. *Int. J. Mol. Sci.* 2020;21:2882.

[10] Kulik K, Sadowska K, Wielgus E, Pacholczyk-Sienicka B, Sochacka E, Nawrot B. Different oxidation pathways of 2-selenouracil and 2-thiouracil, natural components of transfer rna. *Int. J. Mol. Sci.* 2020;21:1–18.

[11] Vašková J, Kočan L, Vaško L, Perjési P. Glutathione-Related Enzymes and Proteins: A Review. *Molecules* 2023;28:1447.

[12] Georgiou-Siafis SK, Tsiftsoglou AS. The Key Role of GSH in Keeping the Redox Balance in Mammalian Cells: Mechanisms and Significance of GSH in Detoxification via Formation of Conjugates. *Antioxidants* 2023;12:1953.

[13] Iwaoka M, Arai K. From Sulfur to Selenium. A New Research Arena in Chemical Biology and Biological Chemistry. *Curr. Chem. Biol.* 2013;7:2–24.

[14] Beld J, Woycechowsky KJ, Hilvert D. Selenoglutathione: Efficient oxidative protein folding by a diselenide. *Biochemistry* 2007;46:5382–5390.

[15] Kanamori A, Egawa N, Yamasaki S, Ikeda T, Rocha MJ da, Bortolatto CF, Savegnago L, Brüning CA, Iwaoka M. Antioxidative and Antiglycative Stress Activities of Selenoglutathione Diselenide. *Pharmaceuticals* 2024;17:1049.

[16] Frank W. Synthesen von selenhaltigen peptiden, II. Darstellung des Se-analogen oxydierten Glutathions (Se-Se-glutathion). *Hoppe. Seylers. Z. Physiol. Chem.* 1964;339:214–221.

[17] Theodoropoulos D, Schwartz IL, Walter R. Synthesis of Selenium-Containing Peptides. *Biochemistry* 1967;6:3927–3932.

[18] Tamura T, Oikawa T, Ohtaka A, Fujii N, Esaki N, Soda K. Synthesis and Characterization of the Selenium Analog of Glutathione Disulfide. *Anal. Biochem.* 1993;208:151–154.

[19] Yoshida S, Kumakura F, Komatsu I, Arai K, Onuma Y, Hojo H, Singh BG, Priyadarsini KI, Iwaoka M. Antioxidative Glutathione Peroxidase Activity of Selenoglutathione. *Angew. Chemie Int. Ed.* 2011;50:2125–2128.

[20] Shimodaira S, Asano Y, Arai K, Iwaoka M. Selenoglutathione Diselenide: Unique Redox Reactions in the GPx-Like Catalytic Cycle and Repairing of Disulfide Bonds in Scrambled Protein. *Biochemistry* 2017;56:5644–5653.

[21] Iwaoka M, Ooka R, Nakazato T, Yoshida S, Oishi S. Synthesis of Selenocysteine and Selenomethionine Derivatives from Sulfur-Containing Amino Acids. *Chem. Biodivers.* 2008;5:359–374.

[22] Shimodaira S, Iwaoka M. Improved synthetic routes to the selenocysteine derivatives useful for Boc-based peptide synthesis with benzylic protection on the selenium atom. *ARKIVOC* 2016;2017:260–271.

[23] Flögel O, Casi G, Hilvert D, Seebach D. Preparation of the β³-Homoselenocysteine Derivatives Fmoc-β³hSec(PMB)-OH and Boc-β³hSec(PMB)-OH for Solution and Solid-Phase-Peptide Synthesis and Selenoligation. *Helv. Chim. Acta* 2007;90:1651–1666.

[24] Yonezawa T, Yamaguchi M, Ninomiya M, Koketsu M. Application of bis-2-(trimethylsilyl)ethyl diselenide to the synthesis of selenium-containing amino acid derivatives. *Tetrahedron* 2017;73:6085–6091.

[25] Lapcinska S, Arsenyan P. Selenocysteinyl electrophiles efficiently promote the formation of coumarin and quinolinone cores by 6-endo-dig cyclization. *New J. Chem.* 2021;45:16625–16634.

[26] Cowie DB, Cohen GN. Biosynthesis by Escherichia coli of active altered proteins containing selenium instead of sulfur. *Biochim. Biophys. Acta* 1957;26:252–261.

[27] Shrift A, Virupaksha TK. Seleno-amino acids in selenium-accumulating plants. *Biochim. Biophys. Acta - Gen. Subj.* 1965;100:65–75.

[28] Van Dorst SH, Peterson PJ. Selenium speciation in the soil solution and its relevance to plant uptake. *J. Sci. Food Agric.* 1984;35:601–605.

[29] Dernovics M, Far J, Lobinski R. Identification of anionic selenium species in Se-rich yeast by electrospray QTOF MS/MS and hybrid linear ion trap/orbitrap MSn. *Metallomics* 2009;1:317–329.

[30] Far J, Preud'homme H, Lobinski R. Detection and identification of hydrophilic selenium compounds in selenium-rich yeast by size exclusion-microbore normal-phase HPLC with the on-line ICP-MS and electrospray Q-TOF-MS detection. *Anal. Chim. Acta* 2010;657:175–190.

[31] Rao Y, McCooeye M, Windust A, Bramanti E, D'Ulivo A, Mester Z. Mapping of selenium metabolic pathway in yeast by liquid chromatography-orbitrap mass spectrometry. *Anal. Chem.* 2010;82:8121–8130.

[32] Arnaudguilhem C, Bierla K, Ouerdane L, Preud'homme H, Yiannikouris A, Lobinski R. Selenium metabolomics in yeast using complementary reversed-phase/hydrophilic ion interaction (HILIC) liquid chromatography-electrospray hybrid quadrupole trap/Orbitrap mass spectrometry. *Anal. Chim. Acta* 2012;757:26–38.

[33] Ruszczyńska A, Konopka A, Kurek E, Torres Elguera JC, Bulska E. Investigation of biotransformation of selenium in plants using spectrometric methods. *Spectrochim. Acta - Part B Atomic Spectrosc.* 2017;130:7–16.

[34] Kieliszek M, Błazejak S. Speciation analysis of selenium in Candida utilis yeast cells using HPLC-ICP-MS and UHPLC-ESI-Orbitrap MS techniques. *Appl. Sci.* 2018;8:1–14.

[35] Gao F, Pang Y, Wang Y, Yang X, Song W, Nie X, Tan Z, Zhou J, Xin Y, Wng D, Shi H, Lai C, Zhang D. Nanocellulose/Selenoglutathione-Enhanced Antioxidant, Elastic, Antibacterial, and Conductive Hydrogels as Strain Sensors. *ACS Sustain. Chem. Eng.* 2024;12:13622–13633.

[36] Beld J, Woycechowsky KJ, Hilvert D. Catalysis of oxidative protein folding by small-molecule diselenides. *Biochemistry* 2008;47:6985–6987.

[37] Beld J, Woycechowsky KJ, Hilvert D. Diselenides as universal oxidative folding catalysts of diverse proteins. *J. Biotechnol.* 2010;150:481–489.

[38] Metanis N, Foletti C, Beld J, Hilvert D. Selenoglutathione-mediated rescue of kinetically trapped intermediates in oxidative protein folding. *Isr. J. Chem.* 2011;51:953–959.

[39] Arai K, Iwaoka M. Flexible folding: Disulfide-containing peptides and proteins choose the pathway depending on the environments. *Molecules* 2021;26:195.

[40] Chatrenet B, Chang JY. The disulfide folding pathway of hirudin elucidated by stop/go folding experiments. *J. Biol. Chem.* 1993;268:20988–20996.

[41] Wedemeyer WJ, Welker E, Narayan M, Scheraga HA. Disulfide bonds and protein folding. *Biochemistry* 2000;39:4207–4216.

[42] Okumura M, Saiki M, Yamaguchi H, Hidaka Y. Acceleration of disulfide-coupled protein folding using glutathione derivatives. *FEBS J.* 2011;278:1137–1144.

[43] Potempa M, Hafner M, Frech C. Mechanism of gemini disulfide detergent mediated oxidative refolding of lysozyme in a new artificial chaperone system. *Protein J.* 2010;29:457–465.

[44] Arai K, Dedachi K, Iwaoka M. Rapid and quantitative disulfide bond formation for a polypeptide chain using a cyclic selenoxide reagent in an aqueous medium. *Chem. - A Eur. J.* 2011;17:481–485.

[45] Arai K, Noguchi M, Singh BG, Priyadarsini KI, Fujio K, Kubo Y, Tokayama K, Ando S, Iwaoka M. A water-soluble selenoxide reagent as a useful probe for the reactivity and folding of polythiol peptides. *FEBS Open Bio* 2013;3:55–64.

[46] Reddy PS, Metanis N. Small molecule diselenide additives for in vitro oxidative protein folding. *Chem. Commun.* 2016;52:3336–3339.

[47] Arai K, Ueno H, Asano Y, Chakrabarty G, Shimodaira S, Mugesh G, Iwaoka M. Protein Folding in the Presence of Water-Soluble Cyclic Diselenides with Novel Oxidoreductase and Isomerase Activities. *ChemBioChem* 2018;19:207–211.

[48] Arai K, Mikami R. Redox Chemistry of Selenols and Diselenides as Potential Manipulators for Structural Maturation of Peptides and Proteins. *Metallomics Res.* 2022;2:rev-1–rev-17.

[49] Beld J, Woycechowsky KJ, Hilvert D. Small-molecule diselenides catalyze oxidative protein folding in vivo. *ACS Chem. Biol.* 2010;5:177–182.

[50] Steinmann D, Nauser T, Beld J, Tanner M, Günther D, Bounds PL, Koppenol WH. Kinetics of tyrosyl radical reduction by selenocysteine. *Biochemistry* 2008;47:9602–9607.

[51] Gebicki JM, Nauser T, Domazou A, Steinmann D, Bounds PL, Koppenol WH. Reduction of protein radicals by GSH and ascorbate: Potential biological significance. *Amino Acids* 2010;39:1131–1137.

[52] Allocati N, Masulli M, Di Ilio C, Federici L. Glutathione transferases: substrates, inihibitors and pro-drugs in cancer and neurodegenerative diseases. *Oncogenesis* 2018;7:1–15.

[53] Khan MAK, Wang F. Chemical demethylation of methylmercury by selenoamino acids. *Chem. Res. Toxicol.* 2010;23:1202–1206.

[54] Pei J, Pan X, Wei G, Hua Y. Research progress of glutathione peroxidase family (GPX) in redoxidation. *Front. Pharmacol.* 2023;14:1147414.

[55] Singh BG, Bag PP, Kumakura F, Iwaoka M, Priyadarsini KI. Role of Substrate Reactivity in the Glutathione Peroxidase (GPx) Activity of Selenocystine. *Bull. Chem. Soc. Jpn.* 2010;83:703–708.

[56] Maiorino M, Aumann KD, Brigelius-Flohe R, Ursini F, van den Heuvel J, McCarthy J, Roveri A, Ursini F, Flohé L. Probing the Presumed Catalytic Triad of Selenium-Containing Peroxidases by Mutational Analysis of Phospholipid Hydroperoxide Glutathione Peroxidase (PHGPx). *Biol. Chem. Hoppe. Seyler*. 1995;376:651–660.

[57] Tosatto SCE, Bosello V, Fogolari F, Mauri P, Roveri A, Toppo S, Flohé L, Ursini F, Maiorino M. The catalytic site of glutathione peroxidases. *Antioxidants Redox Signal.* 2008;10:1515–1525.

[58] Iwaoka M, Tomoda S. A Model Study on the Effect of an Amino Group on the Antioxidant Activity of Glutathione Peroxidase. *J. Am. Chem. Soc.* 1994;116:2557–25561.

[59] Sarma BK, Mugesh G. Glutathione peroxidase (GPx)-like antioxidant activity of the organoselenium drug ebselen: Unexpected complications with thiol exchange reactions. *J. Am. Chem. Soc.* 2005;127:11477–11485.

[60] Orian L, Mauri P, Roveri A, Toppo S, Benazzi L, Bosello-Travain V, Palma AD, Maiorino M, Miotto G, Zaccarin M, Polimeno A, Flohé L, Ursini F. Selenocysteine oxidation in glutathione peroxidase catalysis: an MS-supported quantum mechanics study. *Free Radic. Biol. Med.* 2015;87:1–14.

[61] Masuda R, Kimura R, Karasaki T, Sase S, Goto K. Modeling the Catalytic Cycle of Glutathione Peroxidase by Nuclear Magnetic Resonance Spectroscopic Analysis of Selenocysteine Selenenic Acids. *J. Am. Chem. Soc.* 2021;143:6345–6350.

[62] Iwaoka M, Oba H, Matsumura K, Yamanaka S, Shimodaira S, Kusano S, Asami T. Antioxidant Activity of a Selenopeptide Modelling the Thioredoxin Reductase Active Site is Enhanced by NH···Se Hydrogen Bond in the Mixed Selenosulfide Intermediate. *Curr. Chem. Biol.* 2022;16:44–53.

[63] Watanabe N, Forman HJ. Autoxidation of extracellular hydroquinones is a causative event for the cytotoxicity of menadione and DMNQ in A549-S cells. *Arch. Biochem. Biophys.* 2003;411:145–157.

[64] Carroll L, Gardiner K, Ignasiak M, Holmehave J, Shimodaira S, Breitenbach T, Iwaoka M, Ogilby PR, Pattison DI, Davies MJ. Interaction kinetics of selenium-containing compounds with oxidants. *Free Radic. Biol. Med.* 2020;155:58–68.

[65] Thornalley PJ. Glyoxalase I – structure, function and a critical role in the enzymatic defence against glycation. *Biochem. Soc. Trans.* 2003;31:1343–1348.

[66] Distler MG, Palmer AA. Role of glyoxalase 1 (Glo1) and methylglyoxal (MG) in behavior: Recent advances and mechanistic insights. *Front. Genet.* 2012;3:250.

[67] Ogasawara Y, Tanaka R, Koike S, Horiuchi Y, Miyashita M, Arai M. Determination of methylglyoxal in human blood plasma using fluorescence high performance liquid chromatography after derivatization with 1,2-diamino-4,5-methylenedioxybenzene. *J. Chromatogr. B* 2016;1029–1030:102–105.

[68] Richard MJ, Guiraud P, Didier C, Seve M, Flores SC, Favier A. Human Immunodeficiency Virus Type 1 Tat Protein Impairs Selenoglutathione Peroxidase Expression and Activity by a Mechanism Independent of Cellular Selenium Uptake: Consequences on Cellular Resistance to UV-A Radiation. *Arch. Biochem. Biophys*. 2001;386:213–220.

Chemical synthesis and diselenide metathesis in selenocysteine-containing peptides

Ying He, Hironobu Hojo*

Institute for Protein Research, Osaka University

Abstract

Selenoproteins, the functional form of the essential trace element selenium, play a vital role in maintaining redox homeostasis in humans. Selenocysteine (Sec), which constitutes the active center of many selenoproteins, is introduced to the polypeptide chain by a unique biosynthetic insertion mechanism, making the expression of selenoproteins through biological means challenging. Compared to its analogue cysteine (Cys), Sec exhibits a lower redox potential, facilitating the oxidation of selenol groups to form diselenide bonds. These diselenide bonds are more resistant to reduction than disulfide bonds, providing an enhanced stability to peptides under reducing conditions. On the other hand, due to the larger atomic radius of selenium, the dissociation energy of the diselenide bond is lower than that of the disulfide bond, rendering them more prone to diselenide metathesis. This mini-review summarizes the use of Sec for the chemical synthesis of proteins, Sec-containing peptides and the selenoproteins. The diselenide metathesis reaction of Sec-containing peptides is also reviewed.

Statements about COI: The authors declare no conflict of interest associated with this manuscript.

1. Introduction

1.1 Selenium and selenoproteins

Selenoproteins are the primary form of selenium, an essential trace element, that functions in our body. The selenium atom in selenoproteins exists as Sec, the 21st genetically encoded amino acid, which usually constitutes the active center of selenoproteins and has garnered significant attention in biochemistry and biology.

The Swedish chemist Jöns Jacob Berzelius first discovered selenium while re-examining a red sediment found in a sulfuric acid plant in 1818 [1]. Initially, selenium was considered as a toxic element, largely due to reports by Kurt Franke and others linking it to a series of livestock diseases [2]. However, in 1973, Rotruck made a pivotal discovery by identifying selenium as a crucial component of erythrocyte glutathione peroxidase (RBC-GPx) [3]. Subsequently, in 1976, Stadtman's group demonstrated the presence of selenium, in the form of Sec, as the active center of clostridial glycine reductase selenoprotein in *Clostridium sticklandii* [4]. In 1978, Tappel's group further identified Sec as an essential component of the catalytic

*Correspondence

Hironobu Hojo

Institute for Protein Research, Osaka University,

Osaka 565-0871, Japan.

Tel ; +81-6-6879-8601

E-mail ; hojo@protein.osaka-u.ac.jp

site of glutathione peroxidase (GPx) in rat liver [5]. These findings demonstrated the biological significance of selenium. With the advancement of molecular biology, 25 selenoproteins have been identified in humans [6], in which Sec constitutes the active center, playing a critical role in maintaining redox homeostasis. These proteins are related to human diseases such as diabetes, cancer and immune diseases [7].

1.2 The comparison of selenocysteine and cysteine

Sec is an analogue of Cys, in which the sulfur atom is replaced by selenium (**Fig. 1**). Both selenium and sulfur belong to the chalcogen family and share similar chemical properties. However, compared to sulfur, selenium has a higher polarizability due to its larger atomic radius, which makes it more nucleophilic.

	Cysteine (Cys)	Selenocysteine (Sec)
pK_a	8.3	5.2
E_0	−180 mV	−381 mV
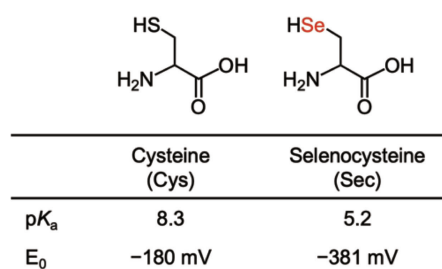
Fig. 1. | Structure, pK_a, and redox potential of Cys and Sec.

On the other hand, compared to Cys, Sec has a lower pK_a (pK_a of Sec selenol = 5.2, pK_a of Cys thiol = 8.3), which means that the selenol group in Sec more readily liberates a proton to form selenolate, whereas the thiol group in Cys remains as the protonated thiol form at physiological pH [8]. As a result, under physiological conditions, Sec exhibits a higher nucleophilicity. In addition, the diselenide bond ($E_0 = -381$ mV) in Sec has a lower reduction potential than the disulfide bond ($E_0 = -180$ mV) in Cys, meaning Sec is more easily oxidized to form diselenide dimers, which are less prone to be reduced compared to disulfides [9].

Given these chemical properties, Sec has broad applications in biochemistry. Its higher nucleophilicity can enhance reaction rates and improve enzyme catalytic activity. The lower redox potential of the diselenide bond realizes the preferential formation of the diselenide bond to the disulfide bond, which makes it useful in studying the oxidative protein folding pathway of the disulfide-rich peptide by substituting a part of the disulfide to diselenide bond. The difference in the pK_a between selenol and thiol also provides a detection method for Sec. For example, as shown in **Fig. 2**, BESThio (3'-(2,4-dinitrobenzenesulfonyl)-2',7'-dimethylfluorescein) is a fluorescent probe for selenols, which only reacts with Sec at pH 5.8, while keeping thiols intact [10].
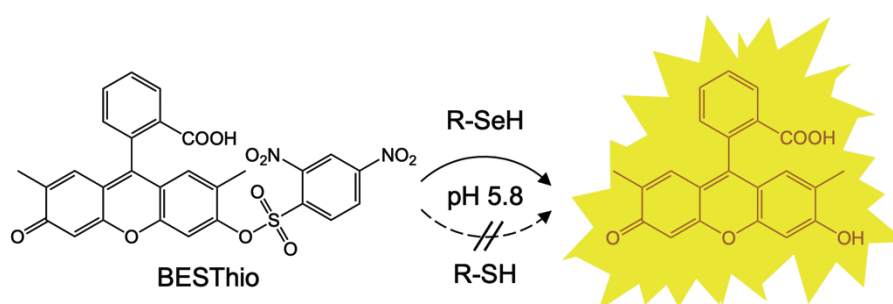
Fig. 2. | Detection of Sec based on the different pK_a of Sec and Cys.

1.3 Biosynthesis of selenoproteins

Sec is a genetically-encoded amino acid. As the stop codon, UGA is used for its incorporation in the growing polypeptide chain, a noncanonical insertion mechanism has been developed to direct the selenoprotein synthesis. The Sec insertion sequence (SECIS) element guides the translation of the stop codon UGA into Sec [11]. In prokaryotes, the SECIS element is located downstream of the UGA codon encoding Sec, whereas in eukaryotes, the SECIS element resides in the 3′ untranslated region (3′UTR) of the mRNA.

As shown in **Fig. 3**, the first step in Sec biosynthesis involves the aminoacylation of tRNA^{Sec} with serine (Ser), catalyzed by seryl-tRNA synthetase (SerRS), to form Ser-tRNA^{Sec}. In prokaryotes, Ser in Ser-tRNA^{Sec} is converted to Sec by selenocysteine synthase (SelA). The structure of SelA contains pyridoxal 5'-phosphate (PLP). PLP forms a Schiff base with the amino group of Ser-tRNA, leading to the 2,3-elimination of H_2O, resulting in the formation of an aminoacrylyl-tRNA intermediate. This intermediate then reacts with a selenium donor (selenophosphate), yielding Sec, which is subsequently released from SelA [12]. In eukaryotes, after the formation of Ser-tRNA^{Sec}, *O*-phosphoseryl-tRNA^{Sec} kinase (PSTK) phosphorylates Ser-tRNA^{Sec} to generate *O*-phosphoseryl-tRNA^{Sec} (Sep-tRNA^{Sec}). Subsequently, Sec-tRNA^{Sec} is formed from Sep-tRNA^{Sec} through selenocysteinyl-tRNA synthase (SepSecS) [13].

In prokaryotes, the insertion of Sec requires the Sec-specific elongation factor SelB, which recognizes the SECIS element and facilitates the incorporation of Sec into the polypeptide chain [14]. The insertion of Sec in eukaryotes involves the SECIS binding protein 2 (SBP2) and Sec-specific elongation factor (eEFSec) to recognize the SECIS element and to recruit Sec-tRNA^{Sec} to the ribosome [15]. However, other components involved in this process, as well as their specific roles, remain poorly understood.

Since the biosynthesis of the selenoprotein is regulated by both cis-acting elements and trans-acting factors, the recombinant expression of selenoproteins is highly complex and challenging.
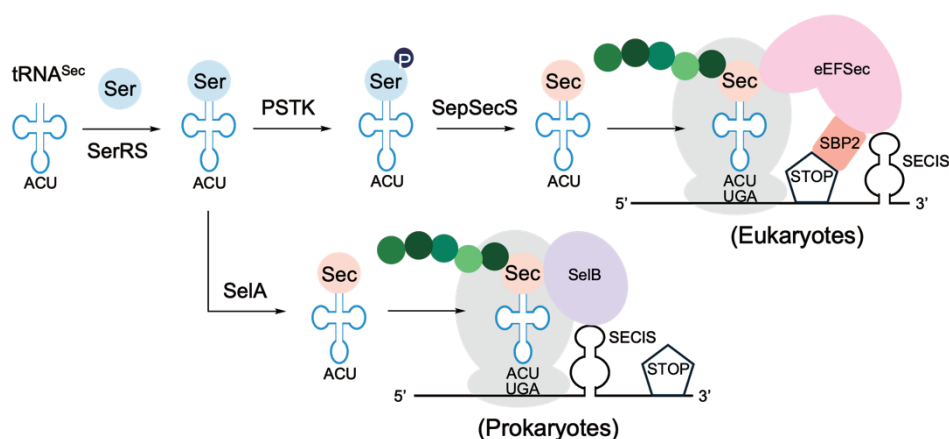
Fig. 3. | **Biosynthesis of Sec in prokaryotes and in eukaryotes.**

1.4 Glutathione Peroxidases (GPxs)

Glutathione peroxidases (GPxs) are a well-characterized family of antioxidant enzymes in the human body that play a critical role in maintaining the cellular redox balance by reducing reactive oxygen species (ROS), by-products of cellular oxidative respiration. GPxs reduce hydrogen peroxide (H_2O_2) to water and organic hydroperoxides (ROOH) to alcohol (ROH), thereby preventing oxidative damage of biomolecules like DNA, proteins and lipids. In humans, there are eight types of GPx, five of which (GPx-1, GPx-2, GPx-3, GPx-4, and GPx-6) contain Sec at their active centers, while the other three (GPx-5, GPx-7, GPx-8) use Cys as their active site residue [16]. The active center of GPx consists of four amino acids: Gln, Asn, Trp, and either Sec or Cys [17]. Studies have shown that mutating Sec to Cys in murine GPx results in a 1000-fold decrease in enzymatic activity [18].

GPx-1 is one of the most abundantly expressed selenoproteins in humans. It presents in all cells and is known

as cytosolic GPx or classic GPx [16, 19]. As shown in **Fig. 4**, the catalytic mechanism of GPx-1 is as follows: upon interaction with peroxides, the selenol group in the active center of GPx-1 is oxidized to the selenenic acid (GPx-SeOH) intermediate, while the peroxide is reduced. GPx-SeOH then reacts with one reduced glutathione (GSH) molecule to form the selenosulfide intermediate (GPx-SeSG). A second molecule of GSH subsequently reduces GPx-SeSG back to the original selenol group (GPx-SeH) restoring its activity, and generates one molecule of oxidized glutathione (GSSG) at the same time [20]. GPx-1 is closely linked to human health and is associated with several cancers, including breast, lung, and prostate cancers, as well as diabetes and cardiovascular diseases [19].
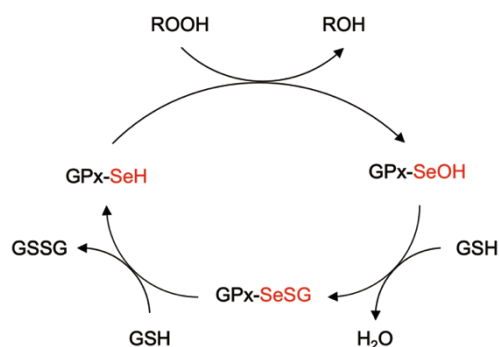
Fig. 4. | **Catalytic cycle of GPx.**

In conclusion, although selenium is the only trace element whose incorporation as Sec is genetically regulated and is closely linked to human health, the functions of all the selenoproteins have not yet been fully elucidated. However, the biosynthesis of selenoproteins is complicated due to the unique mechanism of Sec incorporation regulated by both the cis- and trans-acting factors.

In this mini-review, we focus on the chemical synthesis of selenopeptides (Sec-peptides) and selenoproteins by solid-phase peptide synthesis (SPPS), Sec-mediated native chemical ligation (NCL), and the recently discovered but still enigmatic diselenide metathesis found in diselenide bond-containing peptides.

2. Chemical synthesis of Sec-containing peptides

2.1 Solid-phase peptide synthesis (SPPS)

Solid-phase peptide synthesis, which is routinely used for the synthesis of peptides, was invented by Merrifield in 1963 [21]. The significant contribution of this method to this field also earned him the Nobel Prize in Chemistry in 1984. The main concept of the method is to couple the N-protected amino acid to a solid support, followed by deprotection of the amino group and subsequent amide bond formation with the next N-protected amino acid, allowing stepwise peptide elongation. Compared to solution-phase synthesis, SPPS is simpler to operate, because the synthesis can be simply realized by the addition of an activated amino acid and removal of the deprotection reagent. However, a major limitation is that the polypeptides exceeding 50 amino acids are usually obtained with a significantly lower purity and yield by this method.

In SPPS, the N-terminal protection of amino acids is typically achieved using either the 9-fluorenylmethoxycarbonyl (Fmoc) or *tert*-butoxycarbonyl (Boc) group, which are removed under basic or acidic conditions, respectively. Due to the high reactivity, protection of the -SeH group of Sec is required during the chain elongation. The most common and commercially-available protecting group is the 4-methoxyphenylmethyl (PMB) group. PMB deprotection is achieved under various conditions, such as HF, Lewis acids, or oxidative methods like iodine or dimethyl sulfoxide (DMSO) in TFA [22]. Inspired by the work of Tung about sulfur-based linkages on resin [23], Hondal developed a milder deprotection method using 2,2′-dithiobis(5-nitropyridine) (DTNP), an electrophilic disulfide, in TFA [24]. The method was further improved into the two-step procedure combining the ascorbolysis [25].

Another recently developed commercially-available Fmoc building block has the xanthenyl (Xan) protecting

group [26], which can be removed using the TFA cocktail (TFA/TIS/H$_2$O). Flemer successfully used Fmoc-Sec(Xan)-OH to synthesize the Sec-substituted analogue of the Stromelysin 1 matrix metalloproteinase inhibitor (MMP3-I) and the Sec-containing glutaredoxin analogue fragment, Lys[16]-Grx(10–17) designed by Moroder [27], observing minor by-products containing such as dehydroalanine (dHA) and selenenic acid derivative [26].

2.2 Sec-substituted peptide analogue

Due to the chemical similarity between selenium and sulfur, as well as the lower redox potential of Sec compared to Cys, the diselenide bond is more stable than the disulfide bond in the presence of reducing agents. The approach of replacing Cys with Sec in peptides was first used by Moroder to study the oxidative folding of the reduced Sec-analogue of human endothelin-1 (ET-1) which contains two disulfide bridges [28]. By replacing Cys[3] and Cys[11] with Sec, Moroder and colleagues synthesized [Sec[3], Sec[11], Nle[7]]-ET-1. Air oxidation achieved the target peptide with the diselenide bond between Sec[3] and Sec[11] and the disulfide bond between Cys[1] and Cys[15]. No mixed Se-S bond isomer by the thiol/diselenide exchange reaction was observed. The results also confirmed that the Sec-analogue retained the same structure and receptor-binding properties as the native ET-1. The results showed that by replacing one of the Cys pairs in the Cys-rich peptides by Sec residues, the oxidative folding can be steered so that the diselenide bond is preferentially formed. This method has been successfully used for analysis of the folding pathway and accelerating folding reaction [29, 30]. Similar Sec-analogues have also been investigated, such as the bee venom apamin, a peptide highly resistant to isomer formation due to its stable disulfide bonds [31, 32], conotoxins, neurotoxic peptides from marine cone snail venom [33-37], interleukin-8 [38], and the *Ecballium elaterium* trypsin inhibitor II (EETI-II) [39].

Notably, Prof. Iwaoka, Inaba and our group also replaced the A-chain Cys[7] and B-chain Cys[7] residues in bovine pancreatic insulin (BPIns) to synthesize the [C7U[A], C7U[B]]-BPIns, and through biological assays, we found that this analogue exhibited an increased resistance to degradation by the insulin-degrading enzyme (IDE) and had an extended half-life [40]. This enhanced activity was attributed to the higher propensity of oligomer formation of the diselenide-substituted BPIns compared to BPIns, due to the stronger interaction between the diselenide bonds than the disulfide bonds [41]. Similarly, Metanis' group designed a Sec-analogue of human insulin by replacing Cys[6] and Cys[11] in the A-chain with Sec while retaining the two interchain disulfide bonds, demonstrating that [C6U[A], C11U[A]]-insulin also retained biological activity with an enhanced thermodynamic stability and increased resistance to reduction and enzymatic digestion [42]. The similar internal diselenide bond replacement applied to the insulin prescription drug, glargine, also enhanced its thermodynamic stability [43].

In 2022, our laboratory replaced all six Cys in the human epidermal growth factor (EGF) with Sec, successfully synthesizing Se-EGF with a comparable biological activity, structure and enhanced stability under reducing conditions in the presence of reduced glutathione [44]. Despite the presence of three diselenide bonds, the folding of Se-EGF was efficient and obtained isomorphous products.

These studies highlight the possibility and potential of Sec-substitution to achieve directional folding and increased stability of Cys-rich peptides in therapeutic use.

3. Synthesis of Sec-containing proteins by the ligation method
3.1 Native chemical ligation (NCL) and thioester method

The SPPS is a well-established and widely used method for chemical peptide synthesis. However, it is not suitable for the synthesis of peptides containing more than 50 amino acid residues due to several challenges that arise as the peptide chain lengthens. These challenges include peptide aggregation and accumulation of missing amino acid by-products, all of which lead to a reduced purity and yield. To overcome the limitation of SPPS, various chemical ligation methods have been developed to synthesize longer polypeptides by assembling shorter peptide segments.

The most commonly used method is the native chemical ligation (NCL, **Fig. 5. (A)**) method, developed by Kent and colleagues in 1994 [45]. NCL is an efficient and chemoselective ligation method performed in an aqueous environment at neutral pH without protection of the side-chain functional groups. NCL enables the ligation of

the peptide segments with a C-terminal thioester and an N-terminal Cys. The thiol group of the N-terminal Cys attacks the carbonyl carbon of the C-terminal thioester of the other segment, forming a thioester bond, which then undergoes an intramolecular *S-N* acyl shift to form the native amide bond. They successfully synthesized human interleukin-8 (IL-8), a 72-residue protein by NCL (**Fig. 6**). The basics of this reaction was already developed by Wieland and coworkers in 1953 [46] by achieving ligation between the valine thioester and Cys.

NCL represents a milestone in protein chemical synthesis. However, its application is limited by the low abundance of Cys in proteins (1.9%). To expand the applicability of this method, Dawson introduced a metal-based desulfurization reaction in 2001 [47].
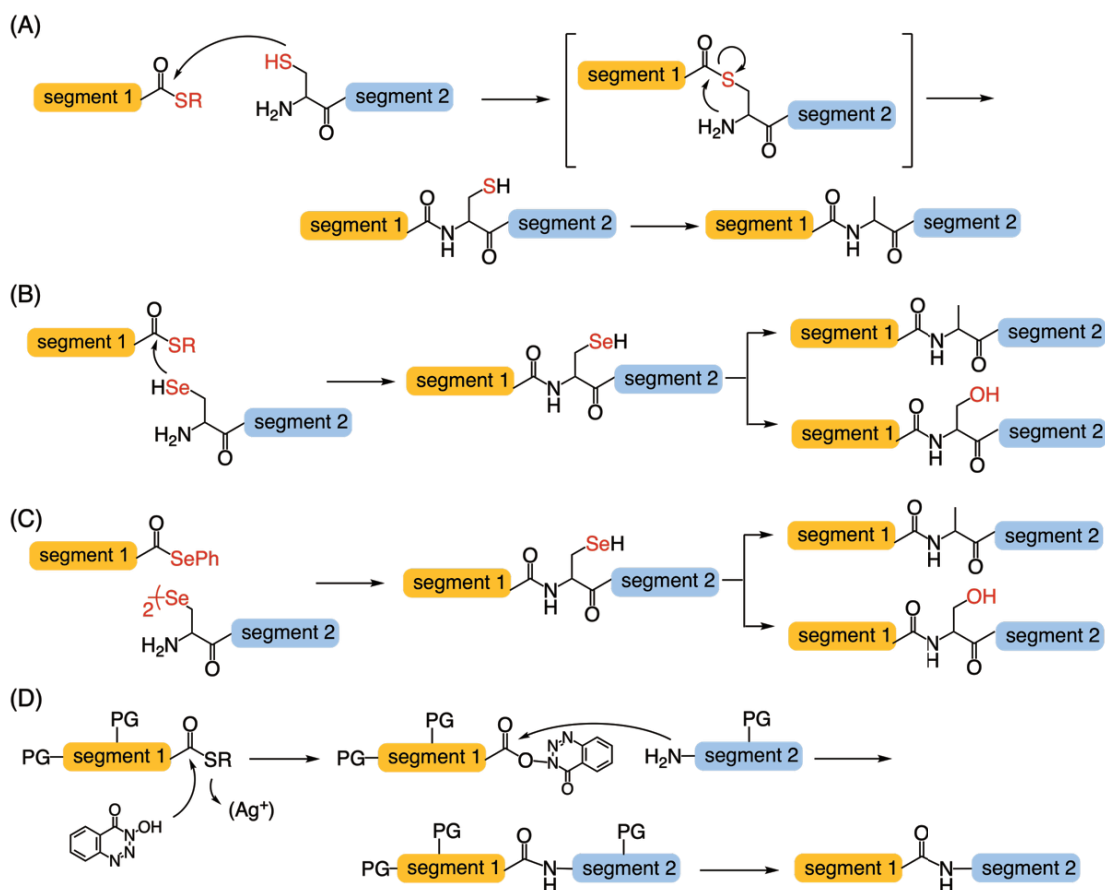

Fig. 5. (A) Native chemical ligation (NCL) and desulfurization of Cys. (B) Sec-mediated NCL and deselenization of Sec. (C) Diselenide-selenoester ligation (DSL) and deselenization of Sec. (D) Thioester method and deprotection of amino and thiol protecting groups (PG).
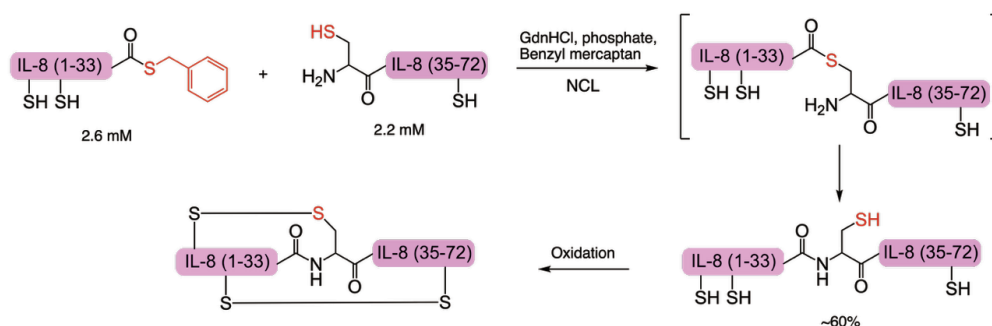

Fig. 6. Synthesis of [A33]IL-8 by the NCL.

This approach realizes the ligation at the abundant (7.8%) alanine (Ala) site by ligation at the Cys site, followed by the Raney nickel or Pd/Al$_2$O$_3$ mediated desulfurization reaction to convert Cys to Ala. In 2007, Danishefsky, inspired by Hoffmann's report on the desulfurization reaction between mercaptans and trialkylphosphine in 1956 [48], introduced a mild, radical-mediated desulfurization reaction [49]. The desulfurization conditions involved the use of a water-soluble radical initiator, 2,2′-azobis[2-(2-imidazolin-2-yl)propane] dihydrochloride (VA-044), a thiol to provide a hydrogen atom, and TCEP for the phosphoranyl radical. These mild conditions are compatible with the synthesis of various peptides and glycopeptides. Subsequent studies combined desulfurization with the design of thiolated amino acids to expand the NCL-desulfurization chemistry's scope [50-57]. However, the lack of selectivity in desulfurization has limited its use in biologically-expressed proteins.

Before the development of NCL, our laboratory developed the thioester method shown in **Fig. 5. (D)** for chemical protein synthesis in 1991 [58] inspired by Blake's work about the Ag$^+$-activated condensation of a peptide bearing a thiocarboxy group at its C-terminus with another peptide segment [59]. In the thioester method, the C-terminal thioester group is activated by a silver ion, converting the segment into the corresponding active ester, which is then attacked by the amino group of the N-terminal segment, forming an amide bond. To realize the chemoselective reaction, the side chain amino and thiol groups requires protection. Instead, in principle, there is no limitation in the selection of the ligation site. We also discovered that aryl thioesters can undergo aminolysis without Ag$^+$ activation [60]. By exploiting the difference in the reactivity of the aryl and alkyl thioesters, it is possible to assemble three peptide fragments in a one-pot reaction [61-65]. Additionally, our laboratory utilized selenoester chemistry to develop a one-pot four-segment coupling strategy by the thioester method, which was successfully applied to the synthesis of superoxide dismutase (SOD) [66].

In 2020, we successfully synthesized Se-ferredoxin (Se-Fd), in which the four Cys residues coordinating the [2Fe-2S] cluster were replaced with Sec using a one-pot three-segment coupling by the thioester method as shown in **Fig. 7** [67]. The 97-residue ferredoxin (Fd) was divided into three peptide segments. These included the side chain amino and selenol group protected Fd (1–33) with a C-terminal aryl thioester, Fd (34–73) with a C-terminal alkyl thioester, and Fd (74–97). To prepare the thioesters, we introduced *N*-alkylcysteine at the C-terminus of the peptide chains. This allowed for an intramolecular *N*-to-*S* acyl shift, followed by an intermolecular thioester exchange reaction to obtain the Fd (1–33) and Fd (34–73) thioesters. This approach, developed by our laboratory, has proven effective for generating peptide thioester by the Fmoc method [68]. The first ligation step, achieved using a Ag$^+$-free thioester method, involved coupling of the Fd (1–33) aryl thioester with the Fd (34–73) alkyl thioester to produce Fd (1–73) alkyl thioester. Subsequently, Fd (74–97) was added together with Ag$^+$ to promote the second ligation via a Ag$^+$-activated thioester method, producing the full-length Fd (1–97) in one-pot. After
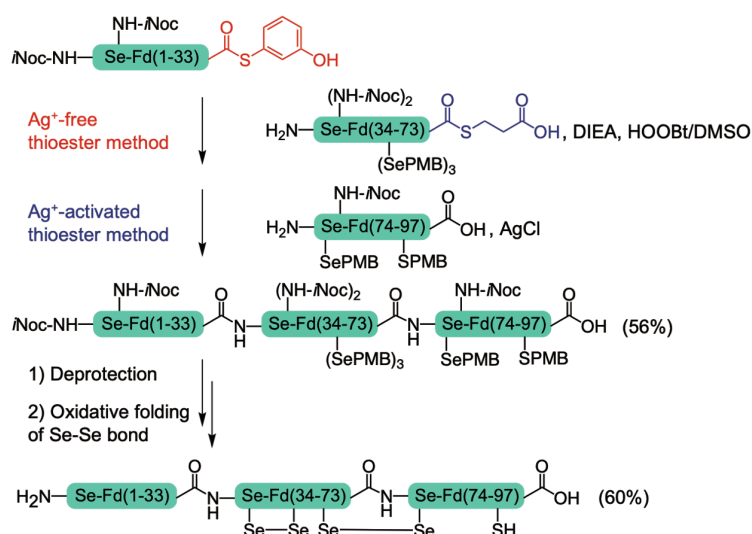

Fig. 7. | **One-pot ligation of Se-ferredoxin (Se-Fd) by thioester method.**

deprotection and [2Fe-2S] cluster incorporation, Se-Fd was successfully synthesized. Circular dichroism (CD) and biochemical assays indicated that Se-Fd retained a structure similar to the wild-type Fd, though its catalytic activity was slightly decreased. This decrease in activity is likely due to the lower redox potential of selenium, which may impact the efficiency of electron transfer in the Fe cluster.

3.2 Sec-mediated NCL

To overcome the inherent limitations of the NCL-desulfurization strategy, a method using the N-terminal Sec instead of Cys for site-specific ligation was developed (**Fig. 5. (B)**). The mechanism of the Sec-mediated NCL is similar to traditional NCL. The selenol group attacks the acyl carbon, forming a selenoester, followed by a *Se-N* acyl shift to form a native peptide bond. This approach was independently proposed by three different groups in 2001 [69-71].

Due to the higher nucleophilicity of selenol compared to thiol, Sec-mediated NCL proceeds faster than the conventional NCL. Because of Sec's lower pK_a, selenol is more readily deprotonated, allowing the reaction to occur at a lower pH, which helps to avoid potential side reactions such as thioester hydrolysis. Another advantage of Sec is its selective deselenization even in the presence of Cys. In 2005, Metanis and Payne reported methods to convert Sec to Ala or Ser via deselenization [72, 73]. Compared to desulfurization, the deselenization conditions are milder and do not require the use of radical initiators. In 2010, Dawson demonstrated the deselenization of a 10-residue peptide containing a Se-S bond using excess TCEP and DTT, achieving Sec-to-Ala conversion without affecting Cys [74]. They also applied this method to 38 residues of glutaredoxin 3 (Grx3(1-38)), where Cys[11] and Cys[14] were mutated to Sec, and Ala[38] was mutated to Cys. Sec[11] and Sec[14] were successfully converted to Ala with only minimal desulfurization observed at Cys[38] by their method [74].

Due to the lower redox potential of Sec, the segment with the N-terminal Sec often forms the diselenide dimer or Se-S bond with other compounds [75]. Therefore, the use of a reducing agent is essential in Sec-NCL. Thiol-based reducing agents are preferable in Sec-NCL since commonly used reducing agents like TCEP can cause deselenization [76].

In recent years, there have been several examples of proteins synthesized using Sec-NCL. The bovine pancreatic trypsin inhibitor (C38U-BPTI), whose Cys[38] was substituted with Sec, was synthesized, followed by oxidative folding of two disulfide bonds and one Se-S bond (**Fig. 8**). Cyclization of a peptide containing an N-terminal Sec and a C-terminal thioester can also be achieved by Sec-NCL [69, 77]. Additionally, Sec-NCL has been applied in semi-synthetic strategies, such as the synthesis of C110U-RNase A and C112U-azurin [70, 78].
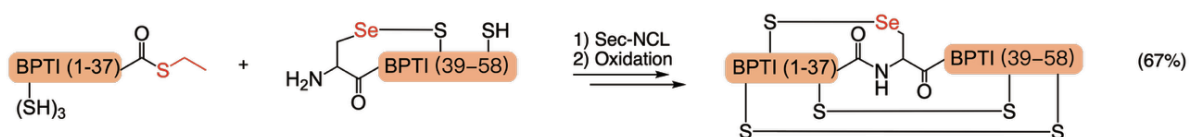
Fig. 8. | Synthesis of C38U-BPTI by the Sec-mediated NCL.

3.3 Diselenide-selenoester ligation (DSL) and reductive DSL (rDSL)

Due to the low redox potential of Sec, selenopeptides tend to exist as diselenide dimers. Therefore, as already described, a reducing agent is needed to reduce diselenide or Se-S bonds into reactive selenolates during the Sec-NCL process. The choice of the reducing agent is critical as it directly affects the rate and the yield of Sec-NCL. Overly strong reducing agents may induce deselenization, while weak reducing agents may not fully reduce the diselenide or Se-S bonds, leading to a decreased ligation efficiency.

To address this issue, Payne's group introduced a method called diselenide-selenoester ligation (DSL), shown in **Fig. 5 (C)**, in 2015, which does not require reducing agents [79]. This reaction occurs between a C-terminal aryl

selenoester and an N-terminal diselenide dimer. Compared to NCL, DSL proceeds extremely fast, completing in just a few minutes, and it resolves the challenge of the ligation at sterically-hindered sites. The proposed mechanism involves the release of phenylselenoate from the C-terminal aryl selenoester through hydrolysis, aminolysis or acyl substitution. This phenylselenoate then attacks the diselenide bond, generating selenolate, which forms a native peptide bond through a mechanism similar to NCL.

In 2020, the same group developed a refined approach, known as reductive DSL (rDSL), by employing TCEP as a reducing agent to generate selenolate and diphenyl diselenide (DPDS) as a radical scavenger to avoid deselenization while accelerating the formation of selenolate [80]. This method realized the ligation at a concentration as low as 50 nM. Additionally, after extracting DPDS by ether, they succeeded in a viable and efficient photodeselenization reaction in the presence of TCEP and GSH under light irradiation (254 nm) for 30 seconds.

The possibility of ligation at a low concentration by rDSL allows it to be used for synthesizing hydrophobic proteins without the need for hydrophilic tags, and subsequent one-pot photodeselenization further improved both the yield and efficiency of the synthesis. For example, the synthesis of various therapeutic tesamorelins, the palmitoylated variants of the transmembrane lipoprotein phospholemman (FXYD1, **Fig.9**), adiponectin (19-107), haemathrin 1, haemathrin 2, and peptide-oligonucleotide conjugates [80-82].
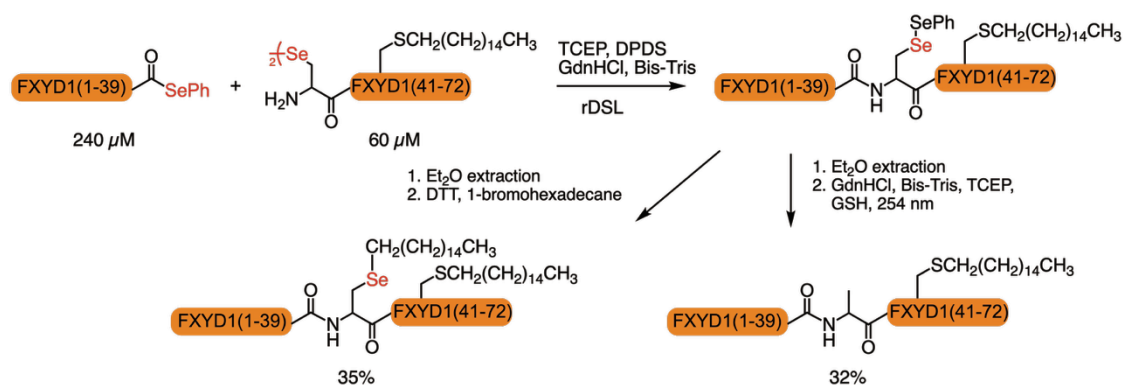
Fig. 9. │ **The synthesis of palmitoylated FXYD1 by one-pot rDSL-alkylation and rDSL-photodeselenization.**

3.4 Chemical synthesis of selenoproteins

The functions of many selenoproteins remain unclear, due to the complexity involved in their biosynthetic pathway as already described. However, the application of the aforementioned chemical synthetic methods has enabled the synthesis of several human selenoproteins.

In 2016, Metanis and colleagues successfully synthesized human selenoprotein M (SelM) and W (SelW) [83]. Mature human SelM (24-145) consists of 122 amino acids and is widely expressed in mammalian tissues, particularly in the brain, implying that it is closely associated with brain function [84]. SelM contains a CXXU redox motif which is similar to the CXXC active site in thioredoxins (Trx), conferring antioxidant properties [83, 85]. The protein was divided into four segments with ligation sites at Gly^{47}-Sec^{48}, Gly^{77}-Ala^{78}, and Asn^{106}-Ala^{107}. Ala^{78} and Ala^{107} were mutated to Sec to facilitate Sec-NCL, followed by deselenization to convert them to Ala. The introduction of the C-terminal thioester employed the Dawson linker [86, 87]. The four peptide segments were: SelM (24-47) with a C-terminal thioester, SelM (48-77) and SelM (78-106) with N-terminal selenazolidine (Sez) and C-terminal thioesters, and SelM (107-145). $Sez^{48,78}$ were used to protect the N-terminal Sec and prevent deselenization. Methionine (Met) was replaced with the norleucine (Nle) to prevent oxidation. The first Sec-NCL ligated SelM (78-106) and SelM (107-145), and subsequent $MeONH_2$ treatment converted Sez^{78} to Sec, forming SelM (78-145) with unprotected Sec^{78} and Sec^{107}. The second Sec-NCL ligated SelM (48-77) to SelM (78-145) followed by deselenization of Sec^{78} and Sec^{107} under anaerobic conditions using DTT and TCEP to form Ala^{78} and Ala^{107}, then

followed by the conversion of Sez[48] to Sec. During deselenization, partial Sez deprotection led to the observation of minor three deselenized products. The final Sec-NCL yielded full-length SelM with a Se-S bond. The folding of the final protein was confirmed by CD comparison with structurally similar Trx proteins.

Selenoprotein W (SelW), which contains 86 residues, is expressed in muscle, brain, and spleen tissues [88]. It also features a CXXU motif and is associated with intracellular redox processes, bone remodeling, and diseases such as non-alcoholic fatty liver disease (NAFLD), although its functions are not fully understood [89, 90]. SelW was divided into two segments with a ligation site between Ile[36] and Sec[37]. Met was similarly replaced with Nle. The C-terminal thioester of SelW (2-36) was prepared using the Dawson linker. The two segments SelW (2-36) and SelW (37-87) were successfully ligated via Sec-NCL, forming a SelW with a Se-S bond and a free Cys. The folding of the final protein was verified by CD analysis [83].

In 2017, Payne et al. synthesized a homodimeric Selenoprotein K (SelK) via one-pot DSL-deselenization [91]. SelK consists of 93 amino acids. SelK was divided into two segments: SelK (2-60) with a selenoester and SelK (61-94) with an N-terminal (β-Se)-Asp. Met was replaced with Nle. DSL gave the full-length SelK (2-94) forming a diselenide bond between Sec[61] and Sec[92] with part of the product retaining the extra SelK (2-60) linked to the side chain selenol group. Hydrazinolytic removal of the extra SelK (2-60), followed by selective deselenization of (β-Se)-Asp using TCEP gave the desired SelK dimer.

In 2022, He and colleagues achieved the semi-synthesis of selenoprotein F (SelF) (**Fig. 10**), [92]. Mature SelF consists of 134 amino acids, including one Sec and seven Cys, and its function remains unclear. SelF was synthesized in three segments, ligated by two NCL at Gly[41]-Cys[42] and Gln[74]-Ala[75]. To stabilize the peptide hydrazide precursor, Gln[74] was mutated to Ala, and Ala[75] was mutated to Cys to afford NCL. The three segments were SelF (1-41) with a C-terminal thioester, Cys- and Sec-protected SelF (42-74) with a C-terminal thioester, and SelF (75-134). SelF (75-134) was biologically expressed due to aspartimide formation. SelF (42-134) was synthesized by the first NCL followed by desulfurization under mild condition by reducing the amount of radical initiator VA044 and reaction
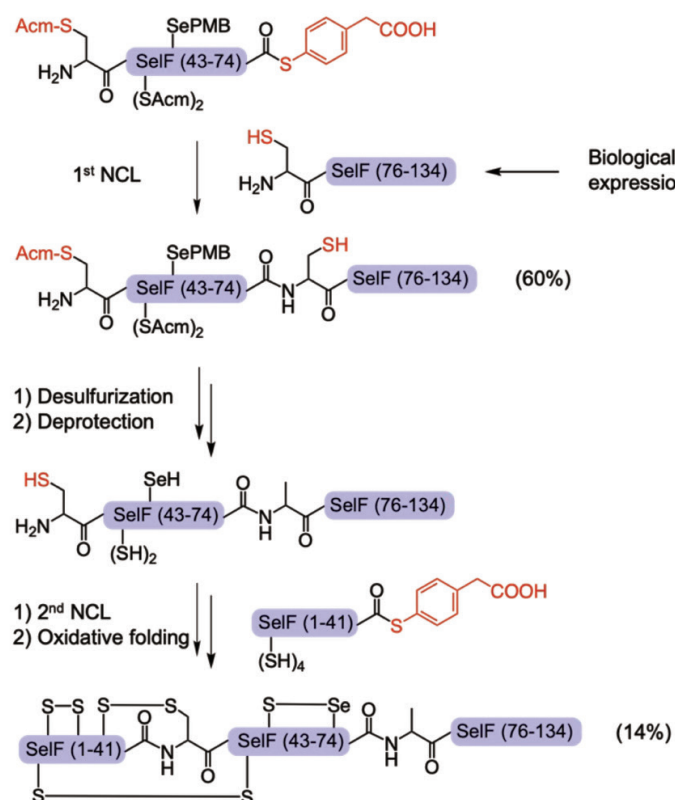

Fig. 10. | Semi-synthesis of selenoprotein F.

time. The deprotection of acetamidomethyl (Acm) and also PMB group was achieved by Pd^{2+} followed by DTT treatment. The reduction of diselenide dimer was then performed with TCEP and ascorbate. Finally, the second NCL yielded the full-length SelF (1-134). One Se-S bond and three disulfide bonds were formed by oxidative folding. Other selenoproteins, such as selenoprotein H and S, were also synthesized via semi-synthetic methods [93, 94].

4. Diselenide metathesis of Sec-containing peptides

Although the isomorphic substitution of disulfide bonds with diselenide bonds is commonly used to enhance protein stability under reducing conditions, the larger atomic radius of selenium leads to a lower bond dissociation energy for diselenide bonds compared to disulfide bonds (Se-Se bond: 172 kJ/mol, S-S bond: 240 kJ/mol), making diselenide bonds more prone to be broken under external influences [95]. Diselenide bonds function as dynamic covalent bonds (DCBs) and can undergo metathesis reactions under defined conditions, such as light irradiation or heat. This property has garnered significant attention in recent years for application in self-healing materials, fluorescent probes, organic synthesis, selective surface modification, and drug delivery systems [96-101].

In 2019, Stefanowicz discovered that the diselenide bond metathesis also occurs in short peptides containing Sec (**Fig. 11**). They dissolved two selenopeptide dimers in methanol and observed the formation of heterodimers after 30 minutes of light irradiation (400-700 nm wavelength) [102].
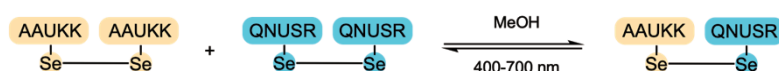
Fig. 11. | **Diselenide metathesis of model peptide in methanol by light irradiation.**

Following this, our group found that the metathesis reaction can even occur in neutral aqueous buffer solutions without reducing agents in the dark and exhibits a pH dependency. This suggests that diselenide bonds may be inherently unstable [103]. To find the conditions that can keep the diselenide bonds stable and to further investigate the reaction mechanism for broader applications, we studied the inter- and intramolecular metathesis reactions of three bioactive peptides (both the wild type and Sec-substituted analogues) under physiological conditions in the dark; i.e., oxytocin, α-conotoxin ImI, and apamin. Oxytocin has one intramolecular disulfide bond, while conotoxin and apamin have two intramolecular disulfide bonds. We found that Se-oxytocin was stable under a low-concentration (10 μM) in the dark. However, the intermolecular diselenide metathesis happened at higher concentrations, leading to polymerization. Se-α-conotoxin ImI showed similar results to Se-oxytocin. Additionally, it formed isomers via intramolecular diselenide metathesis, regardless of the concentration (**Fig. 12**). Interestingly, the ratio of the diselenide isomer to Se-conotoxin matched that observed during oxidative folding of Se-conotoxin. In contrast, Se-apamin exhibited no metathesis which might be due to the inherent stability of its tertiary structure, as the wild-type apamin explicitly forms the product with native disulfide bond pairing in the oxidative folding reaction [31].
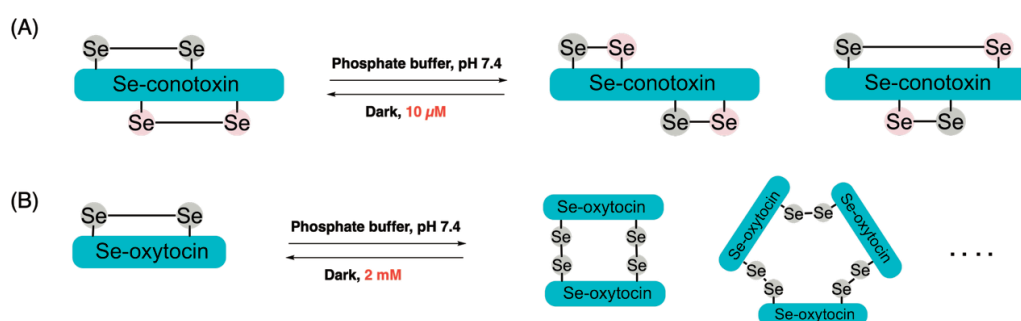
Fig. 12. | **Diselenide metathesis of Sec-peptides.**
(A) Intramolecular metathesis under diluted conditions, **(B)** Intermolecular metathesis under higher concentration.

This indicates that selenopeptides with stable tertiary structures are resistant to diselenide metathesis reactions. We observed a similar behavior when synthesizing the Sec-substituted epidermal growth factor (Se-EGF) [44].

The mechanism behind diselenide metathesis remains debated. In 2014, Xu proposed that the light-driven diselenide metathesis is facilitated by light-induced selenium radicals, a hypothesis supported by the inhibition of the reaction upon adding the radical scavenger (2,2,6,6-tetramethylpiperidin-1-yl)oxyl (TEMPO) [104]. However, the diselenide isomerization observed by us occurs under dark conditions, which excludes the proposed reaction mechanism by Xu in our case. We found that the production of diselenide isomers was accelerated under reducing conditions in the presence of GSH, suggesting that the selenol group generated by reducing agents can promote isomer formation. Therefore, our isomerization reaction is not selenol mediated. In 2022, Zhu suggested a mechanism of metathesis in the absence of light driven by the ease of polarization of the diselenide bond, which is accelerated in polar solvents [105]. This mechanism agrees with our group's observations.

5. Conclusion and outlook

Selenopeptides and selenoproteins remain an important topic of research in molecular biology, biochemistry, and medicinal chemistry. However, the unique biosynthetic insertion mechanism of Sec into proteins makes the biological expression of selenoproteins challenging. To address this, chemical synthesis methods for selenopeptide and selenoprotein have been developed, such as NCL, Sec-NCL, DSL, and rDSL. Moreover, deselenization reactions allow for selective conversion of Sec to Ala or Ser in the presence of the unprotected Cys, broadening the scope of NCL. Due to the higher nucleophilicity of the selenol group compared to the thiol group, these methods offer faster reaction rates and extend the reaction concentration down to 50 nM, making the synthesis of highly-hydrophobic proteins feasible. Selenoproteins can also be synthesized by the thioester method.

Sec also has a significant potential for various applications. With a lower redox potential than thiol, selenol can form diselenide bonds more rapidly in the presence of Cys and is more resistant to reduction than disulfide bonds, which can be exploited in protein folding studies. Additionally, given the similar chemical properties of Se and S, Sec-substituted peptide analogues generally retain a very similar biological activity with the native Cys peptides while being more stable under reducing conditions.

On the other hand, diselenide bonds, as dynamic covalent bonds, can undergo diselenide metathesis under certain conditions, making them suitable for applications in self-healing materials, drug delivery systems, and fluorescent probes. This diselenide metathesis reaction has also been observed in proteins, and although the exact mechanism remains unclear, it is believed to hold a significant potential for further applications.

References
[1]   Weeks ME. The discovery of the elements. VI. Tellurium and selenium. *J. Chem. Educ.* 1932; 9(3): 474-485.
[2]   Franke KW. A new toxicant occurring naturally in certain samples of plant foodstuffs I: Results obtained in preliminary feeding trials. *J. Nutr.* 1934; 8: 597–608.
[3]   Rotruck JT, Pope AL, Ganther HE, Swanson AB, Hafeman DG, Hoekstra W. Selenium: biochemical role as a component of glutathione peroxidase. *Science.* 1973; 179(4073): 588-590.
[4]   Cone JE, Del Rio RM, Davis JN, Stadtman TC. Chemical characterization of the selenoprotein component of clostridial glycine reductase: identification of selenocysteine as the organoselenium moiety. *Proc. Natl. Sci. U. S. A.* 1976; 73(8): 2659-2663.
[5]   Forstrom JW, Zakowski JJ, Tappel AL. Identification of the catalytic site of rat liver glutathione peroxidase as selenocysteine. *Biochemistry* 1978; 17(13): 2639-2644.
[6]   Kryukov GV, Castellano S, Novoselov SV, Lobanov AV, Zehtab O, Guigó R, Gladyshev VN. Characterization of mammalian selenoproteomes. *Science.* 2003; 300(5624): 1439-1443.
[7]   Rayman MP. Selenium and human health. *Lancet.* 2012; 379(9822): 1256–1268.
[8]   Poole LB. The basics of thiols and cysteines in redox biology and chemistry. *Free Radic. Biol. Med.* 2015; 80: 148–157.
[9]   Besse D, Siedler F, Diercks T, Kessler H, Moroder L. The redox potential of selenocystine in unconstrained cyclic peptides. *Angew. Chem. Int. Ed.* 1997; 36(8): 883–885.
[10] Maeda H, Katayama K, Matsuno H, Uno T. 3'-(2, 4-Dinitrobenzenesulfonyl)-2', 7'-dimethylfluorescein as a fluorescent probe for selenols. *Angew. Chem. Int. Ed.* 2006; 45(11): 1810-1813.
[11] Walczak R, Westhof E, Carbon P, Krol A. A novel RNA structural motif in the selenocysteine insertion element of eukaryotic selenoprotein mRNAs. *RNA.* 1996; 2(4): 367–379.

[12] Forchhammer K, Böck A. Selenocysteine synthase from *Escherichia coli*. Analysis of the reaction sequence. *J. Biol. Chem.* 1991; 266(10): 6324–6328.

[13] Xu XM, Carlson BA, Mix H, Zhang Y, Saira K, Glass RS, Berry MJ, Gladyshev VN, Hatfield DL. Biosynthesis of selenocysteine on its tRNA in eukaryotes. *PLoS Biol.* 2006; 5(1): e4. DOI: 10.1371/journal.pbio.0050004

[14] Baron C, Heider J, Böck A. Interaction of translation factor SELB with the formate dehydrogenase H selenopolypeptide mRNA. *Proc. Natl. Acad. Sci.* 1993; 90(9): 4181-4185.

[15] Cain A, Krahn N. Overcoming challenges with biochemical studies of selenocysteine and selenoproteins. *Int. J. Mol. Sci.* 2024; 25(18): 10101-10118.

[16] Stolwijk JM, Garje R, Sieren JC, Buettner GR, Zakharia Y. Understanding the redox biology of selenium in the search of targeted cancer therapies. *Antioxidants (Basel).* 2020; 9(5): 420-444.

[17] Tosatto SCE, Bosello V, Fogolari F, Mauri P, Roveri A, Toppo S, Flohé L, Ursini F, Maiorino M. The catalytic site of glutathione peroxidases. *Antioxid. Redox Signal.* 2008; 10(9): 1515-1526.

[18] Rocher C, Lalanne JL, Chaudiere J. Purification and properties of a recombinant sulfur analog of murine selenium-glutathione peroxidase. *Eur. J. Biochem.* 1992; 205(3): 955-960.

[19] Lubos E, Loscalzo J, Handy DE. Glutathione peroxidase-1 in health and disease: from molecular mechanisms to therapeutic opportunities. *Antioxid. Redox Signal.* 2011; 15(7): 1957-1997.

[20] Maia LB, Maiti BK, Moura I, Moura JJG. Selenium—more than just a fortuitous sulfur substitute in redox biology. *Molecules.* 2023; 29(1): 120-155.

[21] Merrifield RB. Solid phase peptide synthesis. I. The synthesis of a tetrapeptide. *J. Am. Chem. Soc.* 1963; 85(14): 2149-2154.

[22] Flemer SJr. Selenol protecting groups in organic chemistry: Special emphasis on selenocysteine Se-protection in solid phase peptide synthesis. *Molecules.* 2011; 16(4): 3232-3251.

[23] Galande AK, Weissleder R, Tung CH. An effective method of on-resin disulfide bond formation in peptides. *J. Comb. Chem.* 2005; 7(2): 174–177.

[24] Harris KM, Flemer SJr, Hondal RJ. Studies on deprotection of cysteine and selenocysteine side-chain protecting groups. *J. Pep. Sci.* 2007; 13(2): 81-93.

[25] Marie SEJ, Ruggles EL, Hondal RJ. Removal of the 5-nitro-2-pyridine-sulfenyl protecting group from selenocysteine and cysteine by ascorbolysis. *J. Pep. Sci.* 2016; 22(9): 571-576.

[26] Flemer SJr. Fmoc-Sec(Xan)-OH: synthesis and utility of Fmoc selenocysteine SPPS derivatives with acid-labile sidechain protection. *J. Pep. Sci.* 2015; 21(1): 53-59.

[27] Besse D, Moroder L. Synthesis of selenocysteine peptides and their oxidation to diselenide-bridged compounds. *J. Pep. Sci.* 1997; 3(6): 442-453.

[28] Pegoraro S, Fiori S, Rudolph BS, Watanabe TX, Moroder L. Isomorphous replacement of cystine with selenocystine in endothelin: Oxidative refolding, biological and conformational properties of [Sec^3, Sec^{11},Nle^7]-endothelin-1. *J. Mol. Biol.* 1998; 284(3): 779-792.

[29] Metanis N, Hilvert D. Strategic use of non-native diselenide bridges to steer oxidative protein folding. *Angew. Chem. Int. Ed.* 2012; 51(23): 5585-5588.

[30] Metanis N, Hilvert D. Harnessing selenocysteine reactivity for oxidative protein folding. *Chem. Sci.* 2015; 6(1): 322-325.

[31] Pegoraro S, Fiori S, Cramer J, Rudolph BS, Moroder L. The disulfide-coupled folding pathway of apamin as derived from diselenide-quenched analogs and intermediates. *Protein Sci.* 1999; 8(8): 1605–1613.

[32] Fiori S, Pegoraro S, Rudolph BS, Cramer J, Moroder L. Synthesis and conformational analysis of apamin analogues with natural and non-natural cystine/selenocystine connectivities. *Biopolymers.* 2000; 53(7): 550-564.

[33] Armishaw CJ, Daly NL, Nevin ST, Adams DJ, Craik DJ, Alewood PF. α-selenoconotoxins, a new class of potent α$_7$ neuronal nicotinic receptor antagonists. *J. Biol. Chem.* 2006; 281(20): 14136-14143.

[34] Walewska A, Zhang MM, Skalicky JJ, Yoshikami D, Olivera BM, Bulaj G. Integrated oxidative folding of cysteine/selenocysteine containing peptides: improving chemical synthesis of conotoxins. *Angew. Chem. Int. Ed.* 2009; 48(12): 2221–2224.

[35] Muttenthaler M, Nevin ST, Grishin AA, Ngo ST, Choy PT, Daly NL, Hu SH, Armishaw CJ, Wang CIA, Lewis RJ, Martin JL, Noakes PG, Craik DJ, Adams DJ, Alewood PF. Solving the α-conotoxin folding problem: efficient selenium-directed on-resin generation of more potent and stable nicotinic acetylcholine receptor antagonists. *J. Am. Chem. Soc.* 2010; 132(10): 3514–3522.

[36] Gowd KH, Yarotskyy V, Elmslie KS, Skalicky JJ, Olivera BM, Bulaj G. Site-specific effects of diselenide bridges on the oxidative folding of a cystine knot peptide, ω-selenoconotoxin GVIA. *Biochemistry.* 2010; 49(12): 2741–2752.

[37] de Araujo AD, Callaghan B, Nevin ST, Daly NL, Craik DJ, Moretta M, Hopping G, Christie MJ, Adams DJ, Alewood PF. Total synthesis of the analgesic conotoxin MrVIB through selenocysteine-assisted folding. *Angew. Chem. Int. Ed.* 2011; 50(29): 6527–6529.

[38] Rajarathnam K, Sykes BD, Dewald B, Baggiolini M, Clark LI. Disulfide bridges in interleukin-8 probed using non-natural disulfide analogues: Dissociation of roles in structure from function. *Biochemistry.* 1999; 38(24): 7653-7658.

[39] Walewska A, Jaśkiewicz A, Bulaj G, Rolka K. Selenopeptide analogsof EETI-II retain potent trypsin inhibitory activities. *Chem. Biol. Drug Des.* 2011; 77(1): 93–97.

[40] Arai K, Takei T, Okumura M, Watanabe S, Amagai Y, Asahina Y, Moroder L, Hojo H, Inaba K, Iwaoka M. Preparation of selenoinsulin as a long-lasting insulin analogue. *Angew. Chem. Int. Ed.* 2017; 56(20): 5522-5526.

[41] Arai K, Okumura M, Lee YH, Katayama H, Mizutani K, Lin Y, Park SY, Sawada K, Toyoda M, Hojo H, Inaba K, Iwaoka M. Diselenide-bond replacement of the external disulfide bond of insulin increases its oligomerization leading to sustained activity. *Commun. Chem.* 2023; 6(1): 258-267.

[42] Weil KO, Rege N, Lansky S, Shalev DE, Shoham G, Weiss MA, Metanis N. Substitution of an internal disulfide bridge with a diselenide enhances both foldability and stability of human insulin. *Chem. Eur. J.* 2019; 25(36): 8513-8521.

[43] Weil KO, Dhayalan B, Chen YS, Weiss MA, Metanis N. Se-Glargine: Chemical synthesis of a basal insulin analogue stabilized by an internal diselenide bridge. *ChemBioChem.* 2024; 25(5): e202300818. DOI: 10.1002/cbic.202300818.

[44] Takei T, Tanaka H, Okumura N, Takao T, Moroder L, Hojo H. Chemical synthesis of per-selenocysteine human epidermal growth factor. *J. Pep. Sci.* 2023; 29(5): e3464. DOI: 10.1002/psc.3464

[45] Dawson P, Muir TW, Clark LI, Kent SB. Synthesis of proteins by native chemical ligation. *Science.* 1994; 266(5186): 776-779.

[46] Wieland T, Bokelmann E, Bauer L, Lang HU, Lau H. Über peptidsynthesen. 8. Mitteilung bildung von S-haltigen peptiden durch intramolekulare wanderung von Aminoacylresten. *Justus Liebigs Ann. Chem.* 1953; 583(1): 129-149.

[47] Yan LZ, Dawson PE. Synthesis of peptides and proteins without cysteine residues by native chemical ligation combined with desulfurization. *J. Am. Chem. Soc.* 2001; 123(4): 526–533.

[48] Hoffmann FW, Ess RJ, Simmons TC, Hanzel RS. The desulfurization of mercaptans with trialkyl phosphites. *J. Am. Chem. Soc.* 1956; 78(24): 6414.

[49] Wan Q, Danishefsky SJ. Free-radical-based, specific desulfurization of cysteine: a powerful advance in the synthesis of polypeptides and glycopolypeptides. *Angew. Chem. Int. Ed.* 2007; 46(48): 9248-9252.

[50] Crich D, Banerjee A. Native chemical ligation at phenylalanine. *J. Am. Chem. Soc.* 2007; 129(33): 10064–10065.

[51] Haase C, Rohde H, Seitz O. Native chemical ligation at valine. *Angew. Chem. Int. Ed.* 2008; 47(36): 6807–6810.

[52] Harpaz Z, Siman P, Kumar KSA, Brik A. Protein synthesis assisted by native chemical ligation at leucine. *ChemBioChem.* 2010; 11(9): 1232–1235.

[53] Chen J, Wang P, Zhu JL, Wan Q, Danishefsky SJ. A program for ligation at threonine sites: application to the controlled total synthesis of glycopeptides. *Tetrahedron.* 2010; 66(13): 2277–2283.

[54] Ding H, Shigenaga A, Sato K, Morishita K, Otaka, A. Dual kinetically controlled native chemical ligation using a combination of sulfanylproline and sulfanylethylanilide peptide. *Org. Lett.* 2011; 13(20): 5588-5591.

[55] Malins LR, Cergol KM, Payne RJ. Peptide ligation-desulfurization chemistry at arginine. *ChemBioChem.* 2013; 14(5): 559–563.

[56] Thompson RE, Chan B, Radom L, Jolliffe KA, Payne RJ. Chemoselective peptide ligation-desulfurization at aspartate. *Angew. Chem. Int. Ed.* 2013; 52(37): 9723-9727.

[57] Pasunooti KK, Yang R, Banerjee B, Yap T, Liu CF. 5-Methylisoxazole-3-carboxamide-directed palladium-catalyzed γ-C (sp³)–H acetoxylation and application to the synthesis of γ-mercapto amino acids for native chemical ligation. *Org. Lett.* 2016; 18(11): 2696-2699.

[58] Hojo H, Aimoto S. Polypeptide synthesis using the *S*-alkyl thioester of a partially protected peptide segment. Synthesis of the DNA-binding domain of c-Myb protein (142-193)-NH$_2$. *Bull. Chem. Soc. Jpn.* 1991; 64(1): 111-117.

[59] Blake J. Peptide segment coupling in aqueous medium: silver ion activation of the thiolcarboxyl group. *Int. J. Pep. Protein Res.* 1981; 17(2): 273-274.

[60] Hojo H, Murasawa Y, Katayama H, Ohira T, Nakahara Y, Nakahara Y. Application of a novel thioesterification reaction to the synthesis of chemokine CCL27 by the modified thioester method. *Org. Biomol. Chem.* 2008; 6(10): 1808-1813.

[61] Asahina Y, Kamitori S, Takao T, Nishi N, Hojo H. Chemoenzymatic synthesis of the immunoglobulin domain of Tim-3 carrying a complex-type *N*-glycan by using a one-pot ligation. *Angew. Chem. Int. Ed.* 2013; 52(37): 9733-9737.

[62] Asahina Y, Kanda M, Suzuki A, Katayama H, Nakahara Y, Hojo H. Fast preparation of an *N*-acetylglucosaminylated peptide segment for the chemoenzymatic synthesis of a glycoprotein. *Org. Biomol. Chem.* 2013; 11(41): 7199-7207.

[63] Asahina Y, Komiya S, Ohagi A, Fujimoto R, Tamagaki H, Nakagawa K, Sato T, Akira S, Takao T, Ishii A, Nakahara Y, Hojo H. Chemical synthesis of *O*-glycosylated human interleukin-2 by the reverse polarity protection strategy. *Angew. Chem. Int. Ed.* 2015; 54(28): 8226-8230.

[64] Hojo H, Takei T, Asahina Y, Okumura N, Takao T, So M, Suetake I, Sato T, Kawamoto A, Hirabayashi Y. Total synthesis and structural characterization of caveolin-1. *Angew. Chem. Int. Ed.* 2021; 60(25): 13900-13905.

[65] Hojo H, Suetake I. Chemical synthesis of palmitoylated histone H4. *ARKIVOC.* 2021; 2021(4): 186-197.

[66] Takei T, Andoh T, Takao T, Hojo H. One-pot four-segment ligation using seleno- and thioesters: synthesis of superoxide dismutase. *Angew. Chem. Int. Ed.* 2017; 56(49): 15708-15711.

[67] Takei T, Ando T, Takao T, Ohnishi Y, Kurisu G, Iwaoka M, Hojo H. Chemical synthesis of ferredoxin with 4 selenocysteine residues using a segment condensation method. *Chem. Commun.* 2020; 56(91): 14239-14242.

[68] Hojo H, Onuma Y, Akimoto Y, Nakahara Y, Nakahara Y. *N*-Alkyl cysteine-assisted thioesterification of peptides. *Tetrahedron Lett.* 2007; 48(1): 25-28.

[69] Quaderer R, Sewing A, Hilvert D. Selenocysteine-mediated native chemical ligation. *Helv. Chim. Acta.* 2001; 84(5): 1197-1206.

[70] Hondal RJ, Nilsson BL, Raines RT. Selenocysteine in native chemical ligation and expressed protein ligation. *J. Am. Chem. Soc.* 2001; 123(21): 5140-5141.

[71] Gieselman MD, Xie L, Van Der Donk WA. Synthesis of a selenocysteine-containing peptide by native chemical ligation. *Org. Lett.* 2001; 3(9): 1331-1334.

[72] Dery S, Reddy PS, Dery L, Mousa R, Dardashti RN, Metanis N. Insights into the deselenization of selenocysteine into alanine and serine. *Chem. Sci.* 2015; 6(11): 6207-6212.

[73] Malins LR, Mitchell NJ, McGowan S, Payne RJ. Oxidative deselenization of selenocysteine: applications for programmed ligation at serine. *Angew. Chem. Int. Ed.* 2015; 54(43): 12716-12721.

[74] Metanis N, Keinan E, Dawson PE. Traceless ligation of cysteine peptides using selective deselenization. *Angew. Chem. Int. Ed.* 2010; 49(39): 7049-7053.

[75] Malins LR, Mitchell NJ, Payne RJ. Peptide ligation chemistry at selenol amino acids. *J. Pep. Sci.* 2014; 20(2): 64-77.

[76] Gieselman MD, Xie L, van Der Donk WA. Synthesis of a selenocysteine-containing peptide by native chemical ligation. *Org. Lett.* 2001; 3(9): 1331-1334.

[77] Shimodaira S, Takei T, Hojo H, Iwaoka M. Synthesis of selenocysteine-containing cyclic peptides via tandem *N*-to-*S* acyl migration and intramolecular selenocysteine-mediated native chemical ligation. *Chem. Commun.* 2018; 54(83): 11737-11740.

[78] Berry SM, Gieselman MD, Nilges MJ, van der Donk WA, Lu Y. An engineered azurin variant containing a selenocysteine copper ligand. *J. Am. Chem. Soc.* 2002; 124(10): 2084–2085.

[79] Mitchell NJ, Malins LR, Liu X, Thompson RE, Chan B, Radom L, Payne RJ. Rapid additive-free selenocystine-selenoester peptide ligation. *J. Am. Chem. Soc.* 2015; 137(44): 14011–14014.

[80] Chisholm TS, Kulkarni SS, Hossain KR, Cornelius F, Clarke RJ, Payne RJ. Peptide ligation at high dilution via reductive diselenide-selenoester ligation. *J. Am. Chem. Soc.* 2020; 142(2): 1090-1100.

[81] Kulkarni SS, Watson EE, Premdjee B, Conde FKW, Payne RJ. Diselenide–selenoester ligation for chemical protein synthesis. *Nat. Protoc.* 2019; 14(7): 2229-2257.

[82] Liczner C, Hanna CC, Payne RJ, Wilds CJ. Generation of oligonucleotide conjugates via one-pot diselenide-selenoester ligation–deselenization/alkylation. *Chem. Sci.* 2022; 13(2): 410-420.

[83] Dery L, Reddy PS, Dery S, Mousa R, Ktorza O, Talhami A, Metanis N. Accessing human selenoproteins through chemical protein synthesis. *Chem. Sci.* 2017; 8(3): 1922-1926.

[84] Korotkov KV, Novoselov SV, Hatfield DL, Gladyshev VN. Mammalian selenoprotein in which selenocysteine (Sec) incorporation is supported by a new form of Sec insertion sequence element. *Mol. Cell Biol.* 2002; 22(5): 1402-1411.

[85] Nunes LGA, Cain A, Comyns C, Hoffmann PR, Krahn N. Deciphering the role of selenoprotein M. *Antioxidants (Basel).* 2023; 12(11): 1906-1922.

[86] Blanco CJB, Dawson PE. An efficient Fmoc-SPPS approach for the generation of thioester peptide precursors for use in native chemical ligation. *Angew. Chem. Int. Ed.* 2008; 47(36): 6851-6855.

[87] Blanco CJB, Nardone B, Albericio F, Dawson PE. Chemical protein synthesis using a second-generation *N*-acylurea linker for the preparation of peptide-thioester precursors. *J. Am. Chem. Soc.* 2015; 137(22): 7197-7209.

[88] Whanger PD. Selenoprotein expression and function—Selenoprotein W. *Biochim. Biophys. Acta.* 2009; 1790(11): 1448-1452.

[89] Kim H, Lee K, Kim JM, Kim MY, Kim JR, Lee HW, Chung YW, Shin HI, Kim T, Park ES, Rho J, Lee SH, Kim N, Lee SY, Choi Y, Jeong D. Selenoprotein W ensures physiological bone remodeling by preventing hyperactivity of osteoclasts. *Nat. Commun.* 2021; 12(1): 2258-2270.

[90] Miao Z, Wang W, Miao Z, Cao Q, Xu S. Role of Selenoprotein W in participating in the progression of non-alcoholic fatty liver disease. *Redox Biol.* 2024; 71: 103114-103128.

[91] Mitchell NJ, Sayers J, Kulkarni SS, Clayton D, Goldys AM, Rozada JR, Pereira PJB, Chan B, Radom L, Payne RJ. Accelerated protein synthesis via one-pot ligation-deselenization chemistry. *Chem.* 2017; 2(5): 703-715.

[92] Liao P, Liu H, He C. Chemical synthesis of human selenoprotein F and elucidation of its thiol-disulfide oxidoreductase activity. *Chem. Sci.* 2022; 13(21): 6322-6327.

[93] Dardashti RN, Laps S, Gichtin JS, Metanis N. The semisynthesis of nucleolar human selenoprotein H. *Chem. Sci.* 2023; 14(44): 12723-12729.

[94] Cheng R, Liu J, Daithankar V, Rozovsky S. Applying selenocysteine-mediated expressed protein ligation to prepare the membrane enzyme selenoprotein S. *Methods Enzymol.* 2022; 662: 159-185.

[95] Kildahl NK. Bond Energy Data Summarized. *J. Chem. Educ.* 1995; 72(5): 423–424.

[96] Kang X, Yuan Y, Xu H, Chen Y. Thermal-and Light-driven Metathesis Reactions Between Different Diselenides. *Chem. Res. Chinese U.* 2022; 38(2): 516-521.

[97] Anugrah DSB, Ramesh K, Kim M, Hyun K, Lim KT. Near-infrared light-responsive alginate hydrogels based on diselenide-containing cross-linkage for on demand degradation and drug release. *Carbohydr. Polym.* 2019; 223(1): 115070-115079.

[98] Han X, Yu F, Song X, Chen L. Quantification of cysteine hydropersulfide with a ratiometric near-infrared fluorescent probe based on selenium–sulfur exchange reaction. *Chem. Sci.* 2016; 7(8): 5098-5107.

[99] Nomoto A, Higuchi Y, Kobiki Y, Ogawa A. Synthesis of selenium compounds by free radical addition based on visible-light-activated Se-Se bond cleavage. *Mini Rev. Med. Chem.* 2013; 13(6): 814-823.

[100] Xia J, Zhao P, Zheng K, Lu C, Yin S, Xu H. Surface modification based on diselenide dynamic chemistry: towards liquid motion and surface bioconjugation. *Angew. Chem. Int. Ed.* 2019; 58(2): 542-546.

[101] Cheng X, Li H, Sun X, Xu T, Guo Z, Du X, Li S, Li X, Xing X, Qiu D. Visible-light-induced diselenide-crosslinked polymeric micelles for ROS-triggered drug delivery. *Molecules.* 2024; 29(16): 3970-3986.

[102] Waliczek M, Pehlivan Ö, Stefanowicz P. Light-driven diselenide metathesis in peptides. *ChemistryOpen.* 2019; 8(9): 1199-1203.

[103] He Y, Takei T, Moroder L, Hojo H. Unexpected diselenide metathesis in selenocysteine-substituted biologically active peptides. *Org. Biomol. Chem.* 2024; 22(30): 6108-6114.

[104] Ji S, Cao W, Yu Y, Xu H. Dynamic diselenide bonds: exchange reaction induced by visible light without catalysis. *Angew. Chem. Int. Ed.* 2014; 53(26): 6781-6785.

[105] Chen S, Lu W, Zhang J, He H, Cang Y, Pan X, Zhu J. Thermally driven diselenide metathesis: polarization process vs radical process. *ACS Macro Lett.* 2022; 11(2): 264-269.

Remodeling of Selenium Metabolism through Adduct Formation of Selenoprotein P with Epigallocatechin Gallate

Takashi Toyama*,‡, Katsuki Sato* , Yoshiro Saito‡

Laboratory of Molecular Biology and Metabolism, Graduate School of Pharmaceutical Sciences, Tohoku University
*These authors equally contributed to this study.
‡These authors jointly supervised.

Abstract

Selenoprotein P (SeP) is the major selenium transport protein in the blood and plays a central role in selenium metabolism by being involved in selenoprotein synthesis via selenium supply in various tissues. On the other hand, excess selenoprotein P, which is increased in patients with diabetes and other diseases, can be a malignant protein that causes metabolic disorders in various tissues through disruption of redox homeostasis. Therefore, developing methods to control selenium metabolism in physiological and pathological conditions are significant. In this study, we focused on epigallocatechin gallate (EGCg), an electrophilic plant component, and newly found that modification of the cysteine residue in SeP by this molecule inhibits its cellular uptake in SH-SY5Ycells. SeP-EGCg adduct failed to induce the expression of glutathione peroxidase, which is synthesized in cells by selenium supply through SeP. These results suggest that EGCg can be a candidate molecule to induce negative remodeling of selenium metabolism by inhibiting SeP incorporation into the cells.

Statements about COI: No potential conflicts of interest were disclosed.

Introduction

Selenium is an essential trace element and is incorporated into our bodies through a variety of dietary sources, including grains and seafood. The incorporated selenium is metabolized to inorganic selenide by multiple steps and the selenocysteine, which is a resulting product of this metabolic cascade, is translated into selenoprotein P (SeP) in the liver. SeP, a secreted protein, is released into the plasma and transports selenium to organs throughout the body[1]. It has been reported that approximately 53% of total plasma selenium is accounted for by SeP[2]. SeP is recognized by low-density lipoprotein (LDL) receptor-related proteins (LRPs) such as ApoER2 and taken up by endocytosis, then degraded by lysosomes to provide selenocysteine to the cytosol[3]. Selenocysteine undergoes further

‡**Correspondence:**
Takashi Toyama[1] , Yoshiro Saito[2]
Laboratory of Molecular Biology , Metabolism, Graduate School of Pharmaceutical Sciences, Tohoku University
C301, 6-3 Aoba, Aramaki, Aoba-ku, Sendai,
Miyagi 980-8578, Japan.
Tel ; +81-22-795-6871
1 e-mail ; takashi.toyama.c6@tohoku.ac.jp
2 e-mail ; yoshiro.saito.a8@tohoku.ac.jp

metabolism by selenocysteine lyase (Scly) to produce inorganic selenide and alanine[4]. This inorganic selenide is used for the synthesis of selenocysteine-tRNA^{sec} and translation of selenoproteins (glutathione peroxidase, etc.), which are important for redox homeostasis[5]. SeP is particularly important for selenium transport to the central nervous system[6]. It is known that radioisotope-labeled SeP is rapidly translocated to the brain when administered to selenium-deficient rat[6]. In addition, the selenium levels and selenoprotein expression in the brain are reduced in SeP KO mice [7, 8]. When SeP KO mice are fed with low-selenium diet, severe neurological deficits are observed[9]. On the other hand, we have found that SeP production is increased in type 2 diabetes patients and have found that inhibition of SeP by neutralizing antibodies improves diabetic pathology in mice[10]. Epidemiological studies revealed that plasma SeP levels increased in type 2 diabetes, and this increase has a significant correlation with insulin resistance[11]. Excess SeP is also related to the decrease in insulin secretion of pancreatic β cells[12]. Furthermore, recent evidence demonstrated the role of SeP expression in ferroptosis sensitivity using patient-derived primary glioblastoma cells[13]. Therefore, excess SeP may have adverse health effects, and it is important to suppress SeP in excessive conditions.

Metabolic remodeling is well understood, especially in the context of cancer studies, by examining metabolomic changes at the level of altered expression of metabolic enzymes. In contrast, its variation in selenium metabolism from selenium uptake to translation to selenoproteins, i.e., metabolic remodeling of selenium, is not well understood. We have recently found that sulforaphane, a phytochemical of broccoli sprouts, suppresses the expression of SeP by promoting its degradation in lysosomes[14]. We also reported that epigallocatechin gallate (EGCg) in tea suppresses its translation via induction of a long noncoding RNA CCDC152, which is located in the antisense region of the SeP gene, in the liver[15]. Therefore, such factors may contribute to the improvement of metabolic pathologies such as diabetes via inhibition of SeP, and in fact, the consumption of sulforaphane and tea has been reported to reduce the risk of type 2 diabetes[16, 17]. However, the details of the mechanism are unknown.

A common chemical property found in sulforaphane and EGCg is electrophilicity. Sulforaphane is covalently bound to cysteine residues in proteins via isothiocyanate groups. Epigallocatechin gallate, on the other hand, has an unsaturated carbonyl group and is known to covalently bind to cysteine and lysine residues in proteins in the same as sulforaphane[18, 19]. Since SeP has 16 cysteine and 10 selenocysteine residues in its polypeptide, the electrophilic molecule may target these residues. Therefore, we considered the possibility that these molecules could functionally inhibit SeP by forming adducts against SeP, thereby inhibiting not only its expression but also its selenium transport function. In this study, we applied the biotin-PEAC$_5$ maleimide labeling (BPML) assay to verify the formation of EGCg adducts on SeP and to elucidate their effects on selenium utilization[20].

Materials and methods

Chemicals

Biotin-PEAC5 maleimide (BPM) was obtained from Dojindo (Kumamoto, Japan) and EGCg was from BioVerde (E5737, Kyoto, Japan). All other chemicals used were of the highest quality commercially available.

SDS-PAGE and western blotting

The protein sample or cells were dissolved in 1% sodium dodecyl sulfate (SDS) buffer, and the protein concentration was determined using a DC protein assay kit (BioRad, CA, USA) with bovine serum albumin as the standard. The protein samples were separated by SDS-PAGE and subjected to Western blotting with the indicated antibodies. The antibodies used in this study are as follows. Anti-Glutathione peroxidase 1 (GPx1) is obtained from abcam (ab108427, Cambridge, UK), anti-GAPDH from (015-25473, WAKO, Osaka, Japan), and anti-SeP monoclonal antibody (BD1) was previously developed and validated[10].

Purification of human SeP

Human SeP was purified from human plasma as we previously reported[21]. Human frozen plasma was provided from the Japanese Red Cross Tohoku Block Blood Center (Human experiment approved No. 25J0012).

BPML and acidic-BPML assay

Biotin-PEAC5 maleimide labeling (BPML) assay and acidic-BPML (aBPML) were performed with slight modifications of the previous report (**Figure 1A**) [20]. Briefly, purified human SeP (20 μg/ml) was reacted with EGCg in 200 mM Tris-HCl (pH 7.0) and incubated at 37°C for 30 min to bind the compound to the protein. Then BPM (30 μM) was added and reacted at 37°C for 30 min for BPML. In the case of acidic-BPML, citric acid buffer (pH 3,200 mM) was added and incubated with BPN at 37°C for 30 min. The sample was desalted by the methanol/chloroform extraction. The desalted precipitate was dissolved by 1×Sample buffer [30 mM Tris-HCl (pH6.8), 5% glycerol, 1% SDS, 2.5% 2-ME] and heated at 95°C for 5 minutes. The sample solution was subjected to SDS-PAGE and detected by Avidin-HRP.

Cell culture

Human neuroblastoma SH-SY5Y cells were obtained from KAC (Kyoto, Japan). The cells were cultured in high glucose DMEM with 10% fetal bovine serum (FBS), 100 U/mL and 100 μg/mL penicillin–streptomycin in a humidified incubator under the conditions of 37 °C, 5% CO_2, and 95% ambient air. Before the experiments, the cells were seeded and pre-cultured for 24 hours in a culture plate. Selenium-deficient medium was prepared by adding 2 μM α-tocopherol, 2.5 mg/mL BSA, 5 μg/mL insulin, and 5 μg/mL transferrin to the DMEM without serum.

Data analysis

Western blotting images were obtained by chemiluminescent imaging system Lumino Graph (Atto, Tokyo, Japan). The bands corresponding to each protein molecular weight were cropped and shown in the figure.
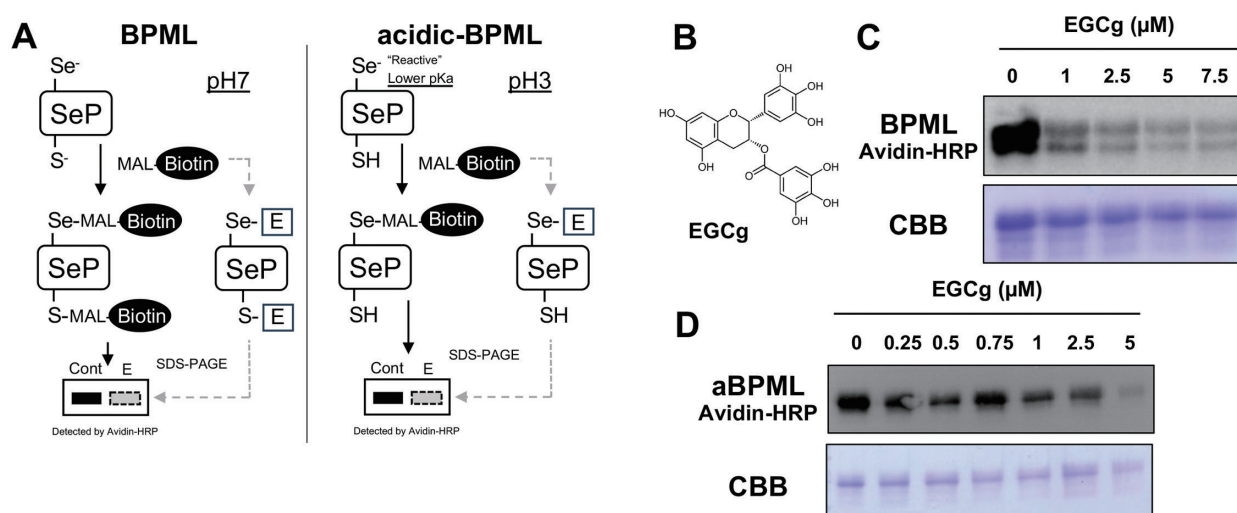
Figure 1. | **Detection of the binding of EGCg to SeP.**
A. Scheme of BPML and acidic-BPML (aBPML).
B. Chemical structure of EGCg.
C. Purified SeP (50 nM) that had been precultured in the indicated concentration of EGCg was subjected to BPML assay.
D. Purified SeP (50 nM) was reacted with an indicated concentration of EGCg and subjected to an aBPML assay. Coomassie brilliant blue (CBB) stain was shown as the loading control.

Results and discussion

EGCg has an unsaturated carbonyl group in its structure and is reported to react with cysteine residues in proteins through covalent bonds (**Figure 1B**). First, to validate the adduct formation of EGCg to SeP, we verified with the BPML assay that detects modification of cysteine or selenocysteine residues. This assay uses biotin-PEAC5-maleimide (BPM), biotin bound to *N*-ethylmaleimide, which selectively reacts with cysteine or selenocysteine, thereby validating the competitive reduction of biotin labeling by the EGCg adduct[20]. The p*K*a value of free cysteine is around 8.3-8.6 and that of free selenocysteine is estimated at approximately 5.2[22]. Thus, under neutral pH conditions, the binding to cysteine and selenocysteine can be examined, while under acidic conditions (acidic-BPML; aBPML), the adduct to selenocysteine can be verified (**Figure 1A**). The BPML result indicates that purified SeP protein was modified by EGCg in a concentration-dependent manner at a concentration of more or less than 1 μM (**Figure 1C**), while in the aBPML, the biotin labeling was inhibited at concentrations more than 5 μM (**Figure 1D**). Under these conditions, the mol ratio of EGCg binding to SeP 50 nM was 1:20 for Cys and 1:100 or higher for selenocysteine. These results indicate that modification of SeP by EGCg occurs for both cysteine and selenocysteine residues but is more likely to occur at low concentrations for cysteine residues. Blood levels of EGCg in humans are known to reach approximately 0.6 μM after drinking 2-3 cup of green tea [23], thus the modifications of cysteine residues of SeP could occur *in vivo*.

Next, the selenium transport activity of SeP modified by EGCg was examined using SH-SY5Y cells, a human neuroblastoma, because this cell line is known to easily take up SeP and use it for selenium metabolism via ApoER2, a major SeP receptor[3]. First, SeP-EGCg conjugates were prepared *in vitro*, and their endocytosis was verified by adding them to the culture medium. The levels of SeP in whole cell lysates were used as an indicator of incorporated SeP. Interestingly, their incorporation was inhibited in a concentration-dependent manner by EGCg at the concentration where modifications to cysteine residues are detected and modifications to selenocysteine residues are not detected (**Figure 2A**). Furthermore, it was verified as the induction of the selenoprotein GPx1 as an indicator of selenium utilization after cellular uptake of SeP. Although SeP induced GPx1 expression of more than 1 nM, this induction was similarly suppressed by pre-incubation with EGCg with a 1:10 mol ratio (**Figure 2B**). Under these conditions, the amount of intracellular SeP was similarly reduced, suggesting that GPx induction was reduced due to uptake inhibition (**Figure 2A, B**). The domain of SeP recognized by ApoER2 is not the N-terminal domain but by the selenium-rich C-terminal domain, and binding to the YWTD β-propeller domain of ApoER2. The
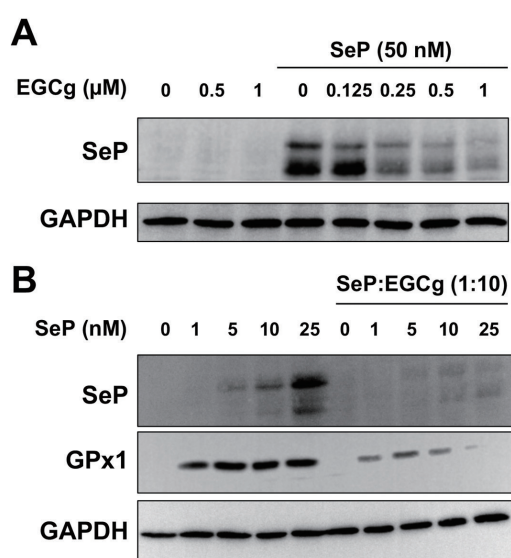
Figure 2. **Inhibition of SeP uptake and production of GPx by EGCg.**

A. Purified SeP was incubated with the indicated concentration of EGCg and then added to the incubation medium of SH-SY5Y cells that had been preculture in serum free medium for 24 hr. After 24 hr, the cells were harvested and subjected to Western blotting.

B. The cells were preculture in selenium deficient medium for 24 hr. Purified SeP was incubated with EGCg at the indicated 10 times higher mol ratio (SeP:EGCg = 1:10) and added to the medium and further incubated for 24 hr. Then the cell lysate was subjected to Western blotting. Control cells with EGCg are in the presence of EGCg (250 nM).

C-terminal domain of SeP contains 9 Cys residues and it is thought that the binding of ApoER2 to SeP is inhibited by modification of these Cys residues. For example, the CQC residue in the C-terminal domain is essential for the binding of SeP to ApoER2, and it has been reported that point mutations at C324 in CQC residue abolish the binding activity[24]. Therefore, it is possible that EGCg binds to the residue, thereby inhibiting uptake of SeP. The bindings of EGCg to Lys residues of SeP are also taken into account, and detailed molecular mechanisms will be elucidated by analyzing binding sites by LC/MS. In addition, when EGCg-SeP containing EGCg-bound selenocysteine is taken up to the cells and degraded by lysosomes, however, it is also possible that the EGCg-modified selenocysteine may not pass through the amino acid transporter of lysosome-cytosol. If it moves to the cytosol, it will be recognized by selenocysteine lyase (SCL), which is essential for selenium metabolism. Thus, the mechanism involved in inhibiting selenium metabolism might not only be the inhibition of uptake of SeP.

In summary, the present study indicates that EGCg forms an adduct to the Cys residues of SeP, presumably by which cellular uptake is inhibited and selenium metabolism is suppressed (**Figure 3**). In this study we used neuronal cells as a model, which show highly efficient SeP uptake, however, it will be necessary to examine the effects in hepatic cells in studies aimed at suppressing diabetes and other diseases that depend on the over-production of SeP. In addition, identifying which Cys residues at which sites are important is an open query, and these are the limitations of this study. At least, the results of this study would indicate that the development of covalent inhibitors that form targeted adducts at the Cys residues of SeP would be promising to trigger metabolic remodeling of selenium, and this could be a piece of important information.
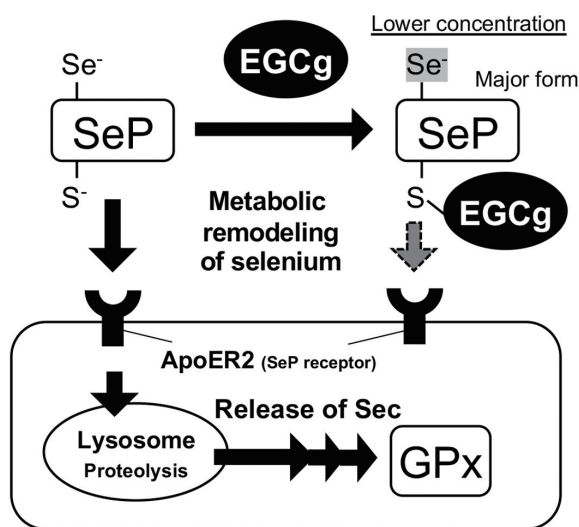
Figure 3. **Metabolic remodeling of selenium by EGCg.**
EGCg covalently binds to cysteine rather than selenocysteine residues of SeP, thereby inhibiting its cellular uptake and suppressing GPx expression, an intracellular selenoprotein. These cascades evoked by EGCg are assumed to be an example of the metabolic remodeling of selenium.

References
[1] Takashi Toyama TK, Kotoko Arisawa, Yoshiro Saito. Takashi Toyama, Takayuki Kaneko, Kotoko Arisawa, Yoshiro Saito. *Metallomics Research.* 2022;2:18-27.
[2] Saito Y, Takahashi K. Characterization of selenoprotein P as a selenium supply protein. *Eur J Biochem.* 2002;269:5746-51.
[3] Mizuno A, Toyama T, Ichikawa A, Sakai N, Yoshioka Y, Nishito Y, et al. An efficient selenium transport pathway of selenoprotein P utilizing a high-affinity ApoER2 receptor variant and being independent of selenocysteine lyase. *J Biol Chem.* 2023;299:105009.
[4] Esaki N, Nakamura T, Tanaka H, Soda K. Selenocysteine lyase, a novel enzyme that specifically acts on selenocysteine. Mammalian distribution and purification and properties of pig liver enzyme. *J Biol Chem.* 1982;257:4386-91.
[5] Palioura S, Sherrer RL, Steitz TA, Soll D, Simonovic M. The human SepSecS-tRNASec complex reveals the mechanism of selenocysteine formation. *Science.* 2009;325:321-5.
[6] Burk RF, Hill KE, Read R, Bellew T. Response of rat selenoprotein P to selenium administration and fate of its selenium. *Am J Physiol.* 1991;261:E26-30.
[7] Hill KE, Wu S, Motley AK, Stevenson TD, Winfrey VP, Capecchi MR, et al. Production of selenoprotein P (Sepp1) by hepatocytes is central to selenium homeostasis. *J Biol Chem.* 2012;287:40414-24.

[8] Hill KE, Zhou J, McMahan WJ, Motley AK, Atkins JF, Gesteland RF, et al. Deletion of selenoprotein P alters distribution of selenium in the mouse. *J Biol Chem*. 2003;278:13640-6.

[9] Byrns CN, Pitts MW, Gilman CA, Hashimoto AC, Berry MJ. Mice lacking selenoprotein P and selenocysteine lyase exhibit severe neurological dysfunction, neurodegeneration, and audiogenic seizures. *J Biol Chem*. 2014;289:9662-74.

[10] Mita Y, Nakayama K, Inari S, Nishito Y, Yoshioka Y, Sakai N, et al. Selenoprotein P-neutralizing antibodies improve insulin secretion and glucose sensitivity in type 2 diabetes mouse models. *Nat Commun*. 2017;8:1658.

[11] Misu H, Takamura T, Takayama H, Hayashi H, Matsuzawa-Nagata N, Kurita S, et al. A liver-derived secretory protein, selenoprotein P, causes insulin resistance. *Cell Metab*. 2010;12:483-95.

[12] Kitabayashi N, Nakao S, Mita Y, Arisawa K, Hoshi T, Toyama T, et al. Role of selenoprotein P expression in the function of pancreatic beta cells: Prevention of ferroptosis-like cell death and stress-induced nascent granule degradation. *Free Radic Biol Med*. 2022;183:89-103.

[13] Zheng X, Toyama T, Siu S, Kaneko T, Sugiura H, Yamashita S, et al. Selenoprotein P expression in glioblastoma as a regulator of ferroptosis sensitivity: preservation of GPX4 via the cycling-selenium storage. *Sci Rep*. 2024;14:682.

[14] Ye X, Toyama T, Taguchi K, Arisawa K, Kaneko T, Tsutsumi R, et al. Sulforaphane decreases serum selenoprotein P levels through enhancement of lysosomal degradation independent of Nrf2. *Commun Biol*. 2023;6:1060.

[15] Mita Y, Uchida R, Yasuhara S, Kishi K, Hoshi T, Matsuo Y, et al. Identification of a novel endogenous long non-coding RNA that inhibits selenoprotein P translation. *Nucleic Acids Res*. 2021;49:6893-907.

[16] Axelsson AS, Tubbs E, Mecham B, Chacko S, Nenonen HA, Tang Y, et al. Sulforaphane reduces hepatic glucose production and improves glucose control in patients with type 2 diabetes. *Sci Transl Med*. 2017;9.

[17] Kao YH, Chang HH, Lee MJ, Chen CL. Tea, obesity, and diabetes. *Mol Nutr Food Res*. 2006;50:188-210.

[18] Suhail M, Rehan M, Tarique M, Tabrez S, Husain A, Zughaibi TA. Targeting a transcription factor NF-kappaB by green tea catechins using in silico and in vitro studies in pancreatic cancer. *Front Nutr*. 2022;9:1078642.

[19] Yang H, Landis-Piwowar K, Chan TH, Dou QP. Green tea polyphenols as proteasome inhibitors: implication in chemoprevention. *Curr Cancer Drug Targets*. 2011;11:296-306.

[20] Toyama T, Shinkai Y, Kaji T, Kumagai Y. Convenient method to assess chemical modification of protein thiols by electrophilic metals. *J Toxicol Sci*. 2013;38:477-84.

[21] Saito Y, Hayashi T, Tanaka A, Watanabe Y, Suzuki M, Saito E, et al. Selenoprotein P in human plasma as an extracellular phospholipid hydroperoxide glutathione peroxidase. Isolation and enzymatic characterization of human selenoprotein p. *J Biol Chem*. 1999;274:2866-71.

[22] Peeler JC, Weerapana E. Chemical Biology Approaches to Interrogate the Selenoproteome. *Acc Chem Res*. 2019;52:2832-40.

[23] Janle EM, Morre DM, Morre DJ, Zhou Q, Zhu Y. Pharmacokinetics of green tea catechins in extract and sustained-release preparations. *J Diet Suppl*. 2008;5:248-63.

[24] Kurokawa S, Bellinger FP, Hill KE, Burk RF, Berry MJ. Isoform-specific binding of selenoprotein P to the beta-propeller domain of apolipoprotein E receptor 2 mediates selenium supply. *J Biol Chem*. 2014;289:9195-207.

Formation of Selenium Adducts of Protein in Liver of Rats Administered Supranutritional Level of Selenium

Munehiro Yoshida* , Tingting Wang, Xin Zhang, Ziwen Jin, Ryota Hosomi, Kenji Fukunaga

Laboratory of Food and Nutritional Sciences, Faculty of Chemistry, Materials and Bioengineering, Kansai University

Abstract

The formation of selenium (Se) adducts of protein in the liver of rats administered Se in excess of nutritional requirements was confirmed using high-performance liquid chromatography-inductively coupled plasma mass spectrometry (HPLC-ICPMS). Male Wistar rats aged 4 weeks old were divided into three groups and fed a basal Se-deficient diet or basal diet supplemented with 0.2 or 2.0 μg Se/g of selenite for 4 weeks, respectively. The liver Se concentration and GPX activity were markedly elevated in rats fed the Se-added diet; the 2.0 μg Se/g group showed a higher Se concentration than the 0.2 μg Se/g group, but GPX did not differ between the two groups. HPLC-ICPMS analysis of liver protease hydrolysates led to the detection of only selenocystine in the 0.2 μg Se/g group, while the 2.0 μg Se/g group showed the presence of four unknown Se compounds in addition of selenocystine. In another experiment, rats weighing 250 g and previously fed the Se-deficient diet for 4 weeks were intraperitoneally administered 50 μg Se/day of selenite or L-selenomethionine for 7 days, and their liver protease hydrolysates were analyzed by HPLC-ICPMS. In selenite-treated rats, peaks of several unknown Se compounds other than selenocystine were detected. In selenomethionine-treated rats, selenomethionine was detected in addition to selenocystine. Unknown Se compounds were also present, but the number and height of peaks were smaller than in selenite-treated rats. These results indicate that with supranutritional Se, accumulation in organs occurs in the form of Se adducts on selenite exposure and mainly nonspecific insertion of selenomethionine into positions of methionine residues of proteins on selenomethionine exposure.

Introduction

Selenium (Se) is an essential trace element for higher animals, including humans, but it is also highly toxic [1]. The mechanism of toxicity due to excess Se is considered to depend on the type of Se compound [2]. In the case of inorganic selenium compounds (selenate and selenite), oxidative stress is caused by reactive oxygen species generated during their reduction, and in that of selenomethionine, nonspecific insertion of selenomethionine into sites of methionine residues in general proteins is considered to be responsible for functional disorders caused by excess Se [3, 4]. For example, cataracts induced by oxidative stress derived from selenite administration are frequently used as a model for experimental cataracts, and it has

*Correspondence

Munehiro Yoshida

3-3-35 Yamate, Suita, Osaka 564-8680, Japan

Tel (cell phone); +81 90 9990 1853

E-mail ; gshpx44@xb3.so-net.ne.jp

been shown that oxidative stress also damages major organs including the liver, kidney, and brain in these animal models [5]. In addition to oxidative stress, selenide and methylselenol produced during metabolism of Se compounds are likely to add to various biomolecules. A selenosugar, the main Se molecular species excreted in urine when Se intake is within the normal range, is a compound of methylselenol added to *N*-acetyl-d-galactosamine [6] and can be regarded as a type of Se adduct. Se transport from plasma to organs is considered to involve selenotrisulfide, which is formed by the addition of Se to cysteine residues in albumin, and Se is likely to be added to thiol groups in proteins [7]. Furthermore, it has been reported that in *Arabidopsis thaliana* treated with a low level of selenate, Se is added to the cysteine residue of NAD-dependent glyceraldehyde-3-phosphate dehydrogenase, resulting in a highly active protein with selenol bound to sulfur of cysteine residues [8]. These cases involve physiologically adequate Se exposure, and the Se-adducts formed serve to maintain normal Se metabolism. However, excessive Se-loading is likely to affect cellular functions through nonspecific formation of various Se adducts by highly reactive selenide or methylselenol. Thus, such excessive Se-loading may lead to the formation of nonspecific Se adducts in biomolecules, including functional proteins and DNA. However, no studies have focused on such Se adducts or attempted to detect them. In addition, the amount of nonspecific Se adducts produced may serve as an indicator to determine the upper limit of Se intake or exposure.

In this study, we detected Se adducts in proteins produced in the liver of rats on administering a supranutritional dose of Se equivalent to 10-times their normal Se intake using high-performance liquid chromatography-inductively coupled plasma mass spectrometry (HPLC-ICPMS).

Methods

Se administration to experimental animals

The experimental protocol followed the Guide for the Care and Use of Experimental Animals issued by the Prime Minister's Office of Japan and approved by the Animal Ethics Committee of Kansai University (Approval No. 2203).

In Experiment 1, eighteen 4-week-old male Wistar rats (mean $\pm$ SD of body weight, 80 ± 3 g) purchased from Shimizu Laboratory Supply Co. (Kyoto) were divided into three groups of equal body weight. One group was fed a *Torula* yeast-based Se-deficient basal diet, and the other two groups were fed the basal diet with sodium selenite at a level of 0.2 or 2.0 μg Se/g, respectively, for 4 weeks.

In Experiment 2, eighteen male Wistar rats similar to those in experiment 1 were fed the Se-deficient basal diet for 4 weeks and then divided into three groups of equal body weight. The body weight (mean $\pm$ SD) of rats at the time of initiating intraperitoneal administration was 250 ± 6 g (n=18). The first group received saline, the second group received saline containing sodium selenite, and the third group received saline containing L-selenomethionine intraperitoneally for 7 days. The dose of Se administered was 50 μg/day. During the intraperitoneal administration period, all rats continued to receive the Se-deficient basal diet.

The composition of the basal Se-deficient diet was as follows: *Torula yeast*, 30.1%; sucrose, 56.9%; soybean oil, 8.0%; Se-free AIN93G mineral mixture, 3.5%; AIN93G vitamin mixture, 1.0%; choline bitartrate, 2.0%; DL-methionine, 3.0%. The Se concentration of the basal diet was 9 ng/g. The *Torula* yeast used was kindly supplied by Mitsubishi Corporation Life Science Limited (Tokyo, Japan).

After the end of the rearing or intraperitoneal administration period, the liver was collected under deep anesthesia with isoflurane (MSD Animal Health, Tokyo, Japan) under non-fasting conditions. The collected liver was stored at −30°C until analysis.

Analysis of total Se in liver and assay of glutathione peroxidase (GPX) activity

To approximately 500 mg of fresh liver, 5 mL of nitric acid and 2 mL of perchloric acid were added, and the sample was heated to incineration. Ultrapure water was added to the ashed sample, the volume was increased to 10 mL, and the mixture was passed through a 0.45-μm membrane filter. Then, Se in the filtrate was quantified by ICPMS using ICPM2030 (Shimadzu, Kyoto). The analytical mass number of Se in ICPMS was 82, and indium 115 was used as an internal standard.

Approximately 1 g of fresh liver was homogenized with 9 volumes of saline to prepare a 10% homogenate. GPX activity in the homogenate was measured using *tert*-butyl hydroperoxide as a substrate and monitoring the amount of NADPH consumed in the reduction of the oxidized glutathione produced using glutathione reductase by the decrease in absorbance at 340 nm [9].

Analysis of Se molecular species in liver

Livers were hydrolyzed with protease, and molecular species of Se released were analyzed using HPLC-ICPMS, as follows. Each liver sample was freeze-dried and then pulverized. To facilitate pulverization, the liver samples were defatted with hexane before freeze-drying. To 50 mg of each dried powder sample, 1.92 mL of phosphate buffer (10 mM, pH 7.1) and 5 mg of protease (type XIV derived from *Streptomyces griseus* (Merck KGaA, Darmstadt)) were added, and the mixture was thoroughly stirred and shaken at 37℃. After 24 hours, 0.08 mL of 5 M HCl was added and the mixture was centrifuged at $1,500 \times g$ for 60 min. The supernatant was collected, passed through a 0.45-μm membrane filter, and used as a protease extract. Molecular species of Se in the protease extract were analyzed by HPLC-ICPMS. The HPLC system consisted of an LC-20Ai multi-pump (Shimadzu, Kyoto, Japan), DGU-20A3R on-line degasser (Shimadzu, Kyoto, Japan), and a reversed phase separation column (Develosil® RPAQUEOUSAR column, 4.6 *i.d.* mm × 250 mm, Nomura Chemical, Seto, Japan). The mobile phase was the same as previously used [10]: methanol/distilled water (HPLC grade) (v/v = 0.05/99.95) containing 2.5 mM sodium 1-butanesulfonate, 4 mM malonic acid, and 15.9 mM tetramethylammonium hydroxide. The pH of the mobile phase was adjusted to 2.3 by the dropwise addition of diluted nitric acid. Elution was performed isocratically at 0.5 mL/min and 30℃, and a sample aliquot of 20 μL was injected into the LC system. The eluate was directly applied to the ICPMS nebulizing tube and monitored at ion intensities of m/z 82. Molecular species of Se in the extract were identified by comparison with the retention times of standard Se compounds (sodium selenite, L-selenocystine (Sigma-Aldrich, St. Louis, USA), *Se*-methylselenocysteine hydrochloride (Sigma-Aldrich, St. Louis, USA), L-selenomethionine (Sigma-Aldrich, St. Louis, USA), and selenohomolanthionine (kindly supplied by Prof. Ogra Y, Chiba University, Japan)).

Statistical analysis

Measurements of the total liver Se concentration and GPX activity were tested using one-way ANOVA and Tukey's multiple comparisons. Statistical GraphPad Prism (GraphPad Software, San Diego, USA) was used for these analyses.

Results

In both Experiments 1 and 2, there was no difference in body weight between the experimental groups. The body weight (mean ± SD) was 248 ± 12 (n=18) at the end of the feeding period in Experiment 1 and 274 ± 11 (n=18) at the end of intraperitoneal administration of Se compound in Experiment 2. Thus, the different Se concentrations in the experimental diets (Experiment 1) and intraperitoneal administration of Se compounds (Experiment 2) had no effect on rat growth.

Table 1 summarizes the Se concentration and GPX activity in the liver of each group of rats in Experiment 1. Se concentrations were proportional to the Se concentration of the experimental diet, with rats fed a diet containing a high level of 2.0 μg Se/g having the highest values. In contrast, GPX activity was higher in the two groups fed the selenium-added than selenium-deficient diet, but the different levels of addition had no effect. Therefore, there was no difference between the 0.2 and 2.0 μg Se/g diet group, indicating the saturation of enzyme activity.

Figure 1 shows typical chromatograms of protease hydrolysates from the livers of rats fed diets with different levels of selenium in HPLC-ICPMS. In rats fed the Se-deficient diet (a), only one noise-like peak was detected at around 7-min retention time. In rats fed the diet containing 0.2 μg Se/g selenite (b), a distinct selenocystine peak and the noise-like peak described above were observed. In contrast, four unknown peaks were detected in addition to selenocystine in rats fed diets supplemented with 2.0 μg/g selenite. The peak heights of selenocystine in **Figures 1b and 1c** are nearly identical.

Table 1 │ **Total Se content and GPX activity in livers of rats fed diets with different levels of Se as sodium selenite**

Level of Se addition	Se content (ng/g)	GPX activity (unit/g protein)
None	26 ± 3[a]	44 ± 4[a]
0.2 µg/g	236 ± 20[b]	1219 ± 59[b]
2.0 µg/g	743 ± 41[c]	1181 ± 33[b]

Rats were fed an Se-deficient basal diet, or the basal diet supplemented with selenite at 0.2 or 2.0 µg selenium/diet for 4 weeks. Values are means ± SEM (n=6). Means in the same column not sharing a common superscript differ significantly ($p < 0.05$).
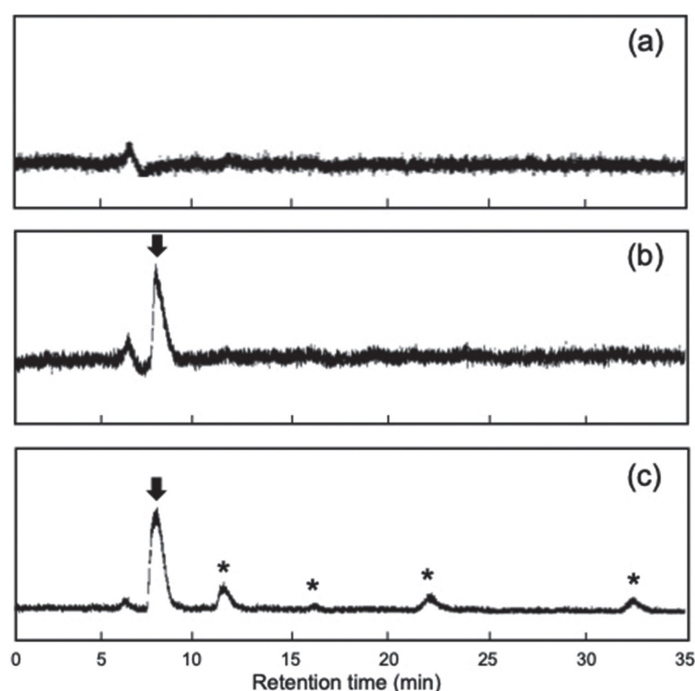
Fig. 1 │ **Chromatograms of protease hydrolysates in livers of rats fed diets with different levels of selenium in HPLC-ICPMS**
Rats were fed a selenium-deficient basal diet (a), or the basal diet supplemented with selenite at 0.2 µg selenium/diet (b) or 2.0 µg selenium/diet (c) for 4 weeks. Although the baseline deviation differs in each chromatogram due to the inconsistent sensitivity of the instrument, the vertical axis (ion intensity in ICPMS) is on the same scale. Black arrows and asterisks indicate the peaks of selenocystine and unknown Se species, respectively.

Table 2 summarizes the Se concentrations and GPX activity in the livers of rats that received the Se compounds intraperitoneally for 1 week in Experiment 2. The Se concentration and GPX activity were markedly increased by administration of the Se compounds. Regarding the effect of the type of Se compound administered, both the Se concentration and GPX activity tended to be higher in rats treated with selenomethionine than in those receiving selenite, but the difference was not significant.

Figure 2 shows typical chromatograms of protease hydrolysates from the livers of rats intraperitoneally administered selenium compounds in HPLC-ICPMS. No distinct peaks were observed in rats not treated with Se compound (a). In rats treated with selenite (b), several unknown Se compound peaks were noted in addition to the distinct selenocystine peak, as in rats fed the experimental diet with an Se concentration of 2.0 µg Se/g in Experiment 1. In rats treated with selenomethionine (c), distinct peaks of selenocystine and selenomethionine were detectable. In addition, unknown peaks were also present, but their number and heights were smaller than in selenite-treated rats.

When the liver powder was analyzed without protease treatment, no peaks derived from Se compounds were observed on HPLC-ICPMS chromatograms in either Experiment 1 or 2.

Table 2 | **Total Se content and GPX activity in livers of rats receiving Se compounds intraperitoneally**

Se compounds received	Se content (ng/g)	GPX activity (unit/g protein)
None	16 ± 2^a	42 ± 5^a
Sodium selenite	414 ± 49^b	917 ± 42^b
Selenomethionine	504 ± 48^b	1020 ± 98^b

Rats were fed a selenium-deficient basal diet. After 4-week feeding, rats received saline, sodium selenite, or L-selenomethionine intraperitoneally for 7 days. The dose of selenium administered was 50 µg/day. Values are means ± SEM (n=6). Means in the same column not sharing a common superscript differ significantly ($p < 0.05$).
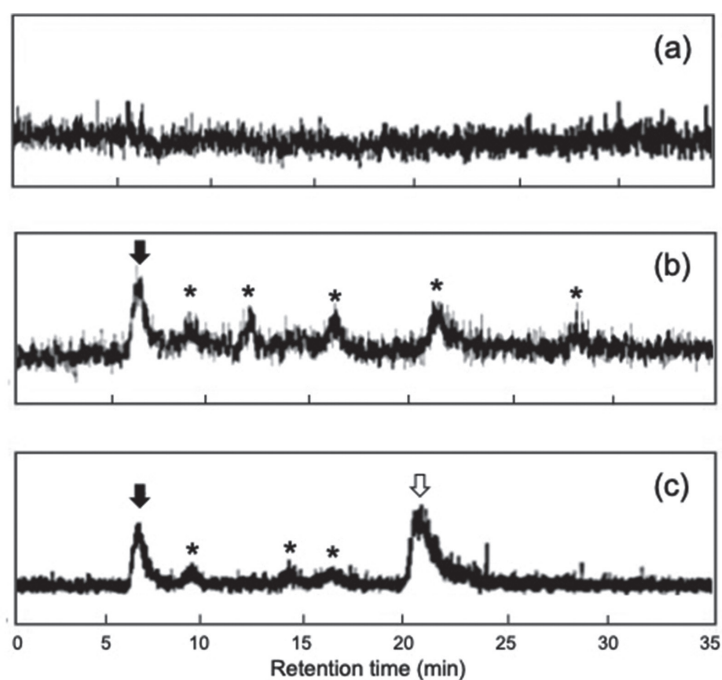

Fig. 2 | **Chromatograms of protease hydrolysates from livers of rats intraperitoneally administered selenium compounds in HPLC-ICPMS**

Rats were fed a selenium-deficient basal diet. After 4-week feeding, rats were divided into three groups: the first group received saline (a), the second group received saline containing sodium selenite (b), and the third group received saline containing L-selenomethionine (c) intraperitoneally for 7 days. The dose of selenium administered was 50 µg/day. Although the baseline deviation differs in each chromatogram due to the inconsistent sensitivity of the instrument, the vertical axis (ion intensity in ICPMS) is on the same scale. Black arrows, white arrow and asterisks indicate the peak of selenocystine, selenomethionine and unknown Se species, respectively.

Discussion

Considering that rats consume a diet equivalent to about 10% of their body weight per day, a diet with an Se concentration of 2.0 µg/g would result in Se intake of 50 µg/day for a rat weighing about 250 g. Thus, Se exposure levels of rats that received the Se compound intraperitoneally in Experiment 2 are comparable to those that consumed the 2.0 µg Se/g diet in Experiment 1. The Se concentration of AIN93G used as a standard semi-purified diet in nutritional studies with rats is 0.2 µg/g [11]. This means that the 0.2 µg Se/g diet in Experiment 1 provides a nutritionally sufficient Se intake. Therefore, the 2.0 µg Se/g diet leads to a supranutritional intake of Se.

In Experiment 1, when 2.0 and 0.2 µg Se/g diet groups were compared, the liver Se concentrations were higher in proportion to the dietary Se concentration, but GPX activity did not differ (**Table 1**). Although only GPX was measured, it is likely that in the 0.2 µg Se/g diet group, where nutritionally sufficient Se intake was achieved, the production of selenoproteins, which incorporate selenocysteine into the peptide chain, was already saturated. In addition, the similar peak height of selenocystine in **Figures 1b and 1c** also means that the selenoprotein production in the two groups is comparable. Therefore, it can be suggested that Se accumulates in the liver of rats

in the 2.0 μg Se/g diet group in a form other than selenoprotein.

HPLC-ICPMS analysis of the extract from the protease-treated liver in Experiment 1 detected only the selenocystine peak derived from selenoprotein in the 0.2 μg Se/g diet group (**Figure 1b**), while four unknown peaks were detected in addition to selenocystine in the 2.0 μg Se/g diet group (**Figure 1c**). Since these peaks were not detected in the absence of protease treatment, we consider that these unknown Se compounds were drived from Se added to the side chains of amino acids. Selenocysteine residues in selenoprotein are unstable, so it is possible that artificial Se species are produced in the process of preparing the protease extract. The amount of selenocysteine residues in the 0.2 μg/g and 2.0 μg/g groups was comparable because the production of selenoprotein was saturated. Therefore, if there was an artificial Se species derived from selenocysteines residues, a peak other than selenocystine should also occur in the 0.2 μg/g group (**Figure 1b**). However, no such peak was observed. Thus, we conclude that Se-adducts of proteins were formed in the livers of rats fed the 2.0 μg Se/g diet.

The peaks, which may be derived from the Se-adducts of proteins, were also observed in the liver of rats treated intraperitoneally with selenite in Experiment 2 (**Figure 2b**). Concerning selenomethionine administration, a large peak of selenomethionine was observed in addition to selenocystine (**Figure 2c**). Unknown peaks were also present, but they were clearly fewer in number and smaller in height than in the case of selenite administration. This means that most of the selenomethionine administered was inserted nonspecifically at sites of methionine residues of general proteins, resulting in low-level formation of Se-adducts of proteins.

The present results indicate that supuranutritional Se intake causes saturation of selenoprotein formation, and that some of the Se not used for selenoprotein formation accumulates as Se-adducts of proteins in the case of selenite and at sites of methionine residues of proteins in the case of selenomethionine. If the formation of Se adducts is used as an index of Se toxicity, this result indicates that selenomethionine is less toxic than selenite. However, this conclusion is tentative because quantitative evaluation of the effect of the substitution of methionine residues in proteins for selenomethionine has not been completed.

The average Se intake of Japanese people is about 100 μg/day, which is within the appropriate range [12]. In a study of chronic poisoning of Se in China, hair loss and changes in nail morphology were reported when Se intake of nearly 1000 μg/day, or approximately 10-times the average Japanese Se intake, continued over a prolonged period [13]. In the present rat experiments, Se adducts were formed in liver proteins after oral or intraperitoneal administration of Se equivalent to 10 times the appropriate Se intake. Thus, it is possible that Se adducts were produced in the livers and other organs in these Chinese Se-poisoning cases.

In a study of mice, Se administered orally at 4 mg/kg body weight in the form of sodium selenite for 28 days resulted in an average increase in reactive oxygen species and malondialdehyde concentrations in livers, but no significant differences were observed [14]. The dose level in the present study (50 μg/250 g = 200 μg/kg for intraperitoneal administration) was less than one-tenth of this. Accordingly, oxidative stress at a toxic level is not considered to have occurred in the present study; Se adduct formation occurs at lower exposures than oxidative stress generation. Considering that the Se dose level in the present study was similar to exposure levels in human chronic-poisoning cases, it is possible that the formation of Se adducts, rather than oxidative stress caused by reactive oxygen species, is responsible for the symptoms of chronic Se-poisoning in humans, such as hair loss and changes in nail morphology.

The formation of Se adducts is not an oxidative stress, but may cause a loss of protein function via changes in protein conformation associated with Se addition. Se adducts could also be generated in DNA, in which case protein synthesis would be inhibited and more significant effects would occur. In the future, it will be necessary to focus on the formation of Se adducts when considering the pathogenic mechanism of Se poisoning.

We have identified selenomethionine as the major Se molecule species in protease hydrolysates of several seafood, chicken meat, and chicken eggs [15]. The present result that selenomethionine was detected only in the liver of rats that consumed selenomethionine indicates that selenomethionine in these animal products is not biosynthesized in the body of each animal species, but is derived from the food and feed of these animal species.

References

[1] Hong LK, Diamond AM. *Selenium. Present Kowledge in Nutririon* (11th ed vol 1). London: Elsevier Inc; 2020. 443–456.

[2] World Health Organization. *Selenium (Environmental Health Criteria Ser 58)*. Geneva: World Health Organization; 1987.

[3] Schrauzer GN. The nutritional significance, metabolism and toxicology of selenomethionine. *Adv Food Nutr Res*. 2003; 47: 73–112.

[4] Wang Y, Jiang L, Li Y, Luo X, He J. Excessive selenium supplementation induced oxidative stress and endoplasmic reticulum stress in chicken spleen. *Biol Trace Elem Res*. 2016; 172: 481–487.

[5] Chen H, Zhou J. Effects of sodium selenite on oxidative damage in the liver, kidney and brain in a selenite cataract rat model. *Biol Trace Elem Res*. 2020; 197: 533–543.

[6] Kobayashi Y, Ogra Y, Ishiwata K, Takayama H, Aimi N, Suzuki KT. Selenosugars are key and urinary metabolites for selenium excretion within the required to low-toxic range. *Proc Natl Acad Sci USA*. 2002; 99: 15932–15936.

[7] Hatanaka M, Hongoh M, Miyauchi M, Hirakawa R, Ono M, Nakayama M. Albumin-mediated selenium transfer by a selenotrisulfide relay mechanism. *Inorg Chem* 2008; 47: 6273–6280.

[8] Takeda T, Fukui Y. Possible role of NAD-dependent glyceraldehyde-3-phosphate dehydrogenase in growth promotion of Arabidopsis seedlings by low levels of selenium. *Biosci Biotech Biochem*. 2015; 79: 1579–1586.

[9] Yoshida M, Yasumoto K, Iwami, K, Tashiro H. Distribution of selenium in bovine milk and selenium deficiency in rats fed casein-based diets, monitored by lipid peroxide level and glutathione peroxidase activity. *Agric Biol Chem*. 1981; 45: 1681–1688.

[10] Sugihara S, Kondo M, Chihara Y, Yuji M, Hattori H, Yoshida M. Preparation of selenium-enriched sprouts and identification of their selenium species by high-performance liquid chromatography-inductively coupled plasma mass spectrometry. *Biosci Biotech Biochem*. 2004; 68: 193–199.

[11] Reeves PG, Nielsen FH, Fahey Jr GC. AIN-93 purified diets for laboratory rodents: Final report of the American Institute of Nutrition Ad Hoc Writing Committee on the reformulation of the AIN-76A rodent diet. *J Nutr*. 1993; 123: 1939–1951.

[12] Yoshida M. Selenium intake and blood selenium level in Japanese. *Nippon Eiyo Shokuryo Gakkaishi (J Jpn Soc Nutr Food Sci)*. 1992; 45: 485–494.

[13] Yang G, Zhou R. Further observations on the human maximum safe dietary selenium intake in a seleniferous area of China. *J Trace Elem Electrolytes Health Dis*. 1994; 8: 159–165.

[14] Kondaparthi P, Deore M, Naqvi S, Flora SJS. Dose-dependent hepatic toxicity and oxidative stress on exposure to nano and bulk selenium in mice. *Environ Sci Pollut Res Int*. 2021; 28: 53034–53044.

[15] Zhang X, Yoshida M. Identification of molecular species of selenium contained in several animal foods. *Trace Nutr Res*. 2020; 37: 1–6

Post-translational modifications to catalytic cysteine by selenium enhance the enzyme activity of glyceraldehyde-3-phosphate dehydrogenase from *Brassica oleracea var. italica.*

Toru Takeda[*], Yuko Minami, Mitsuka Kozaki, Toshiki Takagai, Takayuki Ohnuma

Department of Advanced Bioscience, Graduate School of Agriculture, Kindai University

Abstract

Selenium (Se) was recently shown to be beneficial for plants, and its application to crop production, drug development, and environmental hygiene is expected. The enzyme activities of some proteins were previously reported to be enhanced in plants grown with Se. These increases may be attributed to the binding of Se to catalytic cysteine by post-translational modifications (PTMs), which is a novel mechanism of expression. Therefore, the present study investigated Se binding and increases in enzyme activity by PTMs to cytoplasmic glyceraldehyde-3-phosphate dehydrogenase (GAPC) from broccoli (*B. oleracea var. italica*), which is classified as a Se-accumulating species, *in planta* and *in vitro*. GAPC derived from plants cultivated with 1 μM selenate had more Se bonds and stronger enzyme activity than that from those cultivated without selenate. BES-Thio, a fluorescent probe that identifies thiol or selenol groups, revealed that increases in GAPC activity by Se binding were due to the formation of a selenol group, which is more reactive than a thiol group, on GAPC-catalyzed cysteine by PTMs. Furthermore, purified recombinant GAPC and mutants (C156S, C160S, and C156S/C160S) were reduced and reacted with GSSeSG *in vitro* to investigate Se binding and selenol group generation by PTMs to recombinant GAPC and mutant proteins. The results obtained show that Se binding and selenol group generation by PTMs occurred only at Cys 156, which corresponds to the catalytic Cys. In addition, V_{max}, K_{cat}, and K_{cat}/K_m values of Se binding GAPC synthesized *in vitro* using purified BoGAPC were 1.49-, 1.48-, and 1.86-fold higher, respectively, than those of GAPC. These results indicate that the generation of selenol group at the catalytic Cys of GAPC by PTM improves the enzyme activity.

Statements about Conflict of Interest:

The authors declare no conflict of interest associated with this manuscript.

*Correspondence

Toru Takeda

3327–204 Nakamachi, Nara, 631–8505, Japan.

Tel ; +81–742–43–8179

E-mail ; t_takeda@nara.kindai.ac.jp

Introduction

Selenium (Se) is an essential trace element for most organisms, except higher plants, and is a key component of selenoproteins [1]. Since selenoproteins are involved in

a number of biological functions, mainly as antioxidants, Se deficiency causes lethal diseases through selenoprotein dysfunction [2]. However, Se species exhibit high reactivity *in vivo*, with excessive accumulation being harmful to organisms [3]. Higher plants cannot synthesize selenoproteins and do not require Se to sustain life [4]. Se is recognized as a toxic element because its accumulation is cytotoxic.

Recent research on the application of Se to crop production, phytoremediation, and medicine development revealed its dynamics in higher plants [5]. A low Se concentration exerted diverse beneficial effects on plant growth [6]. Furthermore, various species of plants cultivated with Se exhibited stronger resistance to environmental stresses, such as drought, low temperatures, excessive light, heavy metal toxicity, and pathogens [6-8]. The beneficial effects of Se have been attributed to its regulation of gene expression, and the main target is the antioxidant system [9]. However, many details, including the signaling pathway of Se and the mechanisms underlying beneficial effects due to other factors, currently remain unclear.

We previously revealed that cultivation with trace Se enhanced or modified the functions of specific proteins. In *Chlamydomonas reinhardtii*, Se supplementation induced H_2O_2 reduction activity in glutathione peroxidase homolog (GPXH) [10]. GPXH is an isozyme of glutathione peroxidase (GPX), which is a selenoprotein, which has Cys instead of Sec at its active site, and originally does not exhibit H_2O_2 reduction activity. Verification using several types of mutant GPXH demonstrated that the activation of GPXH was caused by Se binding through post-translational modifications (PTMs) to Cys-38 at the GPXH active site [11]. In *Arabidopsis thaliana*, trace selenate (SeO_4^{2-}) enhanced the enzyme activity of cytosolic glyceraldehyde-3-phosphate dehydrogenase (GAPC), a glycolytic enzyme with catalytic Cys at its active site, and positively affected plant growth [12]. These findings suggest that Se-induced increases in GAPC activity were due to stronger nucleophilic reactivity as a result of the formation of a selenol group (-SeH) by a Se bond to the thiol group (-SH) of catalytic Cys through PTMs. This phenomenon is also predicted to be involved in the mechanisms underlying the beneficial effects of trace amounts of Se on plants, which have not yet been examined in detail. However, the mechanisms by which Se binds to a protein and enhances enzyme activity in plants that do not incorporate Se as Sec during protein translation remain unclear.

We herein propose that Se-induced increases in enzymatic activity are attributed to the conversion of the catalytic Cys thiol group to a selenol group by Se binding via PTMs. In support of this hypothesis, we refer to the nature of Se in enzymatic activity and Se binding by PTMs to non-Se proteins. Sec is an important feature of selenoproteins and is the 21st amino acid at which sulfur in Cys is replaced by Se [13]. The selenol group side chain ($pK_a = 5.2$) of Sec exhibits stronger nucleophilic reactivity under physiological conditions than the thiol group ($pK_a = 8.5$) [14]. Formate dehydrogenase (FDH), a wild-type selenoprotein that contains catalytic Sec, had a higher catalytic constant (K_{cat}) than mutant FDH, in which Sec replaced Cys [15]. The formation of Se-linked catalytic Cys by PTMs has been demonstrated in experiments using bovine liver-derived rhodanese, a protein with catalytic Cys at its active site. *In vitro* analyses revealed that a reaction with glutathione selenotrisulfide (GSSeSG) resulting from the reduction of selenite by glutathione (GSH) was responsible for the conversion of the thiol group in catalytic Cys to a selenol group [16]. Furthermore, reversible PTMs of the Cys residue, such as oxidation, S-nitrosylation, and S-hypersulfhydration, have been shown to function as intracellular signals and modify protein functions. S-sulfhydration, the conversion of the thiol group (Cys-SH) of catalytic Cys to a persulfide group (Cys-SSH), is expected to be a similar phenomenon to that of PTMs by Se due to similarities in the chemical properties of S and Se [17, 18].

The present study investigated Se binding to proteins by PTMs, with a focus on the mechanisms underlying Se binding to catalytic Cys and the resulting enhancements in enzyme activity. *In planta* and *in vitro* experiments were performed using GAPC purified from *Brassica oleracea var. italica*, which has a higher Se accumulation capacity than *Arabidopsis* [19], and its recombinant and mutant forms.

Materials and methods
Plant materials and growth conditions
Broccoli seeds (*B. oleracea var. italica*) were purchased from Nakahara Seeds Product Co., Ltd. (Hakata, Fukuoka, Japan). They were sterilized with NaClO (1% active chlorine) for 10 min, washed twice with sterile water, and

germinated on absorbent cotton medium impregnated with 4.3 g/L Murashige and Skoog basal salt mixture with or without 1 μM selenate in a plant box. Seeds were initially subjected to low temperature conditions (4°C in the dark) for 72 h, followed by dark conditions (room temperature in the dark) for 72 h. Seeds germinated under these conditions were grown in a growth chamber (23°C, 14/10-h light/dark cycle) for 3 days. These steps were performed aseptically, and sterilization was achieved by autoclaving at 121°C for 15 min.

Plasmid construction for the expression of BoGAPC and BoGAPC mutants

Synthetic genes encoding BoGAPC were obtained from Integrated DNA Technologies (IDT) (Coralville, IA, USA). Synthetic genes encoding the single (BoGAPC-C156S and -C160S) and double (BoGAPC-C156S/C160S) mutants of BoGAPC were also obtained from IDT. The EnsemblPlants (http://plants.ensembl.org/index.html) Gene ID for BoGAPC is Bo5g017500. The nucleotide sequences of the genes were optimized for higher expression in *Escherichia coli* without changing the amino acid sequences. The expression vectors for BoGAPC and BoGAPC mutants, pRham-BoGAPC and pRham-BoGAPC mutants (pRham-BoGAPC-C156S, pRham-BoGAPC-C160S, and pRham-BoGAPC-C156S/C160S), were constructed using the Expresso Rhamnose Cloning and Expression System, N-His in accordance with the manufacturer's instructions. The expression of BoGAPC and BoGAPC mutants in *E. coli* 10 G was performed as follows. *E. coli* cells harboring pRham-BoGAPC or pRham-BoGAPC mutants were grown in LB_broth with 50 μg/mL kanamycin to OD600 =0.8 before induction with 0.2 % (w/v) rhamnose. Growth was then continued at 18 °C for 24 h.

Measurement of GAPC activity

Three hundred milligrams of plant material was homogenized in 1 mL of 50 mM potassium phosphate buffer (pH 8.0) containing 1 mM EDTA, 2.5 mM dithiothreitol (DTT), 1 mM GSH, 1% (w/v) polyvinylpyrrolidone, and 10% (v/v) glycerol using a mortar and pestle. The homogenate was centrifuged at $12,000 \times g$ for 10 min and the supernatant was collected as a crude enzyme solution. NAD-dependent GAPC (EC 1.2.1.12) was measured as the increase in absorbance at 340 nm due to the oxidative reduction of NAD^+ to NADH. The reaction mixture contained the enzyme preparation, 0.3 mM glyceraldehyde-3-phosphate (G3P), and 0.15 mM of NAD^+ in 120 μL of assay buffer (15 mM pyrophosphate buffer, 30 mM sodium arsenate, and 2 mM DTT at pH 8.5). The increase in absorbance at 340 nm at 25°C was monitored for three minutes using a microplate reader. All experiments and assays were performed in triplicate.

Purification of GAPC and recombinant proteins

The purification procedure for GAPC was as follows: the crude enzyme solution was centrifuged at $12,000 \times g$ for 30 min and the supernatant was collected. Ammonium sulfate was then dissolved in the solution to 30% saturation. After being left to stand for 30 min, the resulting precipitate was removed by centrifugation and the supernatant was collected for the next step. The enzyme solution was charged onto a HiTrap Phenyl FF high sub column (GE Healthcare) previously equilibrated with buffer A (50 mM potassium phosphate, pH 7.5, 10% (w/w) glycerol, 2.5 mM DTT, 1 mM GSH, and 1 mM EDTA) containing 30% saturated ammonium sulfate, followed by washing with five column volumes of the same buffer. Elution was performed with a linear gradient of 30–0% ammonium sulfate saturation in buffer A. Active fractions were collected and concentrated by ultrafiltration using Amicon ultra-15 (Merck Millipore) for the final step. The concentrated enzyme solution (<1 mL) was applied to a ProteoSEC Dynamic 6-600kDa HR resin (Protein Ark) column previously equilibrated with buffer A containing 0.15 M NaCl. The column was washed with the same buffer, and the active fractions were saved as the purified enzyme preparation.

The recombinant proteins, wild-type BoGAPC, C156S, C160S, and C156S/C160S were purified using the Ni–NTA column and Sephacryl S-100 as previously described [20].

Se quantification

Se concentrations were measured using Hydride Generated-Atomic Fluorescence Spectrometry (HG-AFS: Millennium Excalibur, PSA, Orpington, UK). Measurement conditions were as follows: flow rate, 1 mL/min; injection volume, 100 μL; acid carrier, 50% (v/v) HCl; reductant, and 0.7% (w/v) $NaBH_4$ in 0.1% NaOH. Se concentrations were assessed based on a calibration curve created using selenate.

Synthesis of Se-binding GAPC (Se-GAPC) *in vitro*

Purified GAPC was reduced by DTT and reacted with a reaction mixture containing GSSeSG or selenite at room temperature for 10 min. GAPC after the reaction was separated into GAPC and a low-molecular-weight Se compound using the PD-10 column (GE Healthcare). Eluted fractions were applied to Se measurements by HG-AFS and protein quantification by the UV absorption method at 280 nm, and the selenylation of GAPC was evaluated. GSSeSG solution was prepared by reacting selenite and GSH at a concentration ratio of 1:4 at 24°C for 10 min in 50 mM potassium phosphate (pH 7.4).

Detection of selenol groups with BES-Thio

A 25 μM 3'-(2,4-dinitrobenzenesulfonyl)-2',7'-dimethylfluorescein (BES-Thio, Wako) solution was prepared by dissolving BES-Thio in 99.5% ethanol and diluting it with 50 mM potassium phosphate buffer at pH 5.8. BES-Thio solution was mixed with the sample solution to a final BES-Thio concentration of 22.5 μM, and then incubated at 37°C for 10 min. Fluorescence intensity was measured using a fluorometer (Excitation: 495 nm, Emission: 535 nm).

Results

Purification and Se quantification of GAPC

To examine the synthesis of Se-GAPC and its enzymatic properties *in planta*, we selected the appropriate Se concentration to add to *B. oleracea* during cultivation. The effects on fresh weight and hypocotyl length revealed that selenate at concentrations of 5 μM or higher had a negative effect on the plants (**Fig. S1**). On the other hand, plants supplemented with 1 μM selenate showed no growth inhibition and maintained high GAPC activity compared to the control plants. Therefore, the optimal concentration of selenate to be added during cultivation was determined to be 1 μM to obtain Se-supplemented plants for subsequent experiments. Furthermore, GAPC activity was significantly stronger than that of the control. To elucidate the cause of enhanced GAPC activity following the addition of selenate, GAPC was purified from control and 1 μM selenate-supplemented plants. The results of SDS-
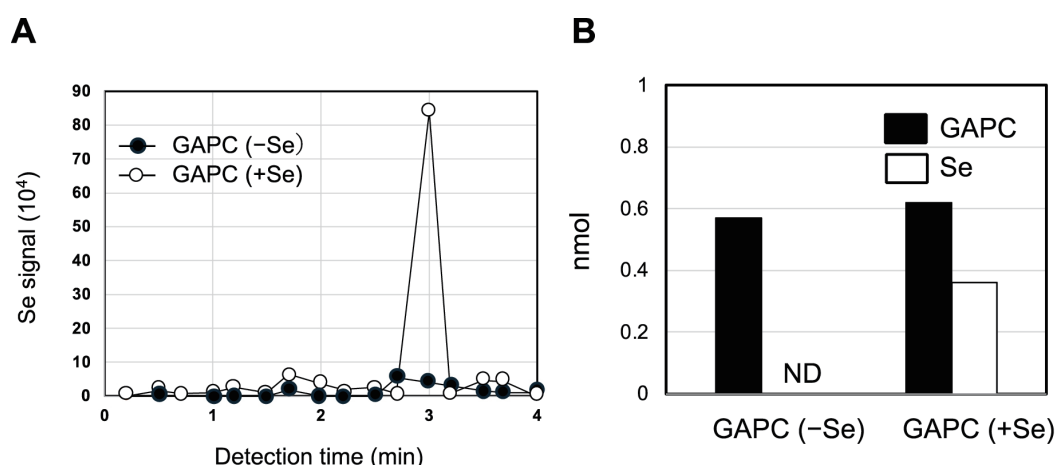
Fig. 1. **Analysis of selenium in purified GAPC(-Se) and GAPC(+Se).**
(A) Detection of selenium in purified GAPC(-Se) and GAPC(+Se) using HG-AFS. Detected fluorescence was applied to the calibration curve prepared from signals of selenite with varying concentrations to calculate the amount of selenium in the sample. (B) The relationship between relative quantities of selenium and purified GAPC. Quantities of purified GAPC were assessed by UV absorbance.

PAGE followed by the silver staining of both samples showed the presence of a single band at a molecular weight of approximately 37,000 Da in the GAPC active fraction by gel filtration chromatography (**Fig. S2**). GAPC active fractions from control and 1 μM selenate-supplemented plants were recovered as GAPC(-Se) and GAPC(+Se), respectively. Comparisons of the specific activities of each purified enzyme confirmed that GAPC(+Se) exhibited 1.37-fold stronger specific activity than GAPC(-Se) (**Table S1**). HG-AFS detected a fluorescence peak, indicating the presence of Se from GAPC(+Se), thereby proving the binding of Se to GAPC(+Se) with enhanced activity (**Fig. 1A**). The results of Se quantification by HG-AFS and protein quantification showed that 0.62 nmol of GAPC(+Se) contained 0.33 nmol Se (**Fig. 1B**).

Mechanisms underlying Se-GAPC synthesis

The results of enzyme activity measurements and Se quantification using purified GAPC demonstrated that Se-GAPC was synthesized *in planta*, which enhanced GAPC activity. Since previous studies reported that Se binding by PTMs in proteins involved GSH *in vivo*, we focused on GSH and investigated the mechanisms underlying the synthesis of Se-GAPC. Using buthionine sulfoximine (BSO), which inhibits GSH biosynthesis, we cultivated GSH-limited plants. The results obtained showed that the addition of 10 μM BSO reduced the total GSH level of both control and 1 μM selenate-supplemented plants to 30% of that without BSO (**Fig. S3A**). Comparisons of GAPC activity between GSH-unrestricted and -restricted plants showed that Se-induced enhancements in GAPC activity were not observed in GSH-restricted plants (**Fig. S3B**). We then attempted to synthesize Se-GAPC *in vitro* for a more detailed investigation, including the enzymatic properties of Se-GAPC. This method was designed based on the result showing that Se binding to catalytic Cys was caused by GSH-mediated PTM. After the reaction between GSSeSG, which was produced by GSH reducing selenite, and reduced GAPC, the mixed solution was applied to a desalting column (PD-10). As a result of separating the reaction mixture containing GAPC and GSSeSG, elution peaks of one GAPC and two Se were detected, and one of the two Se was eluted simultaneously with GAPC. The number of moles of Se eluted simultaneously with GAPC was four-fold that of GAPC (**Fig. 2A**). Since the PD-10 elution pattern of GSSeSG solution only showed one Se peak between elution volumes of 7-11 mL (**Fig. 2B**), the Se elution peak was not consistent with that of GAPC between elution volumes of 7-11 mL in **Fig. 2A**, indicating that low-molecular-weight Se did not bind to GAPC. Based on these results, the reaction between reduced GAPC and GSSeSG generated Se-GAPC, which exhibited 1.6-fold stronger GAPC activity than that of GAPC (**Fig. 2C**).
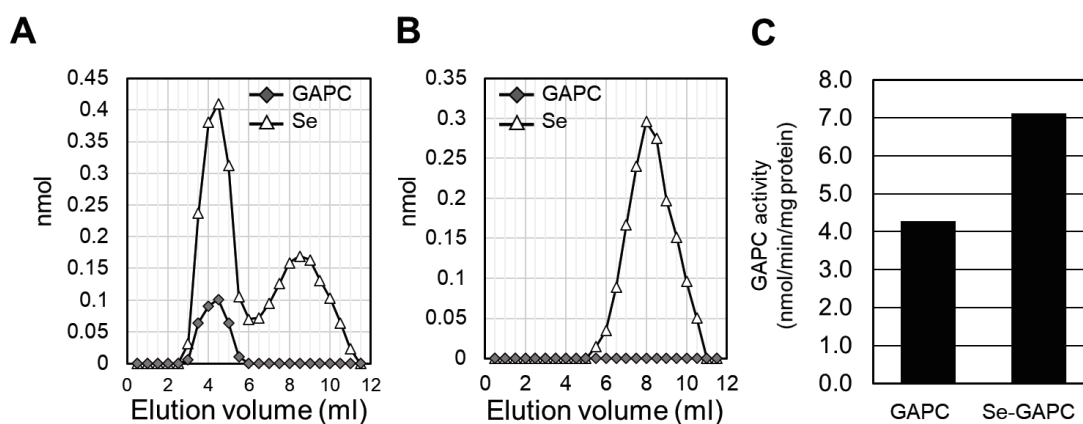
Fig. 2. **Synthesis of Se-GAPC by the reaction between GAPC and GSSeSG *in vitro*. Separation results of the reaction solution containing GAPC and GSSeSG (A) or only GSSeSG (B).**
Separation of the solution was performed using PD-10, with high molecular weights (>5000 Da) and low molecular weights (<1000 Da) being separated into fractions. The amounts of Se and proteins were analyzed by HG-AFS and UV absorption at 280 nm, respectively. (C) Comparison of the enzyme-specific activities of Se-GAPC and GAPC.

Analysis of enzyme properties using Se-GAPC synthesized *in vitro*

Following the successful synthesis of Se-GAPC by the reaction between reduced GAPC and GSSeSG *in vitro*, we conducted a detailed analysis of the properties of Se-GAPC. We compared the fluorescence of BES-Thio to those of GAPC and Se-GAPC at pH 5.8 to prove the hypothesis that the enhanced enzymatic activity of Se-GAPC is due to the conversion of the thiol group (SH) of catalytic Cys to a selenol group (SeH) by Se bonds. BES-Thio fluoresces when deprotected by aromatic nucleophilic substitution with a thiol or selenol group because the pK_a(SeH) of Sec is 5.2, which is markedly lower than the pK_a(SH) of 8.3 for the thiol cysteine (Cys), and selenol acts as a stronger nucleophile than the thiol. **Fig. 3A** shows the results of a preliminary experiment using Cys and Sec as models for the thiol and selenol groups; at pH 5.8, the fluorescence intensity of BES-Thio was stronger for Sec than for Cys. In the experiment using GAPC and Se-GAPC, the same results were obtained for Se-GAPC as those shown in **Fig. 3A;** fluorescence intensity at pH 5.8 was stronger than that of GAPC, which demonstrated that Se formed a selenol group in Se-GAPC (**Fig. 3B**). Reduced and purified recombinant GAPC (BoGAPC) and mutants (C156S, C160S, and C156S/C160S) were then reacted with GSSeSG to confirm the binding of Se to BoGAPC and mutant proteins and
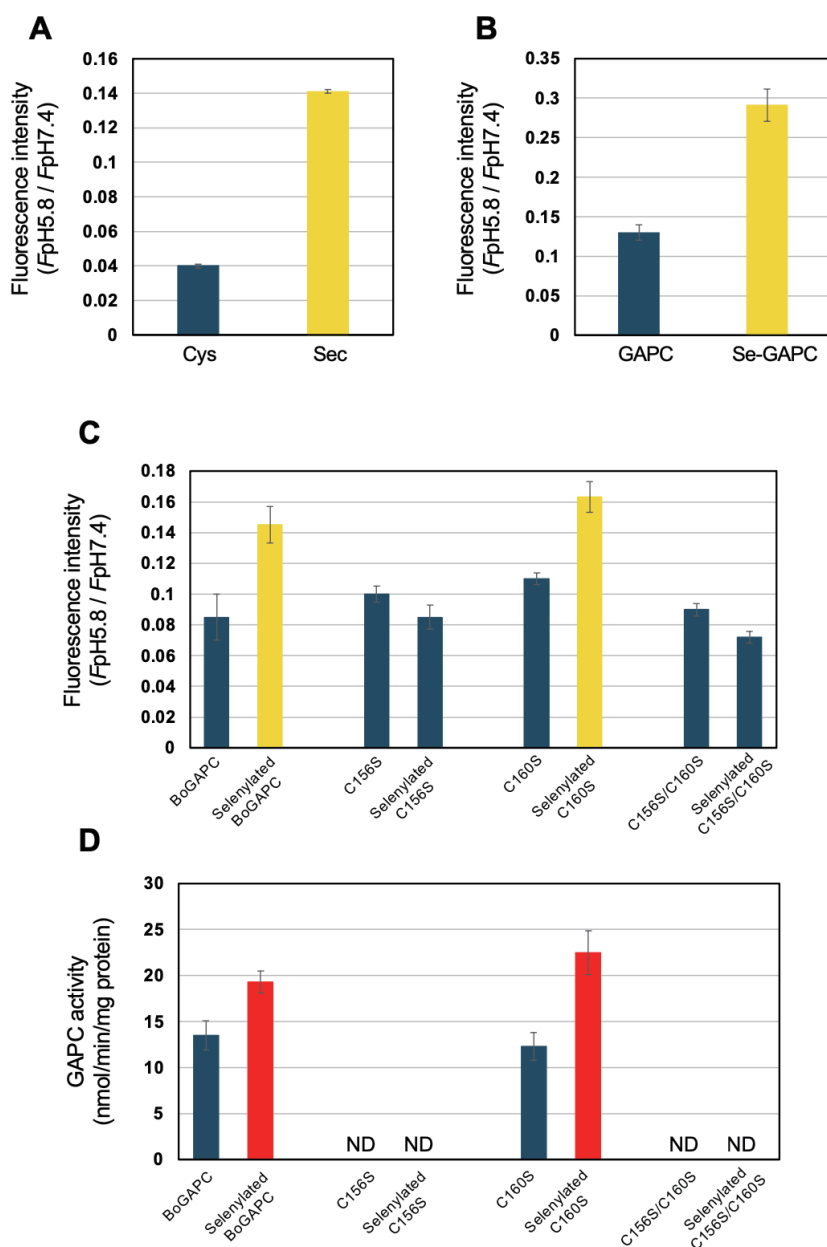
Fig. 3. **Selenol group generation in GAPC from *B. oleracea* and recombinant GAPC (BoGAPC and mutants) depending on selenylation.** Fluorescence intensity from the reaction of each sample with BES-Thio at pH 5.8. (A) Cys(-SH) and Sec(-SeH). (B)GAPC and Se-GAPC. (C) BoGAPC and mutants (C156S, C160S, and the double mutant C156S/C160S). (D) GAPC activity of BoGAPC and mutants (C156S, C160S, and the double mutant C156S/C160S). ND means not detected. Values represent the means ± SD of three experiments.

the generation of selenol groups by PTM. At the same time, the activity of GAPC was measured. No selenol group was detected in the mutant (C156S) in which catalytic Cys was mutated to Ser or in the double mutant (C156S/C160S), and there was no enzyme activity. In contrast, BoGAPC and C160S, in which Cys 156 was conserved, possessed a selenol group and increased enzyme activity, respectively (**Fig. 3C, D**). These results indicate that GAPC with a selenol group at catalytic Cys (selenylated GAPC) exhibited stronger nucleophilic reactivity than GAPC due to the mechanism of action of BES-Thio, which supports enhancements in enzyme activity by Se binding. To investigate the effects of Se binding to catalytic Cys on the activity of GAPC, we performed GAPC activity assays using selenylated GAPC synthesized *in vitro* with BoGAPC. Based on the results obtained, the effects of the selenylation of GAPC were examined by comparing the enzyme properties of GAPC and selenylated GAPC. As shown in **Fig. 4**, two enzyme parameters, K_{cat} and catalytic efficiency (K_{cat}/K_m), showed that selenylated GAPC catalyzed G3P more efficiently than GAPC. The V_{max}, K_{cat} and K_{cat}/K_m values of selenylated GAPC were 1.49-, 1.48- and 1.86-fold higher, respectively, than those of GAPC. These results indicate that the generation of a selenol group to the catalytic Cys of GAPC by PTM increased enzyme activity.

	GAPC	Selenylated GAPC
K_m	0.60	0.45
V_{max}	16.0	23.8
k_{cat}	2.37 min^{-1}	3.51 min^{-1}
k_{cat}/K_m	0.07 M^{-1}sec^{-1}	0.13 M^{-1}sec^{-1}

Fig. 4. **Michaelis-Menten plot of kinetics of GAPC and selenylated GAPC on glyceraldehyde-3-phosphate as the substrate (A). Kinetic characterization of GAPC and selenylated GAPC (B).**
Data are shown as the mean value of triplicate measurements.

Discussion

The selenylation of GAPC was synthesized in *B. oleracea var. italica* grown in the medium containing 1 µM selenate

GAPC(+Se) purified from 1 µM selenate-supplemented plants exhibited stronger enzyme-specific activity and Se binding of 0.5 to 1 mol of GAPC than GAPC(-Se) from control plants. This result confirmed enhancements in enzyme activity by Se binding to proteins, which is consistent with previous findings from *A. thaliana* and *C. reinhardtii* [11, 12]. On the other hand, since GAPC forms homotetramers and has four catalytic Cys sites per molecule, 4 mol of Se is expected to bind to 1 mol of GAPC. However, GAPC(+Se) showed binding of 0.5 mol of Se to 1 mol of GAPC, which was lower than expected. Previous studies using rhodanese, in which Se binding to catalytic Cys in the active center was confirmed, reported that Se was released from rhodanese following the treatment of Se-bound rhodanese with DTT [16]. Therefore, a certain amount of Se is detached from GAPC(+Se) during the process of GAPC purification using a buffer containing DTT, which contributes to maintaining the stability of proteins with catalytic Cys. Although the exact amount of Se binding in GAPC (+Se) before purification remains unknown, it may be higher than the value obtained in the present study.

The reaction by GSSeSG converts GAPC to selenylated GAPC

The results of experiments using GSH-restricted plants suggest the involvement of GSH in the selenylation of Se-GAPC *in planta*. GSH is a biomolecule that plays a role in the maintenance of the cellular redox balance in many
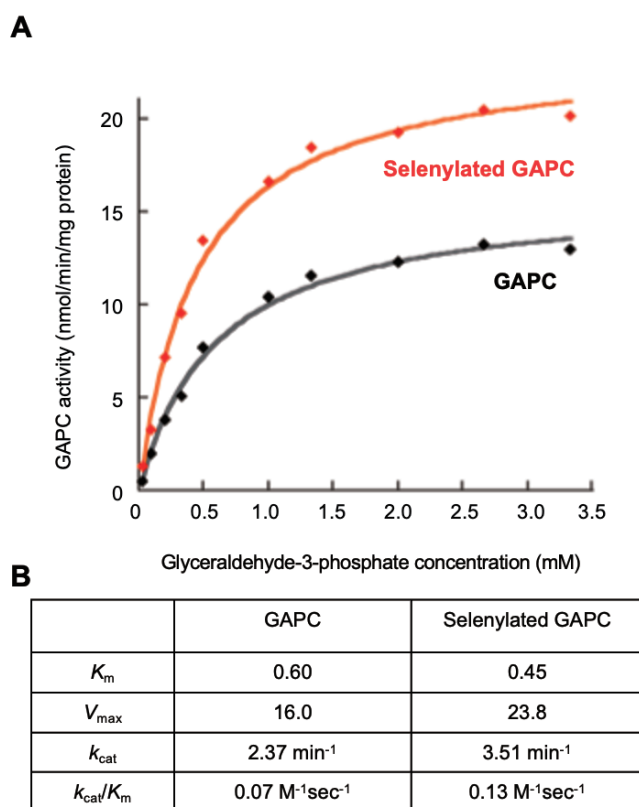
species, including plants, and reduces selenite to GSSeSG, the glutathione selenide anion (GSSe⁻), and HSe⁻ by non-enzymatic reactions [21]. Selenylated GAPC, in which GAPC and Se are bound at a molar ratio of 1:4, was recovered from the *in vitro* reaction of GSSeSG with reduced GAPC. Since GAPC is a homotetramer-forming protein with one catalytic Cys site per subunit, it is reasonable that a 4-fold higher amount of Se than GAPC was recovered. These results clearly demonstrate the role of GSH in Se binding by PTMs to the catalytic Cys of GAPC. However, since GSSeSG is unstable in neutral solution and rapidly decomposes into GSSe- and HSe-, GSSeSG may not be directly involved in the transition of Se to catalytic Cys in the protein. Previous studies on the S-sulfhydration of proteins demonstrated that the gaseous compound sulfide (H_2S) functioned as a sulfur donor to catalytic Cys [22]. Based on these findings, we speculate that HSe- generated by the decomposition of GSSeSG is the direct Se donor to the catalytic Cys. Se binding to Cys in GAPC in plant cells, however, occurs under reducing conditions, not oxidizing conditions. Therefore, as proposed by Ogasawara et al. [16], it is highly likely that Cys in GAPC undergoes thiol exchange with GSSeSG to form Cys-S-Se-SG, which is then reduced by physiological reducing agents such as glutaredoxin and thioredoxin to generate Cys-S-SeH.

Selenylation of GAPC and enhancements in enzyme activity

Experiments using BES-Thio showed that GSSeSG converted the thiol group of the catalytic Cys to a selenol group, resulting in an increase in the nucleophilic reactivity of the catalytic site of selenylated GAPC. Based on previous findings, we speculated that the selenol group of selenylated GAPC was due to S-selenylcysteine (Cys-S-SeH). Se binding to the catalytic Cys of GAPDH, a non-selenoprotein, by a bond similar to the disulfide bond cleaved by DTT was previously confirmed in *E. coli* [23]. The release of Se bound to Cys residues in proteins by a treatment with DTT has also been reported in Se-binding rhodanese[16].

Physiological significance other than enhancements in enzyme activity *in planta*

Previous studies on S-sulfhydration revealed more than 2000 different S-sulfhydrated proteins in *A. thaliana* [22]. Furthermore, S-sulfhydration positively and negatively affected enzyme activities: GAPDH, APX, and ParkinE3 ligase were activated by a NaHS treatment [22,24], while PTP1B enzyme activity was inactivated [25]. Therefore, Se binding to the catalytic Cys of proteins, i.e., S-selenylation, is expected to occur in proteins other than GAPC, resulting in enhanced or inactivated enzyme activity. S-sulfhydration also functions as a stress signaling mechanism by regulating the subcellular localization of various proteins, including GAPC [26-28]. Based on these findings, we hypothesize that the S-selenylation of proteins, including GAPC, is involved in intracellular signaling and may be one of the unidentified Se dynamics in plants.

Furthermore, S-selenylation of GAPC in plant cells maintained in reducing state under non-stress conditions is thought to be one of the mechanisms to avoid damage caused by highly toxic Se compounds, such as selenate randomly taken up via sulfate transporters in the roots, and selenite and Sec produced from selenate via the dissimilatory reduction pathway.

Supplementary data

Table S1. | **Purification of GAPC from *Brassica oleracea var.italica* grown in MS medium with or without 1 μM selenate.**
| Control refers to plants grown in MS medium that does not contain selenate.

Control

	Total protein (mg)	Total activity (μmol/min)	Specific activity (μmol/min/mg protein)	Yield (%)	Purification rate (fold)
Crude extract	91.4	2.41	0.026	100	1.0
Ultra Centrifugation	76.4	2.08	0.027	86.3	1.0
30% ammonium Sulfate Precipitation	48.4	1.30	0.027	53.9	1.0
Hydrophobic Interaction Chromatography	0.94	0.18	0.19	7.47	7.31
Gel Filtration Chromatography	0.008	0.033	4.13	1.37	158.8

1 μM Selenate

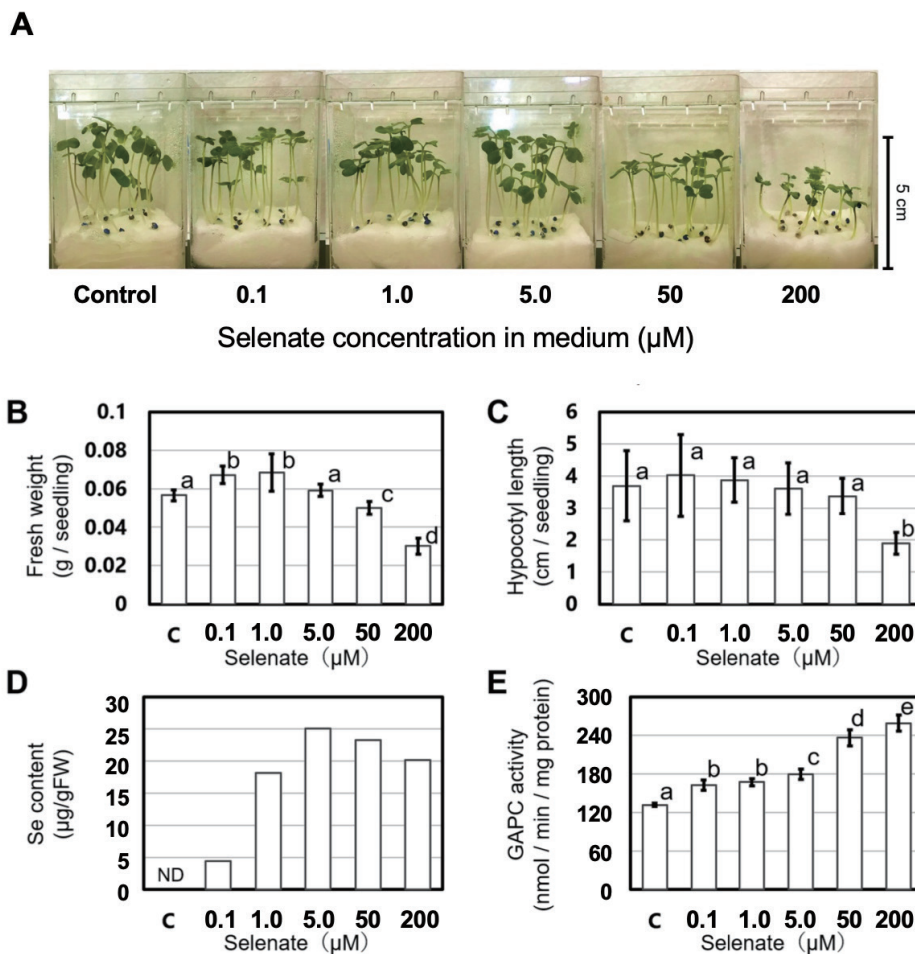|	Total protein (mg)	Total activity (μmol/min)	Specific activity (μmol/min/mg protein)	Yield (%)	Purification rate (fold)
Crude extract	50.3	1.48	0.029	100	1.0
Ultra Centrifugation	42.6	1.24	0.029	83.8	1.0
30% ammonium Sulfate Precipitation	27.5	0.88	0.032	59.5	1.1
Hydrophobic Interaction Chromatography	1.22	0.21	0.17	14.2	5.86
Gel Filtration Chromatography	0.007	0.04	5.71	2.70	196.9

Fig. S1. **Effects of selenate on the growth of *Brassica oleracea var.italica*.**
(A) Growth of plants with MS medium containing 0-200 μM selenate. Control refers to no addition of selenate. (B) Fresh weight as a growth parameter. (n=20). (C) Hypocotyl length as a growth parameter. (n=20). (D) Results on the Se quantification of crude extracts showing the incorporation of Se into plants. (E) GAPC activity in crude extracts prepared from plants grown in various concentrations of selenate (n=3). Different letters represent a significant difference ($p < 0.05$).
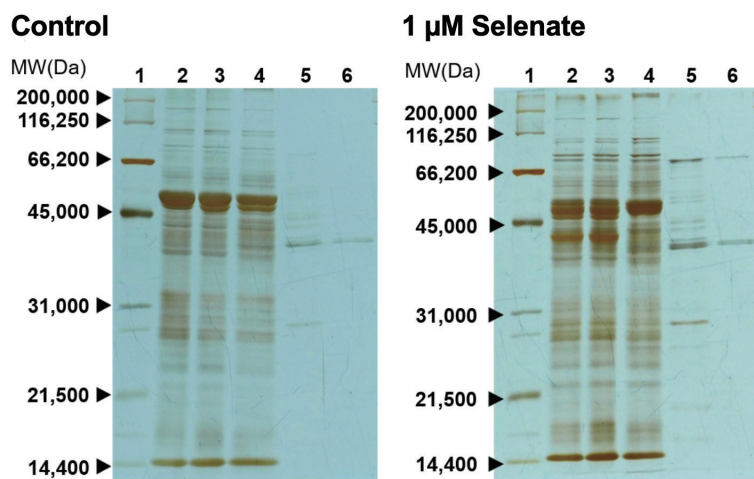

Fig. S2. **Results of silver staining following SDS-PAGE.**
The numbers at the top of the lane indicate the respective applied samples. (1) Protein marker (2) Crude extract (3) Ultra centrifugation (4) 30% ammonium sulfate precipitation (5) Hydrophobic interaction chromatography (6) Gel filtration chromatography
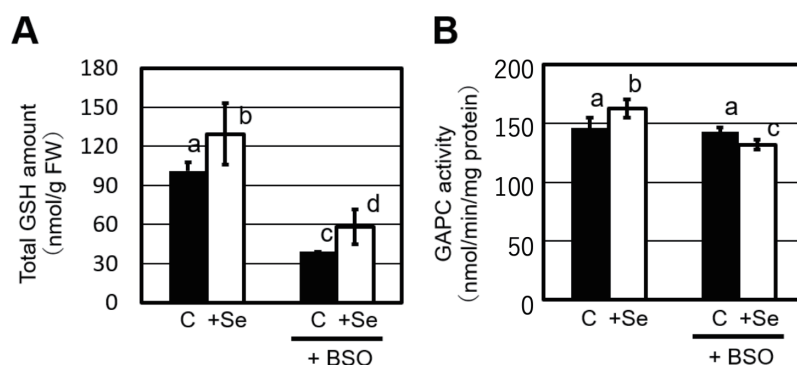
Fig. S3. **Effects of GSH on Se-binding GAPC synthesis *in planta*.**
(A) The amount of GSH in *B. oleracea* (control) and 1 µM selenate-supplemented plants (+Se) and the amount of GSH in plants cultivated in the presence of BSO. GSH-restricted plants were produced by addition of 10 µM BSO to control and 1 µM selenate-supplemented plants. (B) Effects of the restriction of GSH on GAPC activity in control and 1 µM selenate-supplemented plants (n=3). Different letters represent a significant difference ($p < 0.05$).

Data Statement
Data that support the results of the present study are available from the corresponding author, T. T., upon reasonable request.

References
[1] Andreesen JR, Ljungdahl LG. Formate dehydrogenase of *Clostridium thermoaceticum*: incorporation of selenium-75, and the effects of selenite, molybdate, and tungstate on the enzyme. *J Bacteriol.* 1973; 116: 867-873.

[2] Beck MA, Levander OA, Handy J. Selenium deficiency and viral infection. *J Nutr.* 2003; 133: 1463S-1467S.

[3] Cerwenka Jr. EA, Cooper WC. Toxicology of selenium and tellurium and their compounds. *Arch Environ Hearth.* 1961; 3: 189-200.

[4] Obata T, Shirakawa Y. A novel eukaryotic selenoprotein in the haptophyte alga *Emiliania huxleyi*. *J Biol Chem.* 2005; 280: 18462-18468.

[5] Araie H, Shirakawa Y. Selenium utilization strategy by microalgae. *Molecules.* 2009; 14: 4880-4891.

[6] Pilon-Smits EAH, Quinn CF, Tapken W, Malagoli M, Schiavon M. Physiological functions of beneficial elements. *Curr Opin Plant Biol.* 2009; 12: 264-274.

[7] Kumar M, Bijo AJ, Baghel RS, Reddy CRK, Jha B. Selenium and spermine alleviate cadmium induced toxicity in the red seaweed *Gracilaria dura* by regulating antioxidants and DNA methylation. *Plant Physiol Biochem.* 2012; 51: 129-138.

[8] Quinn CF, Prins CN, Freeman JL, Gross AM, Hantzis LJ, Reynolds RJB, Yang Si, Covey PA, Bañuelos GS, Pickering IJ, Fakra SC, Marcus MA, Arathi HS, Pilon-Smits EAH. Selenium accumulation in flowers and its effects on pollination. *New Phytol.* 2011; 192: 727-737.

[9] Hanson B, Garifullina GF, Lindblom SD, Wangeline A, Ackley A, Kramer K, Norton AP, Lawrence CB, Pilon-Smits EAH. Selenium accumulation protects *Brassica juncea* from invertebrate herbivory and fungal infection. *New Phytol.* 2003; 159: 461-469.

[10] Yokota A, Shigeoka S, Onishi T, Kitaoka S. Selenium as inducer of glutathione peroxidase in low-CO_2-grown *Chlamydomonas reinhardtii*. *Plant Physiol.* 1988; 86: 649-651.

[11] Takeda T. Post-translational activation of non-selenium glutathione peroxidase of *Chlamydomonas reinhardtii* by specific incorporation of selenium. *Biochem Biophys Rep.* 2015; 4: 39-43.

[12] Takeda T, Fukui Y. Possible role of NAD-dependent glyceraldehyde-3-phosphate dehydrogenase in growth promotion of *Arabidopsis* seedlings by low levels of selenium. *Biosci Biotechnol Biochem.* 2015; 79: 1579-1586.

[13] Cone JE, Del Rio RM, Davis JN, Stadtman TC. Chemical characterization of the selenoprotein component of clostridial glycine reductase: identification of selenocysteine as the organoselenium moiety. *Proc Natl Acad Sci USA.* 1976; 73: 2659-2663.

[14] Kim IY, Stadtman TC. Selenophosphate synthetase: detection in extracts of rat tissues by immunoblot assay and partial purification of the enzyme from the archaean *Methanococcus vannielii*. *Proc Natl Acad Sci USA.* 1995; 92: 7710-7713.

[15] Axley MJ, Böck A, Stadman TC. Catalytic properties of an *Escherichia coli* formate dehydrogenase mutant in which sulfur replaces selenium. *Proc Natl Acad Sci USA.* 1991; 88: 8450-8454.

[16] Ogasawara Y, Lacourciere G, Stadtman TC. Formation of a selenium-substituted rhodanese by reaction with selenite and glutathione: possible role of a protein perselenide in a selenium delivery system. *Proc Natl Acad Sci USA.* 2001; 98: 9494-9498.

[17] Abe K, Kimura H. The possible role of hydrogen sulfide as an endogenous neuromodulator. *J Neurosci.* 1996; 16: 1066-1071.

[18] Vandiver MS, Snyder SH. Hydrogen sulfide: a gasotransmitter of clinical relevance. *J Mol Med (Berl).* 2012; 90: 255-263.

[19] Neuhierl B, Bock A. On the mechanism of selenium tolerance in selenium-accumulating plants. Purification and characterization of a specific selenocysteine methyltransferase from cultured cells of *Astragalus bisculatus*. *Eur J Biochem.* 1996; 239: 235-238.

[20] Kawamoto D, Takashima T, Fukamizo T, Numata T, Ohnuma T. A conserved loop structure of GH19 chitinases assists the enzyme function from behind the core-functional region. *Glycobiology.* 2022; 32: 356-364.

[21] Turner RJ, Weiner JH, Taylor DE. Selenium metabolism in *Escherichia coli*. *Biometals.* 1998; 11: 223-227.

[22] Aroca A, Serna A, Gotor C, Romero LC. S-Sulfhydration: a cysteine posttranslational modification in plant systems. *Plant Physiol.* 2015; 168: 334-342.

[23] Lacourciere GM, Levine RL, Stadtman TC. Direct detection of potential selenium delivery proteins by using an *Escherichia coli* strain unable to incorporate selenium from selenite into proteins. *Proc Natl Acad Sci USA.* 2002; 99: 9150-9153.

[24] Mustafa AK, Gadalla MM, Sen N, Kim S, Mu W, Gazi SK, Barrow RK, Yang GR, Wang R, Snyder SH. H_2S signals through protein S-sulfhydration. *Sci Signal.* 2009; 2: ra72.

[25] Krishnan N, Fu C, Pappin DJ, Tonks NK. H_2S-Induced sulfhydration of the phosphatase PTP1B and its role in the endoplasmic reticulum stress response. *Sci Signal.* 2011; 4: ra86.

[26] Tristan C, Shahani N, Sedlak TW, Sawa A. The diverse functions of GAPDH: views from different subcellular compartments. *Cell Signal.* 2011; 2: 317-323.

[27] Yang SS, Zhai QH. Cytosolic GAPDH: a key mediator in redox signal transduction in plants. *Biol Plant.* 2017; 61: 417-426.

[28] Couturier J, Chibani K, Jacquot JP, Rouhier N. Cysteine–based redox regulation and signaling in plants. *Front Plant Sci.* 2013; 4: 1-7.

Regular Article

SECIS element variability and its role in selenocysteine versus cysteine utilization in SelD enzymes

Masao Inoue, Riku Aono, Anna Ochi, Yukiko Izu, Toma Rani Majumder, Ming Li, Hisaaki Mihara*

Department of Biotechnology, College of Life Sciences, Ritsumeikan University

Abstract

Selenophosphate synthetase SelD from *Haemophilus influenzae* (HinSelD) has a selenocysteine (Sec) residue at its active site, while its *Escherichia coli* homolog (EcoSelD), which shares 65% amino acid sequence identity, contains cysteine (Cys) instead. This difference prompts questions about the evolutionary divergence between Sec-type and Cys-type SelD enzymes. We used bioinformatics tools to compare the selenocysteine insertion sequence (SECIS) elements of the Sec-type *selD* gene with the corresponding sequence regions of the Cys-type genes. Our analysis showed vital conservation between the UGA Sec codon and SECIS secondary structures. We also tested if HinSelD SECIS could support Sec insertion in *E. coli*. Results indicated that HinSelD SECIS is recognized by *E. coli*, enabling Sec incorporation. Nucleotide differences between HinSelD and EcoSelD SECIS regions affected translation efficiency, with mutants G69A, A75G, G77A, and U84C showing 93%, 81%, 69%, and 69% of wild-type translation levels, respectively. Additionally, the Sec16Cys mutant of HinSelD exhibited a similar expression level compared to the wild-type, suggesting the secondary structure of the SECIS does not inhibit the translation of the preceding UGC codon for Cys.

Statements about COI: The authors have no conflicts of interest associated with this manuscript to declare.

*Correspondence
Hisaaki Mihara
Department of Biotechnology, College of Life Sciences, Ritsumeikan University, 1-1-1 Nojihigashi, Kusatsu, Shiga 525-8577, Japan
Tel ; +81 77 561 2732
E-mail ; mihara@fc.ritsumei.ac.jp

Introduction

Selenium is an essential trace element incorporated into proteins as the selenocysteine (Sec) residue, which plays a crucial role in biological functions [1]. Proteins that specifically incorporate Sec are known as selenoproteins, characterized by their high catalytic activity, making them promising for industrial and pharmaceutical applications. In bacteria, the insertion of Sec into proteins involves four genes: *selA*, *selB*, *selC*, and *selD* [2]. The *selC* gene encodes a tRNA specific for Sec, known as tRNA[Sec], which is charged by seryl-tRNA synthetase (SerRS) to form seryl-tRNA[Sec] [3]. The selenophosphate synthetase SelD catalyzes the formation of selenophosphate from selenide and ATP

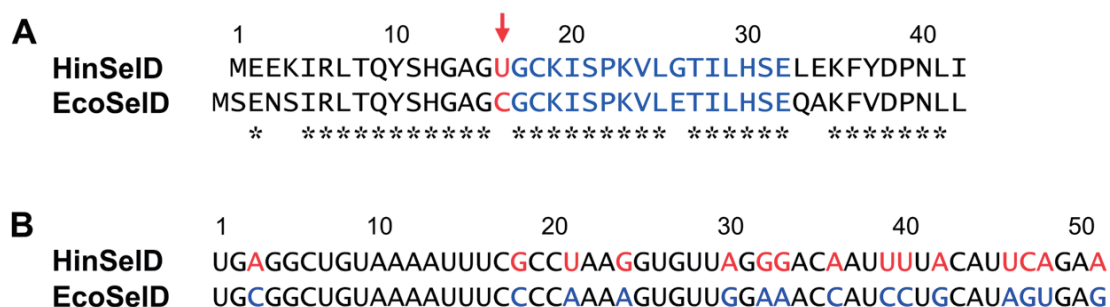**Figure 1.** | **Comparison of the N-terminal amino acid sequences and SECIS element nucleotide sequences of EcoSelD and HinSelD**
(A) Arrows and red text indicate the positions of Sec16 (U) in HinSelD and Cys17 (C) in EcoSelD. Conserved amino acid residues are marked with an asterisk (*), and the amino acid sequences encoded by the SECIS region are highlighted in blue. (B) Nucleotide sequences of the SECIS element in the HinSelD gene and the corresponding region in the EcoSelD gene. Nucleotide differences in the SECIS element of HinSelD and corresponding region of EcoSelD are highlighted in red and blue, respectively.

[4]. The enzyme Sec synthase SelA then converts seryl-tRNA^{Sec} and selenophosphate into Sec-tRNA^{Sec} [2]. On the mRNA of selenoproteins, an in-frame UGA codon is present, along with a selenocysteine insertion sequence (SECIS) element that adopts a stem-loop secondary structure, essential for translating UGA as a Sec codon rather than a stop codon [5]. The specialized translation elongation factor SelB interacts with SECIS, Sec-tRNA^{Sec}, and the ribosome, facilitating the insertion of Sec at the UGA codon [5]. Bacterial SECIS elements share several conserved features: the apical loop, located 16–37 nucleotides downstream of the UGA codon, comprises 3–14 nucleotides and contains at least one guanine (G) residue [6]. Below the apical loop is a stem structure of 4–16 base pairs.

Selenophosphate synthetase SelD with a Sec residue at the active site has been identified in *Haemophilus influenzae* (HinSelD) [7]. HinSelD shares a high sequence homology with *Escherichia coli* SelD (EcoSelD), with 65% identity at the amino acid level. The Sec16 residue in HinSelD corresponds to a cysteine residue (Cys17) in EcoSelD [8]. The surrounding amino acid sequences around the Sec in HinSelD and the Cys in EcoSelD are highly conserved (**Figure 1A**). A comparison of the nucleotide sequences of the SECIS elements between EcoSelD and HinSelD revealed a few nucleotide substitutions, but overall conservation was observed (**Figure 1B**). This observation raises intriguing questions regarding the evolutionary divergence between Sec-type and Cys-type SelD enzymes. In this study, bioinformatics approaches were used to compare the nucleotide sequences and secondary structures of the SECIS regions in Sec-type and Cys-type SelDs from different microorganisms, revealing a high degree of conservation between the presence of the UGA Sec codon and the characteristic secondary structures of the SECIS elements. In addition, we introduced nucleotide substitution in the SECIS element of the HinSelD gene to produce variants, G69A, A75G, G77A, and U84C, based on the comparison with the same region of the EcoSelD gene. The G69A, A75G, G77A, and U84C mutants exhibited translation product levels of 93%, 81%, 69%, and 69%, respectively, of the wild-type, suggesting some flexibility in the recognition of HinSelD SECIS by the *E. coli* translation system. Furthermore, in the Sec16Cys mutant of HinSelD, there was no significant change in expression levels compared to the wild-type, suggesting the secondary structure of the SECIS does not inhibit the translation of the preceding UGC codon for Cys.

Materials and methods

Phylogenetic analysis

The amino acid sequence of HinSelD (R2866_0388) was used as a query for a BLASTp [9] search in KEGG (https://www.genome.jp/kegg/) to retrieve sequences from SelD proteins of 19 *Pasteurellales* species and 14 *Enterobacterales* species, including various *Haemophilus* and *Mannheimia* species. Sequences with shifted start codons, such as

Haemophilus pittmaniae (NCTC13334_01230), *Haemophilus parainfluenzae* (PARA_00030), and *Mannheimia succiniciproducens* (MS1241), were manually corrected to obtain full-length sequences. An outgroup, *Geobacter sulfurreducens* SelD (gsu0607), was included in the alignment. Multiple sequence alignment was performed using Muscle on MEGA7 [10], and a maximum-likelihood phylogenetic tree was constructed using IQ-TREE2 with the LG+G4 model [11]. Bootstrap values were calculated with 1,000 replications using SH-aLRT [12] and Ultrafast Bootstrap [13]. The phylogenetic tree was visualized using iTOL v6 [14].

RNA secondary structure prediction

In the HinSelD gene (R2866_0388), the SECIS element was defined as the 51 nt sequence starting from the 5′ end of the UGA codon for selenocysteine (**Figure 1A**). SECIS-like sequences were extracted from the 34 *selD* gene sequences based on multiple sequence alignment. RNA secondary structures of these SECIS-like sequences were predicted using the MXfold2 Server (http://www.dna.bio.keio.ac.jp/mxfold2/) [15].

Bacterial strain, culture conditions, and preparation of crude extracts

E. coli BL21(DE3) cells transformed with an expression plasmid were cultured in Luria-Bertani (LB) medium containing 0.3% glucose, 1 μM sodium selenite, 10 μM sodium molybdate hydrate, and 100 μg/mL ampicillin at 37°C with shaking until the OD_{600} reached 0.55–0.64. Protein expression was induced by adding 0.1 mM isopropyl β-ᴅ-thiogalactopyranoside (IPTG) or 0.4% lactose, followed by incubation at either 37°C or 30°C for 6 h, with shaking or static conditions. After incubation, cells were harvested by centrifugation, washed twice with phosphate-buffered saline (PBS), and disrupted using ultrasonic sonication UP50H (Hielscher, Teltow, Germany). The lysate was centrifuged at 15,000 × g for 10 min at 4°C. The supernatant was collected as a crude extract.

Plasmid construction

The expression plasmid for HinSelD, pET21aHinSelD, was obtained through synthetic gene production by GenScript (Piscataway, NJ, USA). The expression plasmid for EcoSelD, pET21aEcoSelD, was constructed by inserting the *E. coli selD* gene fragment into the NdeI and BamHI sites of pET21a(+) (Merck KGaA, Darmstadt, Germany). Site-specific mutations in the HinSelD expression plasmid pET21aHinSelD were introduced by GenScript.

Western blotting

Proteins separated by sodium dodecyl sulfate polyacrylamide gel electrophoresis (SDS-PAGE) were transferred to polyvinylidene difluoride (PVDF) membranes (Immobilon-P, Merck Millipore, MA, USA) using a TransBlot SD Semi-dry Transfer Cell (Bio-Rad, CA, USA). An anti-His tag antibody (monoclonal antibody 9C11, FUJIFILM Wako Pure Chemical Corporation, Osaka, Japan) was used as a primary antibody at 1,000-fold dilution. For secondary antibody, anti-mouse IgG(H+L) (Peroxidase Labeled Goat anti-Mouse IgG(H+L) Human Serum Adsorbed, KPL Antibodies & Conjugates, SeraCare, MA, USA) was used at a 14,000-fold dilution. Detection was performed using chemiluminescence (Chemi-Lumi One Super, Nacalai Tesque, Kyoto, Japan) and analyzed with an imaging system (Amersham Imager 600, Cytiva, MA, USA). The band intensities were quantified using ImageJ software [16].

Results and discussion

Phylogenetic analysis of SelD

To investigate the evolutionary relationships between Sec-containing and Cys-containing SelD enzymes, a molecular phylogenetic tree was constructed for SelD enzymes from 34 bacterial species, including those from the order Pasteurellales (which includes *H. influenzae*) and the order Enterobacterales (which includes *E. coli*) (**Figure 2**). The analysis revealed that *Pasteurellales* species harbor both Sec-type and Cys-type SelD enzymes, indicating a diverse evolutionary adaptation within this order. In contrast, SelD enzymes in *Enterobacterales* are predominantly Cys-type, suggesting a possible loss or replacement of the Sec residue during evolution in this lineage.
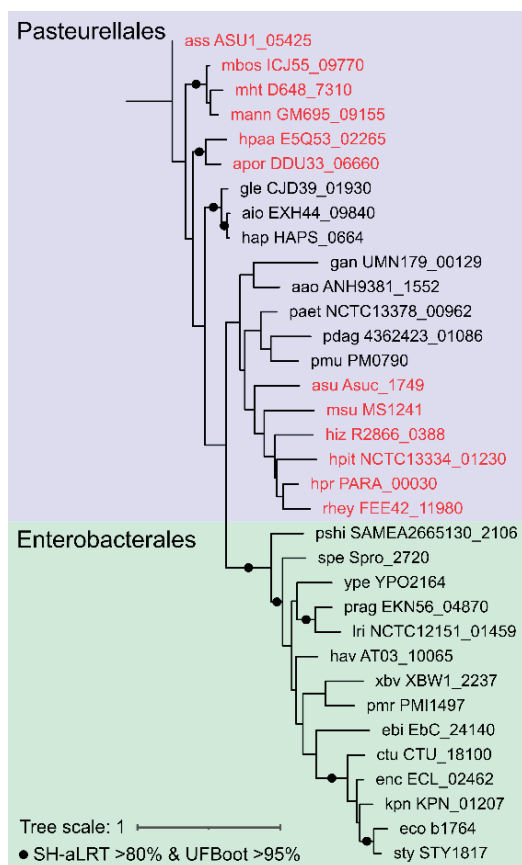
Figure 2. | **Phylogenetic tree of SelD from 34 bacterial species**
Selenocysteine-containing SelD enzymes are indicated in red, while cysteine-containing SelD enzymes are shown in black. SelD sequences used were from *Haemophilus pittmaniae* (NCTC13334_01230), *Haemophilus parainfluenzae* (PARA_00030), *Rodentibacter heylii* (FEE42_11980), *Mannheimia succiniciproducens* (MS1241), *Actinobacillus succinogenes* (Asuc_1749), *Pasteurella aerogenes* (NCTC13378_00962), *Pasteurella multocida* (PM0790), *Pasteurella dagmatis* (4362423_01086), *Aggregatibacter actinomycetemcomitans* (ANH9381_1552), *Gallibacterium anatis* (UMN179_00129), *Glaesserella parasuis* (HAPS_0664), *Actinobacillus indolicus* (EXH44_09840), *Glaesserella* sp. 15-184 (CJD39_01930), *Actinobacillus porcitonsillarum* (DDU33_06660), *Haemophilus parahaemolyticus* (E5Q53_02265), *Actinobacillus suis* (ASU1_05425), *Mannheimia bovis* (ICJ55_09770), *Mannheimia ovis* (GM695_09155), *Mannheimia haemolytica* (D648_7310), *Escherichia coli* (b1764), *Salmonella enterica* (STY1817), *Klebsiella pneumoniae* (KPN_01207), *Enterobacter cloacae* (ECL_02462), *Cronobacter turicensis* (CTU_18100), *Erwinia billingiae* (EbC_24140), *Proteus mirabilis* (PMI1497), *Xenorhabdus bovienii* (XBW1_2237), *Hafnia alvei* (AT03_10065), *Leminorella richardii* (NCTC12151_01459), *Jinshanibacter zhutongyuii* (EKN56_04870), *Yersinia pestis* (YPO2164), *Serratia proteamaculans* (Spro_2720), and *Plesiomonas shigelloides* (SAMEA2665130_2106).

Secondary structure prediction of SECIS elements in SelD genes

We predicted the secondary structures of the SECIS elements and corresponding regions (in the case of Cys-type SelD) in the *selD* genes from 34 bacterial species. For HinSelD (R2866_0388), the SECIS was defined as the 51-nt sequence downstream of the UGA codon that encodes the selenocysteine residue (**Figure 1B**). Using multiple sequence alignment, SECIS regions were extracted from the *selD* nucleotide sequences of the 34 species (**Table 1**). The RNA secondary structures of these SECIS regions were predicted using the MXfold2 Server [15] (**Figure 3 & Supplementary Figure S1**). In Sec-type SelDs, such as those from *Actinobacillus suis* and HinSelD, the predicted secondary structures conformed to the consensus model for SECIS elements. Conversely, in Cys-type SelDs, including EcoSelD, the predicted secondary structures differed significantly from those of the Sec-type SECIS (**Figure 3**). For instance, in the Cys-type *Glaesserella* sp. SelD, the predicted structure resembled the SECIS secondary structure but lacked the characteristic apical loop guanine (G) and had only three base pairs in the stem, deviating from the typical SECIS model. These findings suggest a high degree of conservation between the presence of the UGA codon for Sec and the characteristic secondary structure of SECIS. A comparative analysis of nucleotide sequences specifically focused on the SECIS regions of Sec-type SelD enzymes is shown in **Figure 4A**. The secondary structure predicted from this consensus sequence is depicted in **Figure 4B** and aligns well with previously proposed bacterial SECIS models [6].

Investigation of HinSelD SECIS functionality in *E. coli* and optimization of expression conditions

To examine if the HinSelD SECIS is able to be translated in an *E. coli* host translation system, the expression vector pET21aHinSelD, which produces HinSelD with a C-terminal His-tag, and pET21aEcoSelD expressing C-terminal His-tagged EcoSelD were introduced into *E. coli* BL21(DE3) cells, and various expression conditions were tested. The results from SDS-PAGE and western blot analyses of the crude extracts after cultivation showed that increased

Table 1. SECIS regions from the *selD* nucleotide sequences of the 34 species

| *selD* gene ID	SECIS region
ass:ASU1_05425	UGAGGCUGUAAAAUUUCUCCUAAGGUGUUAGGGACAAUUUUACAAAGUCAG
mbos:ICJ55_09770	UGAGGUUGUAAGAUUUCUCCUAAGGUGUUAGGGACAAUUUUACAAACGCAA
mht:D648_7310	UGAGGCUGUAAAAUUUCGCCUAAGGUGUUAGGGACAAUUUUACAAACUCAA
mann:GM695_09155	UGAGGCUGUAAAAUUUCUCCUAAGGUGUUAGGGACGAUUUUACAAACGCAA
hpaa:E5Q53_02265	UGAGGCUGUAAAAUUUCGCCUAAGGUGUUAGGGACAAUUUUACAUAGCGAA
apor:DDU33_06660	UGAGGCUGUAAAAUUUCUCCUAAGGUGUUAGGGACCAUUUUACAAAGCCAA
gle:CJD39_01930	UGCGGUUGUAAAAUUUCCCCAAAAGUGCUUGAGCAAAUUCUGCAUACAGAA
aio:EXH44_09840	UGUGGCUGUAAAAUUUCCCCGAAAGUGCUUGAACAAAUCUACACAUAGAA
hap:HAPS_0664	UGUGGCUGUAAAAUUUCCCCGAAAGUCCUUGAACAAAUUCUGCACACAGAA
gan:UMN179_00129	UGCGGUUGUAAAAUUUCCCCUAAAGUUUUAGAAACCAUUCUUCACACAGAA
aao:ANH9381_1552	UGUGGUUGUAAAAUCUCGCCUAAGGUAUUAGAGAGUAUUCUGCAUUCAAAA
paet:NCTC13378_00962	UGUGGUUGUAAAAUUUCGCCUAAAGUAUUAGAGACGAUUUUGCAUUCCAAC
pdag:4362423_01086	UGUGGGUGUAAAAUUUCACCAAAAGUGCUUGAGCAAAUUUUACAUUCUGAA
pmu:PM0790	UGCGGCUGUAAAAUUUCGCCGAAAGUCCUCGAAAAGAUUUUACACUCUGAC
asu:Asuc_1749	UGAGGCUGUAAAAUUUCGCCUAAGGUAUUAGGGACUAUUUUACAAACGAAA
msu:MS1241	UGAGGCUGUAAGAUUUCUCCUAAGGUGUUAGGGACUAUUUUACACAGUCAG
hiz:R2866_0388	UGAGGCUGUAAAAUUUCGCCUAAGGUGUUAGGGACAAUUUUACAUUCAGAA
hpit:NCTC13334_01230	UGAGGCUGUAAAAUUUCGCCUAAGGUGUUAGGGACAAUUUUACAAAGCGAA
hpr:PARA_00030	UGAGGUUGUAAAAUUUCGCCUAAGGUGUUAGGGACAAUUUUACAGACUAAA
rhey:FEE42_11980	UGAGGCUGUAAAAUUUCGCCUAAGGUGUUAGGGACAAUUUUACAAACGCAA
pshi:SAMEA2665130_2106	UGUGGGUGUAAAAUCUCGCCUAAAGUGCUGGAUACCAUCUUGCACUCGGAA
spe:Spro_2720	UGCGGUUGUAAAAUCUCACCGAAAGUUCUCGAAACUAUUCUGCACAGCGAG
ype:YPO2164	UGUGGUUGCAAGAUUUCACCAAAAGUUUUGGAUAAAAUUUUGCAUACUGAG
prag:EKN56_04870	UGUGGCUGCAAAAUCUCCCCAAAAGUACUGGAAACGAUCCUGCAUUCUGAG
lri:NCTC12151_01459	UGCGGGUGUAAAAUCUCGCCGAAAGUGUUGGAAACGAUUCUCCACUCCGAG
hav:AT03_10065	UGUGGAUGUAAGAUCUCCCCUAAAGUGUUAGAAACCAUUCUGCACAGCGAA
xbv:XBW1_2237	UGUGGCUGUAAAAUUUCGCCAAAAGUGUUGGAAACUAUUCUGCACAGUGAG
pmr:PMI1497	UGUGGCUGCAAAAUUUCACCAAAAGUUUUGGAAACGAUUUUACAUAGUGAA
ebi:EbC_24140	UGCGGCUGUAAGAUUUCACCCAGCGUGCUGGAGACCAUACUGCACAGCGAU
ctu:CTU_18100	UGCGGUUGUAAAAUUUCCCCGAAAGUGCUGGAAACCAUCCUGCACAGCGAU
enc:ECL_02462	UGCGGUUGUAAAAUUUCCCCAAAGUGCUGGAAACCAUCCUGCACAGUGAA
kpn:KPN_01207	UGUGGUUGUAAAAUUUCCCGAAAGUGCUGGAAACUAUCCUGCAUAGCGAG
eco:b1764	UGCGGCUGUAAAAUUUCCCCAAAAGUGUUGGAAACCAUCCUGCAUAGUGAG
sty:STY1817	UGCGGUUGUAAAAUUUCCCCUAAAGUGCUGGAGACUAUCCUGCAUAGCGAG
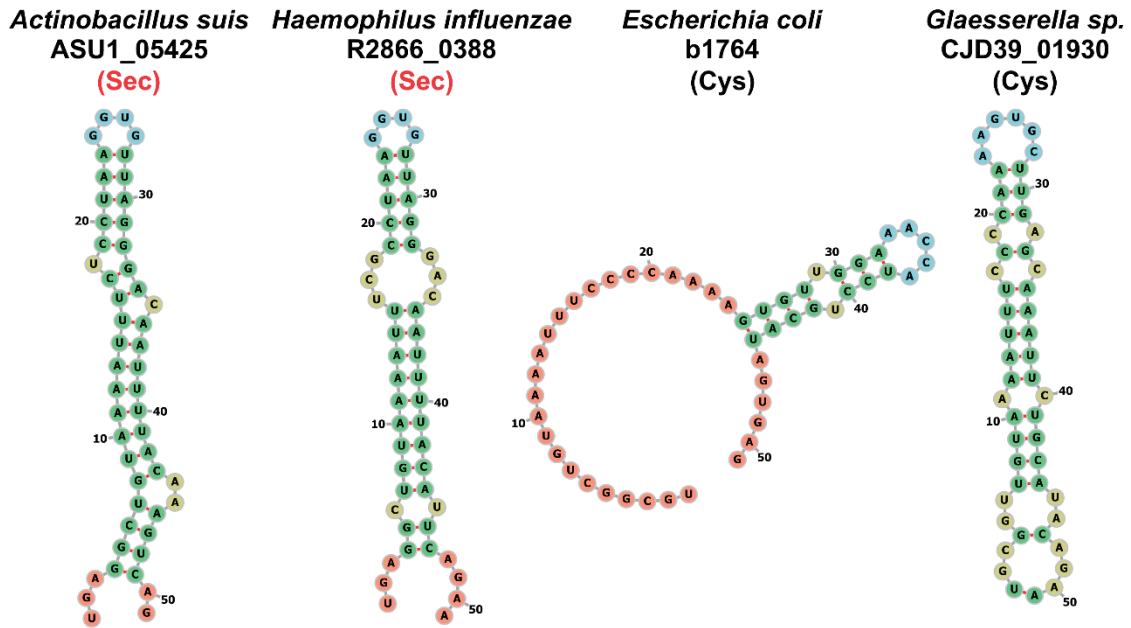
Figure 3. **Prediction of the secondary structure of *selD* SECIS and corresponding regions**

SECIS-like sequences and their corresponding regions were extracted from four representative *selD* nucleotide sequences, and RNA secondary structure prediction was performed using the MXfold2 Server (http://www.dna.bio.keio.ac.jp/mxfold2/). The origin of each SECIS sequence is as follows: *Actinobacillus suis* (Sec-type, ASU1_05425), *Haemophilus influenzae* (Sec-type, R2866_0388), *Escherichia coli* (Cys-type, b1764), *Glaesserella* sp. 15-184 (Cys-type, CJD39_01930).
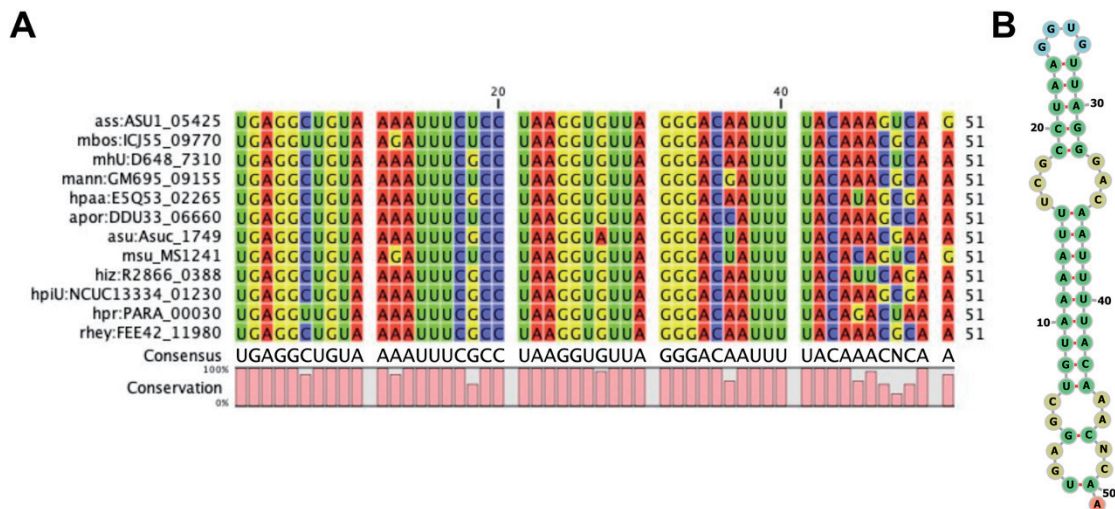

Figure 4. **(A) Comparison of nucleotide sequences of SECIS elements in Sec-type SelD genes. (B) Predicted secondary structure derived from the consensus sequence of SECIS elements in Sec-type SelD genes**

(A) The multiple alignment was created using CLC sequence viewer. (B) The secondary structure predictions were performed using the MXfold2 server (http://www.dna.bio.keio.ac.jp/mxfold2/).

Coomassie Brilliant Blue (CBB)-stained protein bands and immuno-reactive bands around 37 kDa were observed for both HinSelD (calculated molecular mass of 37.2 kDa) and EcoSelD (calculated molecular mass of 37.5 kDa) under IPTG induction, indicating successful expression of HinSelD in *E. coli* (**Figure 5**). This suggests that the HinSelD SECIS is functional for Sec insertion in the *E. coli* host translation system. IPTG induction resulted in higher protein expression levels compared to lactose induction. Based on the results, the optimal expression conditions were determined to be shaking incubation at 37°C with 0.1 mM IPTG, which were employed for subsequent analyses. EcoSelD migrated faster than HinSelD on SDS-PAGE for reasons that remain unclear.
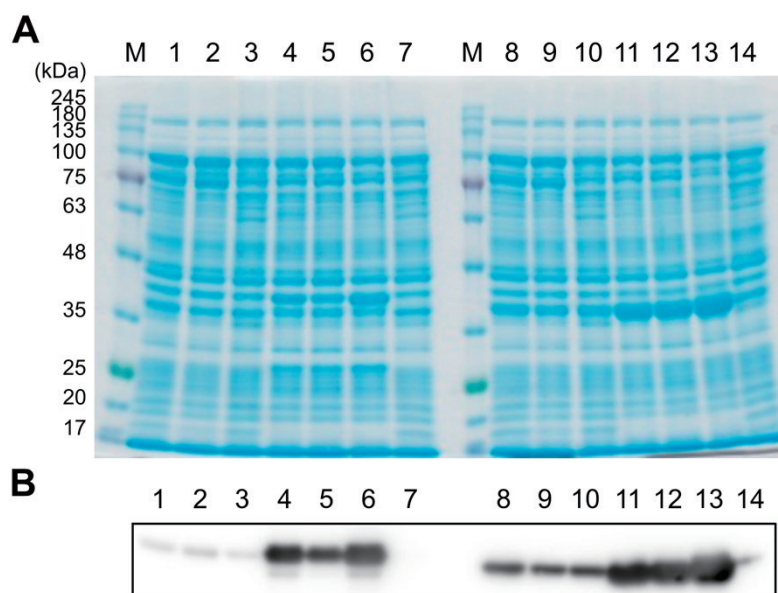

Figure 5. Optimization of expression conditions for HinSelD and EcoSelD
Crude cell extracts (8 µg of protein each) from *E. coli* BL21(DE3) cells carrying either pHinSelD (lanes 1–6) or pEcoSelD (lanes 8–13) were separated on 10% SDS-PAGE gel, stained with CBB (A), and analyzed by Western blotting using an anti-His tag antibody (B). The cultivation conditions were as follows: 0.4% lactose, 37°C, static (lanes 1 and 8); 0.4% lactose, 30°C, static (lane 2 and 9); 0.4% lactose, 37°C, shaking (lane 3 and 10); 0.1 mM IPTG, 37°C, static (lane 4 and 11); 0.1 mM IPTG, 30°C, static (lane 5 and 12); and 0.1 mM IPTG, 37°C, shaking (lane 6 and 13). Lanes M represent the protein marker, while lanes 7 and 14 correspond to crude extracts of *E. coli* BL21(DE3) cells without plasmid, cultivated with 0.1 mM IPTG at 37°C under shaking conditions.

Effects of HinSelD SECIS mutations on Sec insertion in HinSelD

Given that the HinSelD SECIS was functional for a read-through of the UGA codon as Sec in the *E. coli* host, we investigated to determine which regions of the HinSelD SECIS are critical for Sec insertion. By comparing the nucleotide sequences of HinSelD SECIS and EcoSelD SECIS, we designed four HinSelD expression plasmids containing different SECIS variants (**Figure 6**). The first mutant, G69A, involved changing the G in the apical loop of HinSelD SECIS to A, as seen in *E. coli*. The second mutant, A75G, involved altering the upper UA base pair in the upper stem to UG. The third mutant, G77A, involved changing the CG base pair in the lower stem to CA, and the fourth mutant, U84C, involved altering the AU base pair in the lower stem to AC. Additionally, we designed a Sec16Cys mutant enzyme by changing the UGA codon for Sec to UGC for Cys. Using the MXfold2 Server [15], we predicted the secondary structures of these SECIS mutants (G69A, A75G, G77A, U84C) (**Figure 6B**).

    E. coli BL21(DE3) was transformed with expression plasmids containing these HinSelD SECIS variants, and the
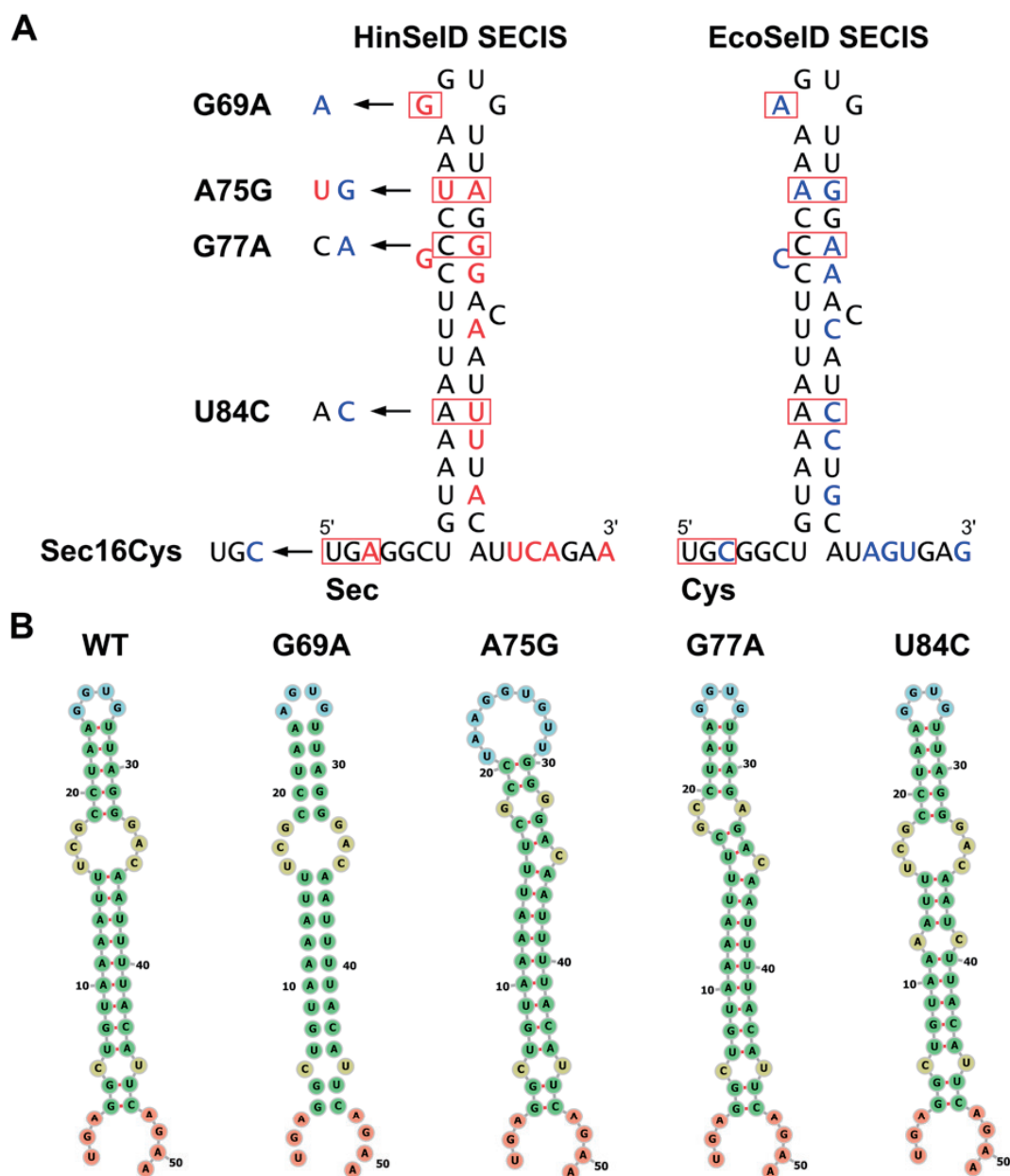
Figure 6. **Comparison of the SECIS elements in HinSelD and EcoSelD and design of site-directed mutations in the HinSelD SECIS element**

(A) Nucleotide differences in the SECIS elements between HinSelD and EcoSelD are highlighted in red and blue, respectively. The secondary structure of the HinSelD SECIS element is shown on the left, and the corresponding region from EcoSelD is displayed on the right for comparison. Although the SECIS element of EcoSelD is predicted not to adopt the secondary structure, it is presented in this way for ease of comparison. The positions where site-directed mutations were introduced in the SECIS elements are indicated and highlighted by black arrows and red rectangles. (B) Secondary structure predictions of SECIS elements of the wild-type HinSelD (WT) and its variants, G69A, A75G, G77A, and U84C. The secondary structure predictions were performed using the MXfold2 server (http://www.dna.bio.keio.ac.jp/mxfold2/).

expression was induced under the conditions mentioned above. The crude extracts were analyzed by SDS-PAGE and Western blot using anti-His tag antibody, and the results are shown in **Figure 7**. Compared to the wild-type HinSelD, all SECIS variants showed decreased expression levels (69–93%). Notably, the G77A mutant exhibited a significant reduction, with expression levels dropping to approximately 69% of the wild type. This was surprising, given that the four base pair stem immediately below the apical loop was predicted to be retained in G77A (**Figure 6B**), predicting a minimal impact [6]. The G69A mutation had the least impact, with expression levels at 93% of the wild type. This result is consistent with the consensus bacterial SECIS model proposed by Zhang and Gladyshev, which requires at least one G among the first two nucleotides in the apical loop [6]. The A75G mutant, predicted to have the most divergent secondary structure from the wild type (**Figure 6D**) and to disrupt the typically essential four base pairs immediately below the apical loop [6], had an impact of about 81% levels on expression. The U84C mutant, which introduced a mutation in the lower stem [6], was presumed to have a mild effect due to the presence of base pairs above and below the mutation site; however, it showed expression levels at 69% of the wild type. None of the mutations caused a drastic decrease in expression, suggesting that significant effects may require multiple mutations. This also implies a degree of flexibility in recognizing SECIS in Sec-type SelD in *E. coli*. On the other hand, the Sec16Cys mutant exhibited expression levels comparable to the wild-type HinSelD and EcoSelD, indicating that the translation efficiency of UGA for Sec is similar to that of UGC for Cys (**Figure 7**). This result suggests that while the SECIS is maintained in the Sec16Cys mutant, the secondary structure of the SECIS does not inhibit the translation of the preceding UGC codon for Cys.

In conclusion, there is strong conservation between the UGA Sec codon and the SECIS secondary structures in *selD* genes. Although nucleotide differences between the HinSelD and EcoSelD SECIS regions play important roles in UGA translation efficiency, with varying impacts depending on their positions, there is also a degree of flexibility in SECIS recognition in Sec-type SelD in *E. coli*. These findings contribute to a deeper understanding of the mechanisms underlying SECIS recognition and the evolution of SECIS elements in bacteria.
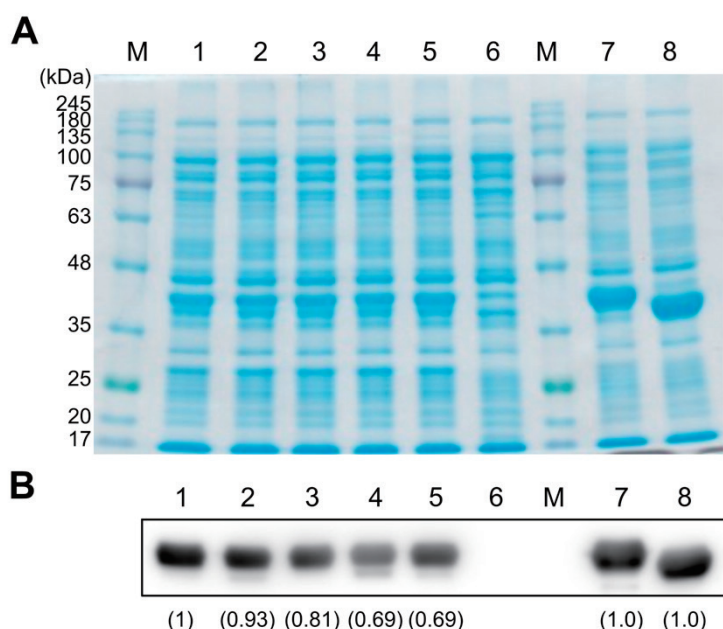

Figure 7. | **Comparison of expression levels of mutant HinSelDs in *E. coli* host cells**
Crude cell extracts (8 μg of protein each) from *E. coli* BL21(DE3) cells expressing wild-type HinSelD (lane 1), G69A (lane 2), A75G (lane 3), G77A (lane 4), U84C (lane 5), Sec16Cys (lane 7), and EcoSelD (lane 8) were separated on 10% SDS-PAGE gel, stained with CBB (A), and analyzed by Western blotting using an anti-His tag antibody (B). Lanes M contain the protein marker, and lane 6 corresponds to the crude extracts of *E. coli* BL21(DE3) cells without plasmid. The band intensities were quantified using ImageJ software based on Western blot analysis.

References
[1] Stadtman TC. Biosynthesis and function of selenocysteine-containing enzymes. *J Biol Chem*. 1991; 266: 16257-16260.

[2] Forchhammer K, Böck A. Selenocysteine synthase from *Escherichia coli*. Analysis of the reaction sequence. *J Biol Chem*. 1991; 266: 6324-6328.

[3] Leinfelder W, Zehelein E, Mandrand-Berthelot MA, Böck A. Gene for a novel tRNA species that accepts L-serine and cotranslationally inserts selenocysteine. *Nature*. 1988; 331: 723-725.

[4] Ehrenreich A, Forchhammer K, Tormay P, Veprek B, Böck A. Selenoprotein synthesis in *E. coli*. Purification and characterisation of the enzyme catalysing selenium activation. *Eur J Biochem*. 1992; 206: 767-773.

[5] Baron C, Heider J, Böck A. Interaction of translation factor SELB with the formate dehydrogenase H selenopolypeptide mRNA. *Proc Natl Acad Sci USA*. 1993; 90: 4181-4185.

[6] Zhang Y, Gladyshev VN. An algorithm for identification of bacterial selenocysteine insertion sequence elements and selenoprotein genes. *Bioinformatics*. 2005; 21: 2580-2589.

[7] Lacourciere GM, Stadtman TC. Catalytic properties of selenophosphate synthetases: comparison of the selenocysteine-containing enzyme from *Haemophilus influenzae* with the corresponding cysteine-containing enzyme from *Escherichia coli*. *Proc Natl Acad Sci USA*. 1999; 96: 44-48.

[8] Kim IY, Veres Z, Stadtman TC. *Escherichia coli* mutant SELD enzymes. The cysteine 17 residue is essential for selenophosphate formation from ATP and selenide. *J Biol Chem*. 1992; 267: 19650-19654.

[9] Altschul SF, Gish W, Miller W, Myers EW, Lipman DJ. Basic local alignment search tool. *J Mol Biol*. 1990; 215: 403-410.

[10] Kumar S, Stecher G, Tamura K. MEGA7: Molecular evolutionary genetics analysis version 7.0 for bigger datasets. *Mol Biol Evol*. 2016; 33: 1870-1874.

[11] Minh BQ, Schmidt HA, Chernomor O, Schrempf D, Woodhams MD, von Haeseler A, Lanfear R. Corrigendum to: IQ-TREE 2: New models and efficient methods for phylogenetic inference in the genomic era. *Mol Biol Evol*. 2020; 37: 2461.

[12] Guindon S, Dufayard JF, Lefort V, Anisimova M, Hordijk W, Gascuel O. New algorithms and methods to estimate maximum-likelihood phylogenies: assessing the performance of PhyML 3.0. *Syst Biol*. 2010; 59: 307-321.

[13] Minh BQ, Nguyen MA, von Haeseler A. Ultrafast approximation for phylogenetic bootstrap. *Mol Biol Evol*. 2013; 30: 1188-1195.

[14] Letunic I, Bork P. Interactive Tree of Life (iTOL) v6: recent updates to the phylogenetic tree display and annotation tool. *Nucleic Acids Res*. 2024; 52: W78-W82.

[15] Sato K, Akiyama M, Sakakibara Y. RNA secondary structure prediction using deep learning with thermodynamic integration. *Nat Commun*. 2021; 12: 941.

[16] Schneider CA, Rasband WS, Eliceiri KW. NIH Image to ImageJ: 25 years of image analysis. *Nat Methods*. 2012; 9: 671-675.
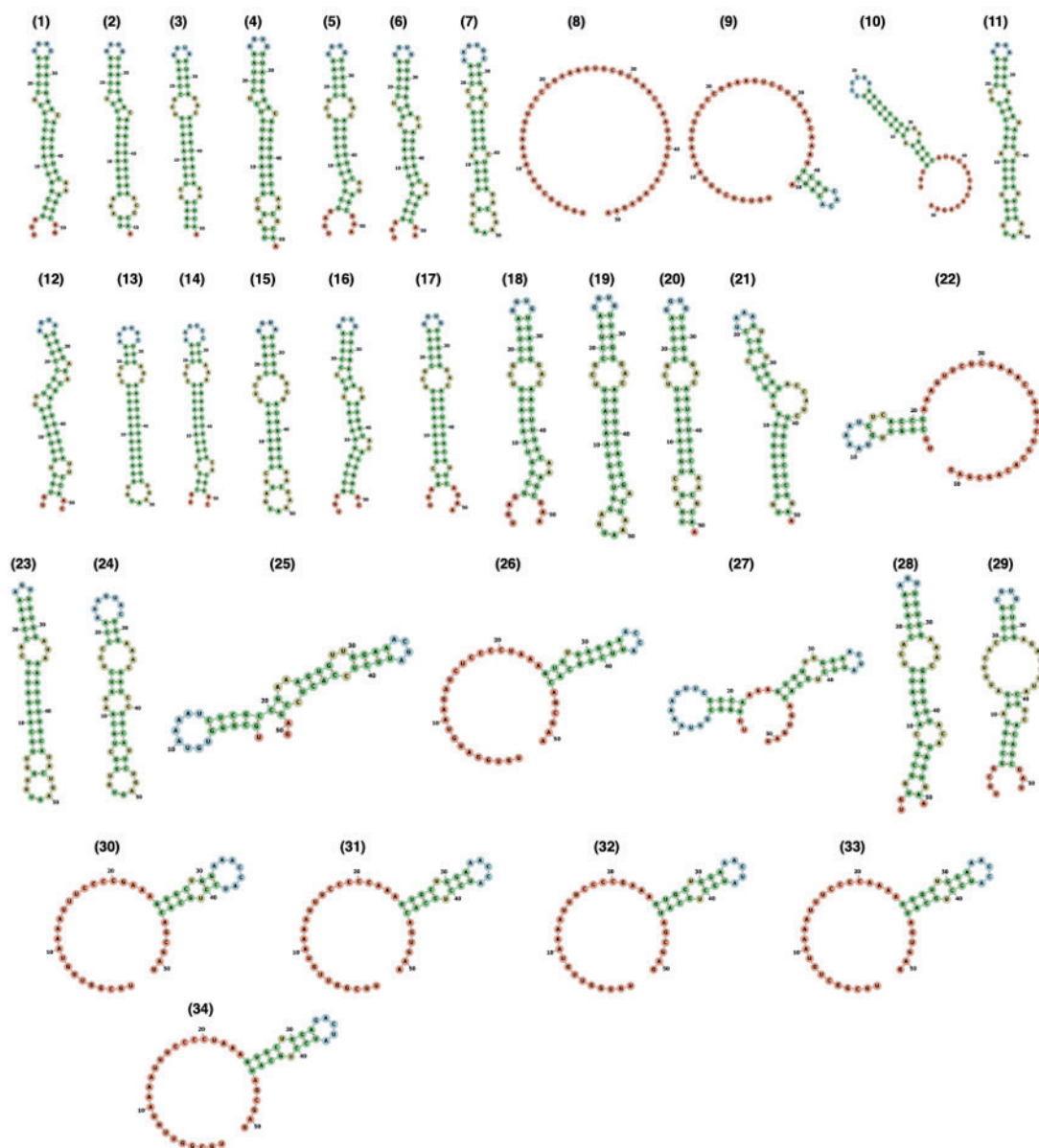
Supplementary data

Figure S1. **Prediction of the secondary structure of *selD* SECIS and corresponding regions**

SECIS-like sequences were extracted from 34 *selD* nucleotide sequences, and RNA secondary structure prediction was performed using the MXfold2 Server (http://www.dna.bio.keio.ac.jp/mxfold2/). The origin of each SECIS sequence is as follows: *Actinobacillus suis* (1, ASU1_05425), *Mannheimia bovis* (2, ICJ55_09770), *Mannheimia haemolytica* (3, D648_7310), *Mannheimia ovis* (4, GM695_09155), *Haemophilus parahaemolyticus* (5, E5Q53_02265), *Actinobacillus porcitonsillarum* (6, DDU33_06660), *Glaesserella* sp. 15-184 (7, CJD39_01930), *Actinobacillus indolicus* (8, EXH44_09840), *Glaesserella parasuis* (9, HAPS_0664), *Gallibacterium anatis* (10, UMN179_00129), *Aggregatibacter actinomycetemcomitans* (11, ANH9381_1552), *Pasteurella aerogenes* (12, NCTC13378_00962), *Pasteurella dagmatis* (13, 4362423_01086), *Pasteurella multocida* (14, PM0790), *Actinobacillus succinogenes* (15, Asuc_1749), *Mannheimia succiniciproducens* (16, MS1241), *Haemophilus influenzae* (17, R2866_0388), *Haemophilus pittmaniae* (18, NCTC13334_01230), *Haemophilus parainfluenzae* (19, PARA_00030), *Rodentibacter heylii* (20, FEE42_11980), *Plesiomonas shigelloides* (21, SAMEA2665130_2106) , *Serratia proteamaculans* (22, Spro_2720), *Yersinia pestis* (23, YPO2164), *Jinshanibacter zhutongyuii* (24, EKN56_04870), *Leminorella richardii* (25, NCTC12151_01459), *Hafnia alvei* (26, AT03_10065), *Xenorhabdus bovienii* (27, XBW1_2237), *Proteus mirabilis* (28, PMI1497), *Erwinia billingiae* (29, EbC_24140), *Cronobacter turicensis* (30, CTU_18100), *Enterobacter cloacae* (31, ECL_02462), *Klebsiella pneumoniae* (32, KPN_01207), *Escherichia coli* (33, b1764), *Salmonella enterica* (34, STY1817).

Regular article

Gene Encoding for Methyltransferase Contributing to Dimethyl Diselenide Synthesis Among Methylated Selenium from *Stutzerimonas stutzeri* NT-I

Osamu Otsuka[1,2]*, Mitsuo Yamashita[1]

[1] Collaborative Research Programs for metal biotechnology, Shibaura Institute of Technology, Tokyo, Japan
[2] KFC Ltd., Saitama, Japan

Abstract

Selenium (Se) is a rare metal refined from the slime byproduct of copper anodes. Selenium circulates globally in various valence states and forms. Soluble selenooxyanions, such as selenate (SeO_4^{2-}) and selenite (SeO_3^{2-}) are converted to volatile dimethyl selenide (DMSe) and dimethyl diselenide (DMDSe) and vaporized. Although some microorganisms synthesize volatile Se compounds, and volatile Se compounds is used for resource recovery and soil remediation, the synthesis pathway of DMDSe has not yet been identified.

We hypothesized that a methyltransferase in the *Stutzerimonas stutzeri* NT-I specific contig is involved in the synthesis of methylated Se in *S. stutzeri* NT-I and cloned the gene encoding the enzyme. We carried out qualitative analysis of synthesized volatile Se compounds using the transgenic *E. coli* DH5α pGEM-mdsN. A novel gene involved in DMDSe synthesis was identified and named *mdsN* and found to encode a class I SAM-dependent methyltransferase. When the *mdsN* was introduced into *E. coli* DH5α, the recombinant *E. coli* DH5α pGEM-mdsN acquired the ability to synthesize DMDSe, which corresponds to 62% of the initial Se concentration. In this paper, we report a novel finding that *E. coli* DH5α pGEM-mdsN, in which *mdsN* from *S. stutzeri* NT-I was transformed into *E. coli* DH5α, synthesized DMDSe from SeO_3^{2-} and Bio-Se[0] from *S. stutzeri* NT-I.

* Correspondence:

Osamu Otsuka
KFC Ltd.
1-19 Ookuwa, Kazo-city, Saitama 347-0010, Japan
Tel : +81-480-76-0095
Fax : +81-480-65-8608
E-mail : ootsuka.osamu@kfc-net.co.jp

Introduction

Selenium (Se) is produced as a by-product of copper in nonferrous metal smelters [1]. Selenium is an industrially important metal resource utilized in photocopiers, glass dyeing, and semiconductor materials, and in pharmaceutical and supplement applications [2]. Moreover, Se circulates in the global environment in various valences and forms. Soluble selenooxyanions, such as selenate (SeO_4^{2-}) and selenite (SeO_3^{2-}), present in the soil are converted to volatile dimethyl selenide (DMSe) and dimethyl diselenide (DMDSe), vaporized, and oxidized in the atmosphere to SeO_4^{2-} and SeO_3^{2-}, which are then

Table 1 | **Volatile selenium–producing microorganisms and associated synthetic substances**

Bacterial strain	Substrate		Substances	Reference
	Concentration	Species		
*Enterobacter cloacae SLD*1a-1	0.01-1.0 mM	SeO_3^{2-}	**DMSe**	[4]
Methylococcus capsulatus (Bath) (NCIBM11132)	20-40 mg·L^{-1}	SeO_3^{2-}	DMSe, DMDSe, DMSeS, Methylselenol, Methylselenoacetate	[5]
	20-40 mg·L^{-1}	Bio-Se^0	DMDSe, DMSeS, DMSe	
	20-40 mg·L^{-1}	Chem-Se^0	DMDSe, DMSeS, DMSe	
Methylosinus trichosporium OB3b (NCIMB 11131)	10-20 mg·L^{-1}	SeO_3^{2-}	DMDSe, DMSeS	[5]
	10-20 mg·L^{-1}	Bio-Se^0	DMDSe, DMSe	
	10-20 mg·L^{-1}	Chem-Se^0	**DMSe**	
Rhodocyclus tenuis DSM 109	1 mM	SeO_4^{2-}	DMDSe, DMSe	[6]
	1 mM	SeO_3^{2-}	**DMSe**	
Rhodobacter sphaeroides DSM 158	114 mg·L^{-1}	SeO_4^{2-}	**DMSe**	[7]
	0.80 mg·L^{-1}	SeO_4^{2-}	—	
	104 mg·L^{-1}	SeO_3^{2-}	DMDSe, DMSeS, **DMSe**	
	0.86 mg·L^{-1}	SeO_3^{2-}	—	
Stenotrophomonas bentonitica	100 mM	SeO_4^{2-}	DMDSe, DMSeS, **DMSe**	[8]
	2 mM	SeO_4^{2-}	—	
	0.1-2 mM	SeO_3^{2-}	**DMDSe**, DMSeS	[9]
Stenotrophomonas maltophilia	0.5 mM	SeO_4^{2-}	**DMDSe**, DMSeS, DMSe	[10]
	0.5 mM	SeO_3^{2-}	**DMDSe**, DMSeS, DMSe	
Stutzerimonas stutzeri NT-I	0.5-5 mM	SeO_4^{2-}	**DMDSe**, DMSeS, DMSe	[11,12]
	0.5-5 mM	SeO_3^{2-}	**DMDSe**, DMSeS, DMSe	
	0.5-5 mM	Bio-Se^0	**DMDSe**, DMSeS, DMSe	
Escherichia coli DH5α pGEM	0.5 mM	SeO_3^{2-}	—	This study
	0.5 mM	Bio-Se^0	—	
Escherichia coli DH5α pGEM-mdsN	0.5 mM	SeO_3^{2-}	**DMDSe**	This study
	0.5 mM	Bio-Se^0	**DMDSe**	

Note: Primary synthesized substances are shown in bold letters. — indicates no substances synthesized.

carried by rainfall [3]. Microorganisms capable of converting SeO_4^{2-} or SeO_3^{2-} into volatile Se compounds have been reported[4-12], suggesting that microbial Se metabolism is involved in global Se cycle.

Among the reports of microorganisms synthesizing volatile Se compounds, there are many reports that multiple methylated selenocompounds such as DMSe and dimethyl selenosulfide (DMSeS) were detected simultaneously (**Table 1**). Some organisms, such as *Enterobacter cloacae* SLD1a-1, synthesize only DMSe [4]. However, to date, no microorganisms that synthesize only DMDSe have been reported. In addition, some microorganisms have different volatile selenium compounds depending on the type of substrate [5,6]. Volatile Se compounds synthesized by *Methylosinus trichosporium* OB3b (NCIMB 11131) include DMDSe and DMSe derived from SeO_3^{2-}, DMDSe and DMSe from bioselenium (Bio-Se^0), and DMSe from elemental selenium(Se^0) [5]. In addition, some microorganisms synthesize volatile Se compounds depending on the substrate concentration [7-9]. However, some microorganisms can synthesize DMDSe in different substrates [10,11]. *Stutzerimonas stutzeri* NT-I reduces SeO_4^{2-}, SeO_3^{2-}, and Se^0 to form DMDSe and DMSeS [11,12]. We previously developed a method to reduce selenooxyanions in solution to volatile

DMDSe and then recover volatile DMDSe with a concentrated nitric acid by utilizing the high SeO_4^{2-} metabolism ability of *S. stutzeri* NT-I [12]. Subsequently, selenium recovered from wastewater was purified to high purity and successfully recycled [12]. It is also used to remove Se from soil by synthesis volatile Se compounds from soluble Se in soil and wastewater [13].

Although some microorganisms synthesize DMDSe and volatile Se compounds, and volatile Se compounds is used for resource recovery and soil remediation, the synthesis pathway of DMDSe has not yet been identified. The ability of *S. stutzeri* NT-I to synthesize DMDSe has been characterized [12]; thus, the DMDSe synthesis pathway can be estimated by analyzing this process. We searched for candidate genes related to DMDSe synthesis from genomic analysis of *S. stutzeri* NT-I and introduced the genes into *Escherichia coli* DH5α to express DMDSe synthesis in recombinant *E. coli* DH5α.

Materials and methods

Growth media and conditions

Stutzerimonas stutzeri NT-I was cultured in Bacto trypticase soy broth (TSB; Becton-Dickinson) or on TSB plates containing 1.5% agar. TSB medium supplemented with ampicillin to a final concentration of 30 µg·mL^{-1} or TSB plate medium with 1.5% agar and 2% Xgal 50 µL per plate was used to cultivate recombinant *E. coli* DH5α. Bacterial growth in the culture medium was calculated from the optical density (OD_{600}) at 600 nm using a spectrophotometer (V-600, JASCO Corporation).

DNA cloning and sequencing

The genomic DNA of *S. stutzeri* NT-I was extracted using ISOPLANT (Nippon Gene Co., Ltd.). Using the extracted DNA as a template, the Se methylation candidate gene *mdsN* from *S. stutzeri* NT-I was amplified via polymerase chain reaction (PCR) using the forward primer 5 '-GCGAGAGATTCTCGAC -3', reverse primer 5'-CTCTCCTGTTCTGAATCAGT -3', and TaKaRa La Taq® polymerase (Takara Bio Inc., Japan). The amplification products were TA-cloned (plasmid pGEM-mdsN) using the pGEM-T Easy Vector System (Promega Corporation). White colonies were selected by blue–white selection. Plasmid pGEM-mdsN was extracted from *E. coli* DH5α, and the sequence of the insert was determined using the forward primer 5 '-GTTTTCCCAGTCACGAC -3' and reverse primer 5 '-CAGGAAACAGCTATGAC -3' on a 3730xl DNA Analyzer (Applied Biosystems, Inc.). The *E. coli* DH5α transformed with the pGEM vector was referred to as the *E. coli* DH5α pGEM-control. The obtained sequences were subjected to a homology search using the BLASTN and BLASTX software, supplied by the National Center for Biotechnology Information.

Bio-selenium preparation

Tryptic soy broth (TSB) medium (Becton Dickinson; 30 g·L^{-1}) was used for cultivating the *S. stutzeri* NT-I. A loopful of a colony of *S. stutzeri* NT-I was inoculated into 50 mL TSB in a 100 mL Erlenmeyer flask and cultivated at 30 °C for 24 h on a rotary shaker at 120 rpm. A total of 0.5 mL of the culture was then transferred into 50 mL TSB in a 100 mL Erlenmeyer flask and cultivated for 12 h under the same conditions. Bacterial cells were harvested by centrifugation at 1,500 × g, 4 °C for 20 min. The harvested bacterial cells were suspended in adding a sterilized saline solution to $OD_{600} = 1.0$, and then used as the pre-culture solution. The TSB cultivation medium (3 L) was placed inside a jar fermenter (Bioneer C500N type 5L (S) supplied by B.E. Marubishi), which was then autoclaved for 15 min at 101.33 kPa and 121 °C. After autoclaved, sodium selenate was added in the TSB medium to the final Se concentration 5 mmol·L^{-1}, which was used as the simulated wastewater. A total of 30 mL of the pre-culture solution was added to this simulated wastewater, cultivation performed under controlled: cultivation temperature, 38 °C; pH, 9.0; agitation speed, 250 rpm; and air flow rate, 1 L·min^{-1}. Selenate in the simulated wastewater is almost completely reduced to SeO_3^{2-} by *S. stutzeri* NT-I in 12 h, while after 48 h approximately 90% of SeO_3^{2-} is reduced to Se^0. After 48 h, air flow was stopped and the cultivation was continued for another 24 h.

The culture was centrifuged at 6,000 × g, 4 °C for 20 min to harvest the mixture of the cells and Se^0. The precipitates were washed with 600 mL of distilled water, and then centrifuged for at 6,000 × g, 4 °C for 20 min. The

supernatant was discarded. Next, 600 mL of 70% ethanol was added to the precipitations, which were recovered by centrifugation at $20,000 \times g$, 4 °C for 20 min. This precipitates were referred to Bio-Se^0. Bio-selenium was then dried by using an automatic oven at 40 °C for 24 h. The color of the Bio-Se^0 was red.

Selenite reduction test

One colony was scraped from a plate of *S. stutzeri* NT-I and recombinant *E. coli* DH5α pGEM-mdsN, *E. coli* DH5α pGEM-control, inoculated into 50 mL of TSB medium (pH 7.0) in a 100 mL volume flask, and cultivated at 30 °C for 24 h on a rotary shaker at 120 rpm. A total of 0.5 mL of the culture was then transferred into 50 mL TSB in a 100 mL Erlenmeyer flask and cultivated for 12 h under the same conditions. Subsequently, bacterial cells were collected by centrifugation ($15,000 \times g$, 20 °C for 5 min), and the collected bacterial cells were suspended in sterile saline and adjusted to an $OD_{600}=1.0$.

Then, 30 mL of the suspension was added to 3 L of TSB medium containing 0.5 mM SeO_3^{2-} and 30 μg·mL^{-1} ampicillin in a 5L-volume jar fermenter (Bioneer-C500 N Model 5 L (S), B.E.MARUBISHI CO., LTD.). Culturing was carried out at 38 °C, pH 7.0, aeration at 1 L·min^{-1}, and agitation speed at 120 rpm. The pH was adjusted using 30% sodium hydroxide solution and 2 N hydrochloric acid solution. Dissolved oxygen (DO) and pH were measured using a DO electrode OX-2500 and a pH combination electrode MPS-220 (B.E. MARUBISHI Co., Ltd.), respectively. The recovery method of volatilized Se compounds was referred to by Winkel *et al.* [14]. The exhaust from the jar fermenter was passed through 150 mL of concentrated nitric acid solution (*i.e.*, a gas trap) dispensed into a 250 mL capacity reagent bottle using a Teflon tube (inner diameter, 5 mm; outer diameter, 6 mm). The cultures and concentrated nitric acid were collected each 24h.

Qualitative methylated selenium

S. stutzeri NT-I, *E. coli* DH5α pGEM-control, and *E. coli* DH5α pGEM-mdsN were each plated with one colony, inoculated into 50 mL of TSB medium in a 100 mL volume flask, and incubated aerobically at 37 °C for 24 h. The culture medium was inoculated into 1 mL TSB medium, incubated under the same conditions for 12 h, and used as the preculture medium. Bacteria were obtained by centrifugation ($2,300 \times g$, 4 °C for 20 min) from the preculture solution. Bacterial cells were washed twice with sterile saline and resuspended in saline to an $OD_{600} = 1.0$. Then, 10 mL of TSB medium was added to a 100 mL volume vial, and Bio-Se^0 or SeO_3^{2-} was added as a substrate to achieve a final Se concentration of 0.5 mM. Then, 100 μL of the resuspension solution was added to the flask, which was then stoppered with butyl rubber and incubated at 37 °C for 12 h with shaking. After 12 h of incubation, 250 μL of the gas-phase sample was collected using a micro-syringe, and the gas-phase components were qualitatively analyzed by GC-MS (FocusGC DSQII, Thermo Fisher Scientific K.K).

Qualitative and quantitative analysis of elements

Before measuring the Se concentration, the samples were centrifuged ($15,000 \times g$, 20 °C for 5 min) to separate the supernatant from the precipitate. The supernatants were filtered with a membrane filter (0.2 μm pore size, Steradisc 13, Kurabo, Osaka, Japan), and the resultant filtrates were used to measure Se concentration. Selenate and SeO_3^{2-} concentrations were determined using an ion chromatography (IC) system (ICS-1100, Thermo Fisher Scientific K.K.) equipped with a DS6 heated conductivity cell detector and an ASRS300 suppressor. An IonPac AS12A separation column (Thermo Fisher Scientific K.K) equipped with an AG12A guard column (Thermo Fisher Scientific K.K) was used. The mobile phase comprised 3 mM sodium carbonate solution prepared with ultrapure water (Barnstead NANO Pure, Thermo Fisher Scientific K.K.) at a flow rate of 1.5 mL·min^{-1}. The total soluble Se concentration in the supernatant was determined using inductively coupled plasma atomic emission spectrometry (ICP-AES) (iCAP 6300 Duo, Thermo Fisher Scientific K.K.). The soluble Se concentrations other than SeO_4^{2-} and SeO_3^{2-} were calculated by subtracting the SeO_4^{2-} and SeO_3^{2-} concentrations from the total soluble Se concentration. The concentrations of the metal elements in the volatile substances collected in gas trap were also measured using ICP-AES. The precipitates were washed with 2 mL of ultrapure water and collected by centrifugation ($15,000 \times g$,

20 °C for 5 min). The washing procedure was repeated twice. Next, the precipitates were digested in a mixed acid solution (1,500 μL of 60% nitric acid solution, and 50 μL of 95% sulfuric acid solution) using a vortex for 10 min. After centrifugation (15,000 × g, 20 °C for 5 min), the supernatants were collected in a volumetric flask. The acid-digestion supernatants were mixed in a volumetric measuring flask with ultrapure water to a total volume of 10 mL. The total Se concentration in the digested samples was determined by ICP-AES. All samples were measured in triplicate, and the average values were used for the analysis.

Analysis of selenium species in the gas phase

The exhausted gaseous samples were analyzed using GC-MS. A fused-silica capillary column (30 m × 0.250 mm (inner diameter)) (DB-624, Agilent Technologies) was used. Splitless injections were performed, and the split valve was opened 1 min after injection. Helium was used as the carrier gas at 1.0 mL·min^{-1}. The column temperature was programmed from 40 to 240 °C at a rate of 10 °C·min^{-1} after being maintained at 40 °C for 5 min and then kept at 240 °C for 1.5 min. Both the injector and the interface (between GC and MS) temperatures were kept at 200 °C. Ionization was performed in the positive ion mode at an ion source temperature of 220 °C. Gaseous samples were injected at 250 μL by 250 μL of gas tight syringe. DMSe, DMDSe, and DMDS (Tokyo Chemical Industry Co., Ltd.) were used as standard solutions.

Results

Cloning of selenium methylation-related gene

The genome of *S. stutzeri* NT-I has been characterized previously, yielding 115 contig sequences with a total contig base number of 63,558,482 bp [15]. Comparative genomic analysis of the reference strain, *Stutzerimonas stutzeri* A1501, revealed 43 contigs unique to *S. stutzeri* NT-I (data not shown). *S. stutzeri* NT-I-specific contigs contained SeO_4^{2-} reduction genes such as the SeO_4^{2-} reduction gene *serA* (Access No. ACV70151), which is a characteristic of *S. stutzeri* NT-I. This suggests that the 43 contigs unique to *S. stutzeri* NT-I characterize its high Se metabolism capacity of *S. stutzeri* NT-I. Genes involved in the synthesis of volatile Se compounds in microorganisms and plants other than *S. stutzeri* NT-I have also been reported. Ranjard *et al*. reported that the gene *tpm*, which encodes thiopurine methyltransferase from *Pseudomonas syringae pathovar pisi*, was transformed into *E. coli* DH10B, and SeO_3^{2-} was added as a substrate to synthesize DMSe and DMDSe [16]. Swearingen *et al.* reported that the gene *ubiE* encoding the ubiquinone/menaquinone biosynthesis C-methyltransferase from *Geobacillus stearothemophilus* V was introduced into *E. coli* K12 to express its ability to synthesize DMSe and DMDSe from SeO_4^{2-} and SeO_3^{2-} [17]. Zhou *et al.* reported that the gene *BoCOQ5-2* encoding COQ5 methyltransferase from *Brassica oleracea varitalica* was transformed into *E. coli* to synthesize DMDSe and DMSe from SeO_4^{2-} [18]. All the enzymes that confer the ability to synthesize volatile Se compounds are methyltransferase genes. However, the genes involved in DMDSe synthesis have not yet been reported.

An open reading frame (ORF) search (ORFFinder NCBI) of 43 contigs unique to *S. stutzeri* NT-I revealed that the gene (Accession No.: PSNT00042, 44319-44918 bp) encoding class I SAM-dependent methyltransferase was included in 43 contigs unique to *S. stutzeri* NT-I. Thus, the gene encoding the class I SAM-dependent methyltransferase was named *mdsN* and designated as a potential selenomethylation gene for *S. stutzeri* NT-I.

The candidate gene *mdsN* was amplified by PCR and subjected to the agarose gel electrophoresis (**Fig. 1**). The PCR amplification product was inserted into the pGEM-T easy vector to transform *E. coli* DH5α. A transformant in which the PCR amplification product of the expected size was inserted was obtained by blue–white selection on the LB-Amp plate medium. The pGEM-mdsN plasmid extracted from the transformant was subjected to restriction enzyme treatment with *Eco*RI. The inserted sequence was excised into an approximately 600 bp fragment (**Fig. 2**). These results indicate that PCR-amplified mdsN could be inserted into the pGEM-easy vector. Sequence analysis of the inserted sequence showed 100% identity with a class I SAM-dependent methyltransferase (Accession No.: PSNT00042, 44319-44918bp) from *S. stutzeri* NT-I registered in NCBI.

E. coli DH5α reduces SeO_3^{2-} and synthesizes Se^0 [19]. However, there is no report on the synthesis of DMDSe and DMSe by the reduction of Se^0 in *E. coli* DH5α. Therefore, *E. coli* DH5α pGEM-control was used as a negative control.
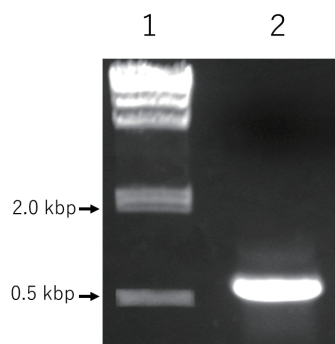
Fig. 1 | **Electrophoresis of PCR products**
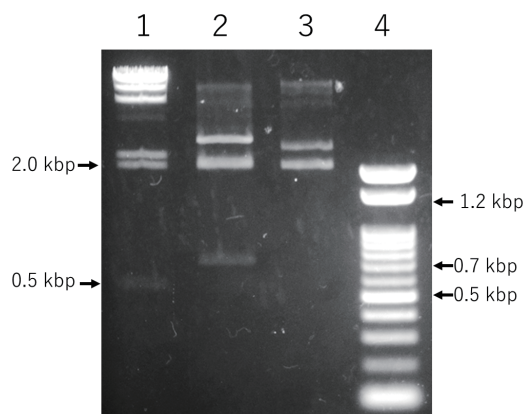Lane 1: λ DNA/HindIII markers;
Lane 2: *mdsN* (about 600 bp)

Fig. 2 | **Electrophoresis of plasmids**
Lane 1: λ DNA/*Hin*dIII markers,
Lane 2: After *Eco*RI restriction enzyme
treatment of pGEM-mdsN;
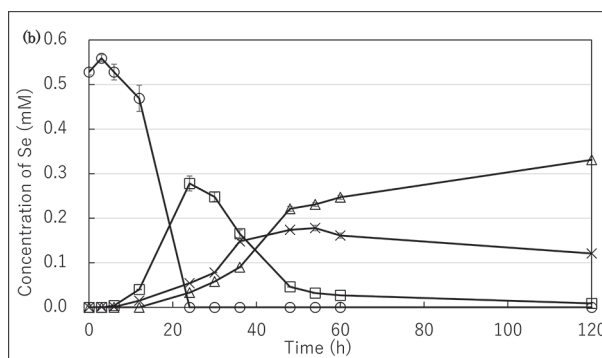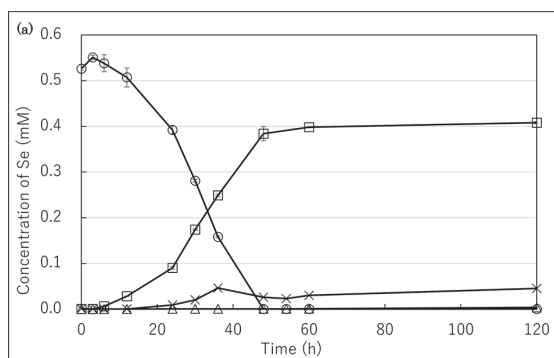Lane 3: pGEM-mdsN;
Lane 4: 100 bp DNA ladder marker.

Fig. 3 | **Time course of selenium concentrations of selenite reduction test**
(a) *E. coli* DH5α pGEM.
(b) *E. coli* DH5α pGEM-mdsN. Circle: Selenite, Square: Elemental selenium, Cross: Soluble Se without selenate and
selenite, Triangle: Volatile selenium (gas trap).

Selenite reduction test of *E. coli* DH5α pGEM-mdsN

E. coli DH5α pGEM-mdsN and negative control *E. coli* DH5α pGEM-control were cultured in TSB medium containing SeO_3^{2-} (**Fig. 3a**). The time course of Se concentrations in the culture medium showed that *E. coli* DH5α pGEM-control reduced SeO_3^{2-} to Se^0 within 48 h after SeO_3^{2-} addition (**Fig. 3a**). Subsequently, Se^0 accounted for 0.41 mM (78% of its initial value) at 120 h. The amount of Se^0 did not decrease between 48 and 120 h. Analysis of metallic elements in the gas trap at 120 h revealed 0.02 mM of sulfur, suggesting that *E. coli* synthesized small amounts of volatilized sulfur compounds (**Table 2**).

Conversely, *E. coli* DH5α pGEM-mdsN reduced SeO_3^{2-} to Se^0 at 24 h after SeO_3^{2-} addition (**Fig. 3b**). Subsequently, elemental selenium decreased from 48 to 120 h to nearly zero. In contrast to the decrease in Se^0 from 48 to 120 h, an increase in Se was detected in the gas trap, suggesting that *E. coli* DH5α pGEM-mdsN synthesized volatilized Se compounds from Se^0 in the culture broth. At 120 h, the Se detected by the gas trap accounted for 62% of the initial value. Analysis of metal elements in the gas trap at 120 h showed that 0.08 mM sulfur and 0.33 mM Se were detected. The amount of Se detected in the gas trap of *E. coli* DH5α pGEM-mdsN was the same as that of *S. stutzeri* NT-I (**Table 2**). Therefore, it was suggested that the transformation of *mdsN* into *E. coli* DH5α had the same high Se methylation ability as that of *S. stutzeri* NT-I. The amount of sulfur produced by *E. coli* DH5α pGEM-mdsN in

Table 2 | **Elemental analysis results in the gas trap (mM)**

Bacterial strain	S	Se
Escherichia coli DH5α pGEM-control	0.02	<0.01
Escherichia coli DH5α pGEM-mdsN	0.08	0.33
Stutzerimonas stutzeri NT-I	0.51	0.37

the gas trap was 4-fold higher than that by *E. coli* DH5α pGEM-control but only approximately 16% of that in the *S. stutzeri* NT-I, suggesting that sulfur volatilization is not enhanced in *E. coli* DH5α pGEM-mdsN.

These results suggest that *mdsN* is strongly involved in the synthesis of volatile Se compounds because it can synthesize volatilized Se compounds in *E. coli* DH5α transfected with the class I SAM-dependent methyltransferase gene from *S. stutzeri* NT-I.

Quantitative determination of volatile selenium compounds

To qualitatively identify the volatile Se compounds synthesized from *E. coli* DH5α pGEM-mdsN with recombinant methyltransferase from *S. stutzeri* NT-I, the gas phase of the culture vessel was analyzed (**Fig. 4**). *S. stutzeri* NT-I synthesizes DMSe and DMDSe when SeO_3^{2-} is used as the substrate, with DMDSe being mainly synthesized (**Fig. 4a**)[11]. When *E. coli* DH5α pGEM-mdsN was incubated with SeO_3^{2-}, only DMDSe was detected in the gas phase (**Fig. 4b**). Conversely, nothing was detected in the gas phase of the culture vessel containing the control *E. coli* DH5α pGEM-control and the negative control experiment containing only SeO_3^{2-} without bacteria (**Fig. 4c, 4f**).

To determine whether volatile Se compounds can be synthesized from Bio-Se^0, a similar experiment was performed by changing the substrate to Bio-Se^0 synthesized by *S. stutzeri* NT-I (**Fig. 5**). The elemental compositions of Bio-Se^0 were quantitatively analyzed using an ICP-AES. Other than Se, inorganic components of Bio-Se^0 comprise six elements: calcium (Ca), potassium (K), magnesium (Mg), sodium (Na), phosphorus (P), and sulfur (S). Bio-selenium was washed with distilled water during its preparation, which removed the TSB medium-derived impurities. Ca, K, Mg, Na, P, and S were suggested to have been derived from bacterial cells. Concentrations of Se in Bio-Se^0 was 11% (mass %)[20]. In the culture of *S. stutzeri* NT-I with Bio-Se^0 as the substrate, DMDSe and a small amount of DMSe were observed, similar to the SeO_3^{2-} added culture (**Fig. 5a**). In contrast, no Se species were detected in the gas phase when Bio-Se^0 alone was added to the TSB medium without bacteria (**Fig. 5d**). Because no turbidity change was observed in the culture solution containing only Bio-Se^0, it is considered that all the *S. stutzeri* NT-I used in the synthesis may have been killed in Bio-Se^0, and there was no microbial contamination in the Bio-Se^0.
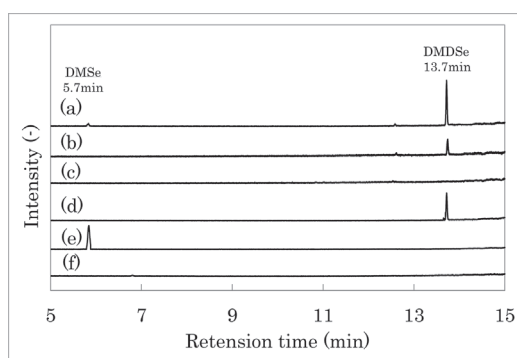

Fig. 4 | **GC-MS spectra of gas phase from selenite reduction test**
(a) *S. stutzeri* NT-I,
(b) *E. coli* DH5α pGEM-mdsN,
(c) *E. coli* DH5α pGEM-control,
(d) DMDSe std,
(e) DMSe std, and (f) selenite without bacteria.

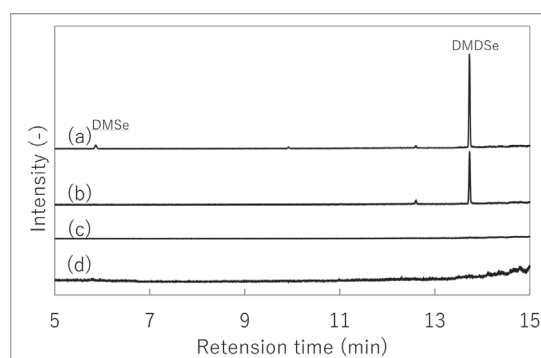**Fig. 5** | **GC-MS spectra of gas phase from Bio-Se^0 reduction test**
(a) *S. stutzeri* NT-I,
(b) *E. coli* DH5α pGEM-mdsN,
(c) *E. coli* DH5α pGEM-control, and
(d) Bio-Se^0 without bacteria.

When Bio-Se^0 was used as a substrate, only DMDSe was detected in the gas phase of *E. coli* DH5α pGEM-mdsN (**Fig. 5b**). In the control experiment, nothing was detected in the gas phase of the culture vessel of *E. coli* DH5α pGEM-control (**Fig. 5c**).

These results suggest that *E. coli* DH5α pGEM-mdsN transfected with the gene encoding class I SAM-dependent methyltransferase acquired the ability to synthesize DMDSe.

Homology analysis of the gene involved in DMDSe synthesis

The *E. coli* DH5α pGEM-mdsN strain acquired the ability to synthesize DMDSe, and the nucleotide sequence of the gene encoding the inserted class I SAM-dependent methyltransferase (Accession No.: PSNT00042, 44319-44918bp) was analyzed. A homology search using BLASTN revealed homology of the nucleotide sequence was 98% with *Stenotrophomonas sp.* As-6 chromosome (Accession No. CP127404). The amino acid sequence showed 100% homology with a class I SAM-dependent methyltransferase (Accession No.: WP_205404086) from *Gammaproteobacteria*. However, the independent synthesis of DMDSe by the class I SAM-dependent methyltransferases of *Gammaproteobacteria* has not yet been reported.

In addition, considering that there might be another enzyme involved in DMDSe synthesis near the class I SAM-dependent methyltransferase, we analyzed the sequence of 5,000 bp around *mdsN* (Accession No.: PSNT00042, 39319-49918 bp) encoding the class I SAM-dependent methyltransferase in the *S. stutzeri* NT-I genome but found no genes involved in Se metabolism (data not shown).

Discussion

We hypothesized that a methyltransferase in the *S. stutzeri* NT-I-specific contig is involved in the synthesis of methylated Se in *S. stutzeri* NT-I and cloned the gene encoding the enzyme. We carried out qualitative analysis of synthesized volatile Se compounds using the transgenic *E. coli* DH5α pGEM-mdsN. A novel gene involved in DMDSe synthesis, that was identified and named *mdsN*. The gene encodes a class I SAM-dependent methyltransferase. When *mdsN* was introduced into *E. coli* DH5α, the recombinant *E. coli* DH5α pGEM-mdsN acquired the ability to synthesize Se to DMDSe, which corresponds to 62% of the initial Se concentration.

The enzymes *tpm*, *ubiE*, and *BoCOQ5-2* involved in the synthesis of both DMSe and DMDSe have been reported [16-18]. However, the genes involved in the synthesis of DMDSe, such as *mdsN*, have not been reported.

The results of qualitative experiments on volatilized Se compounds and SeO_3^{2-} reduction tests in *E. coli* DH5α pGEM-mdsN indicate that the concentration of SeO_3^{2-} decreases and Se^0 increases, followed by a decrease in Se^0. This suggests that *E. coli* DH5α pGEM-mdsN reduces SeO_3^{2-} to Se^0 and then synthesizes DMDSe using Se^0 as a substrate.

These results suggest that *E. coli* DH5α pGEM-mdsN has a pathway to synthesize DMDSe using Se^0 reduced from SeO_3^{2-} as a substrate. The results of qualitative analysis of volatilized Se compounds using Bio-Se^0 (**Figs. 4 and 5**) showed that *S. stutzeri* NT-I synthesized both DMSe and DMDSe, while strain *E. coli* DH5α pGEM-mdsN synthesized only DMDSe. This suggests that *S. stutzeri* NT-I contains genes encoding enzymes involved in DMSe synthesis in addition to class I SAM-dependent methyltransferases. Therefore, further studies on the reaction of *S. stutzeri* NT-I to synthesize methylated Se will lead to the elucidation of DMDSe and DMSe synthetic pathways that have not yet been elucidated.

In this paper, we report a novel finding that *E. coli* DH5α pGEM-mdsN, in which *mdsN* from *S. stutzeri* NT-I was transformed into *E. coli* DH5α, synthesized DMDSe from SeO_3^{2-} and Bio-Se^0 from *S. stutzeri* NT-I. The identification of a novel gene involved in DMDSe synthesis is expected to advance our understanding of the DMDSe synthesis pathway.

References

[1] Wang C. Selenium minerals and the recovery of selenium from copper refinery anode slimes. *J. South. Afr. Inst. Min. Metall.* 2016; 116(6): 593–600. doi: 10.17159/2411-9717/2016/v116n6a16

[2] Srivastava P, Kowshik M. Anti-neoplastic selenium nanoparticles from Idiomarina sp. PR58-8. *Enzyme and Microbial Technology.* 2016; 95: 192–200. doi: 10.1016/j.enzmictec.2016.08.002

[3] Winkel LHE. *et al.* Environmental Selenium Research: From Microscopic Processes to Global Understanding. *Environ. Sci. Technol.* 2012; 46(2): 571–579. doi: 10.1021/es203434d

[4] Dungan RS, Frankenberger WT Jr. Factors affecting the volatilization of dimethylselenide by Enterobacter cloacae SLD1a-1. *Soil Biology and Biochemistry.* 2000; 32(10): 1353-1358. doi: 10.1016/S0038-0717(00)00044-4

[5] Eswayah AS, Smith TJ, Scheinost AC, Hondow N, Gardiner PHE. Microbial transformations of selenite by methane-oxidizing bacteria. *Appl Microbiol Biotechnol.* 2017; 101(17): 6713–6724. doi: 10.1007/s00253-017-8380-8

[6] McCarthy S, Chasteen T, Marshall M, Fall R, Bachofen R. Phototrophic bacteria produce volatile, methylated sulfur and selenium compounds. *FEMS Microbiol Lett.* 1993; 112(1): 93–97. doi: 10.1111/j.1574-6968.1993.tb06429.x

[7] Van Fleet-Stalder V, Chasteen TG, Pickering IJ, George GN, Prince RC. Fate of Selenate and Selenite Metabolized by Rhodobacter sphaeroides. *Appl Environ Microbiol.* 2000; 66(11). doi: 10.1128/aem.66.11.4849-4853.2000

[8] Ruiz-Fresneda MA, *et al.* Combined bioreduction and volatilization of SeVI by Stenotrophomonas bentonitica: Formation of trigonal selenium nanorods and methylated species. *Science of The Total Environment.* 2023; 858(2): 160030. doi: 10.1016/j.scitotenv.2022.160030

[9] Ruiz-Fresneda MA, Eswayah AS, Romero M, Gardiner PHE, Solari PL, Merroun ML. Chemical and structural characterization of SeIV biotransformations by Stenotrophomonas bentonitica into Se0 nanostructures and volatiles Se species. *Environmental Science Nano.* 2020; 2020(7): 2140. doi: 10.1039/D0EN00507J

[10] Dungan RS, Yates SR, Frankenberger WT Jr. Transformations of selenate and selenite by Stenotrophomonas maltophilia isolated from a seleniferous agricultural drainage pond sediment. *Environmental Microbiology.* 2003; 5(4): 287–295. doi: 10.1046/j.1462-2920.2003.00410.x

[11] Kagami T, *et al.* Effective selenium volatilization under aerobic conditions and recovery from the aqueous phase by Pseudomonas stutzeri NT-I. *Water Research.* 2013; 47(3): 1361–1368. doi: 10.1016/j.watres.2012.12.001

[12] Otsuka O, Yamashita M. Selenium recovery from wastewater using the selenate-reducing bacterium Pseudomonas stutzeri NT-I. *Hydrometallurgy.* 2020; 197: 105470. doi: 10.1016/j.hydromet.2020.105470

[13] Otsuka O, Yamashita M. Methods for recovering and recycling selenium from wastewater and soil. *Metallomics Research.* 2022; 2(3): rev28–39. doi: 10.11299/metallomicsresearch.MR202208

[14] Winkel L, Feldmann J, Meharg AA. Quantitative and Qualitative Trapping of Volatile Methylated Selenium Species Entrained through Nitric Acid. *Environ. Sci. Technol.* 2010; 44(1): 382-387. doi: 10.1021/es902345m

[15] Kuroda M, Sei K, Yamashita M, Ike M. Draft Genome Sequence of Stutzerimonas stutzeri NT-I, Which Reduces Selenium Oxyanions into Elemental Selenium and Volatile Selenium Species. *Microbiol Resour Announc.* 2022; 11(12): e01016–22. doi: 10.1128/mra.01016-22

[16] Ranjard L, Nazaret S, Cournoyer B. Freshwater Bacteria Can Methylate Selenium through the Thiopurine Methyltransferase Pathway. *Applied and Environmental Microbiology.* 2003; 69(7): 3784–3790. doi: 10.1128/aem.69.7.3784-3790.2003

[17] Swearingen JW Jr, *et al.* Expression of the ubiE Gene of Geobacillus stearothermophilus V in Escherichia coli K-12 Mediates the Evolution of Selenium Compounds into the Headspace of Selenite- and Selenate-Amended Cultures. *APPLIED AND ENVIRONMENTAL MICROBIOLOGY.* 2006; 72(1): 963-967. doi: 10.1128/AEM.72.1.963-967.2006

[18] Zhou X, *et al.* Involvement of a broccoli COQ5 methyltransferase in the production of volatile selenium compounds. *Plant Physiology.* 2009; 151(2): 528–540. doi: 10.1104/pp.109.142521

[19] Kuroda M, *et al.* Molecular Cloning and Characterization of the srdBCA Operon, Encoding the Respiratory Selenate Reductase Complex, from the Selenate-Reducing Bacterium Bacillus selenatarsenatis SF-1. *J. BACTERIOL.* 2011; 193. doi: 10.1128/JB.01197-10

[20] Otsuka O, Yanaba Y, Yoshikawa T, Yamashita M. Fundamental Studies on Oxidizing Roasting of the 'Bioselenium'. *Mater. Trans.* 2016; 57(7): 1183–1191. doi: 10.2320/matertrans.M2016060